NAVAL POSTGRADUATE SCHOOL

MONTEREY, CALIFORNIA

THESIS

STABILITY CRITERIA ANALYSIS FOR LANDING CRAFT UTILITY

by

Kyriakos Roussopoulos

December 2017

Thesis Advisor:	Fotis A. Papoulias
Co-Advisor	Jarema M. Didoszak

Approved for public release. Distribution is unlimited.

THIS PAGE INTENTIONALLY LEFT BLANK

REPORT DOCUMENTATION PAGE			*Form Approved OMB No. 0704–0188*

1. AGENCY USE ONLY ***(Leave blank)***	**2. REPORT DATE** December 2017	**3. REPORT TYPE AND DATES COVERED** Master's thesis

4. TITLE AND SUBTITLE
STABILITY CRITERIA ANALYSIS FOR LANDING CRAFT UTILITY

5. FUNDING NUMBERS

6. AUTHOR(S) Kyriakos Roussopoulos

7. PERFORMING ORGANIZATION NAME(S) AND ADDRESS(ES)
Naval Postgraduate School
Monterey, CA 93943-5000

8. PERFORMING ORGANIZATION REPORT NUMBER

9. SPONSORING /MONITORING AGENCY NAME(S) AND ADDRESS(ES)
N/A

10. SPONSORING / MONITORING AGENCY REPORT NUMBER

11. SUPPLEMENTARY NOTES The views expressed in this thesis are those of the author and do not reflect the official policy or position of the Department of Defense or the U.S. Government. IRB number ____N/A____.

12a. DISTRIBUTION / AVAILABILITY STATEMENT
Approved for public release. Distribution is unlimited.

12b. DISTRIBUTION CODE

13. ABSTRACT (maximum 200 words)

Currently used Landing Craft Utility (LCU) stability criteria may not be optimal for the typical coastal transits of those vessels. Therefore, this study examines the intact transverse static and dynamic stability of the LCU in order to recommend more appropriate criteria for short-range transits. The analysis mainly uses the Program of Ship Salvage Engineering (POSSE) software and the standard Ship Motion Program (SMP) to model a stochastic sea state, simulate the LCU's loading conditions, and predict the craft's dynamic responses in certain sea state conditions. The LCU's static transverse stability is derived by the POSSE software in terms of righting arm diagrams for different loading conditions, while the SMP software determines the dynamic transverse stability. The SMP analysis is based on seakeeping theory, using sea spectra model techniques to determine the LCU's roll angle dynamic responses.

Based on these simulation results, the study evaluates the currently used stability criteria and arrives at new dynamic stability recommendations and improved operational limits. These may be further refined by using hull appendage implementations in follow-on studies.

14. SUBJECT TERMS
stability, criteria, landing, craft, utility

15. NUMBER OF PAGES 129

16. PRICE CODE

17. SECURITY CLASSIFICATION OF REPORT	**18. SECURITY CLASSIFICATION OF THIS PAGE**	**19. SECURITY CLASSIFICATION OF ABSTRACT**	**20. LIMITATION OF ABSTRACT**
Unclassified	Unclassified	Unclassified	UU

NSN 7540–01-280-5500 Standard Form 298 (Rev. 2–89)
Prescribed by ANSI Std. 239–18

THIS PAGE INTENTIONALLY LEFT BLANK

STABILITY CRITERIA ANALYSIS FOR LANDING CRAFT UTILITY

Kyriakos Roussopoulos
Lieutenant, Hellenic Navy
B.S., Hellenic Naval Academy, 2003

Submitted in partial fulfillment of the
requirements for the degree of

MASTER OF SCIENCE IN MECHANICAL ENGINEERING

from the

NAVAL POSTGRADUATE SCHOOL
December 2017

Approved by: Fotis A. Papoulias
Thesis Advisor

Jarema M. Didoszak
Co-Advisor

Garth V. Hobson
Chair, Department of Mechanical
and Aerospace Engineering

THIS PAGE INTENTIONALLY LEFT BLANK

ABSTRACT

Currently used Landing Craft Utility (LCU) stability criteria may not be optimal for the typical coastal transits of those vessels. Therefore, this study examines the intact transverse static and dynamic stability of the LCU in order to recommend more appropriate criteria for short-range transits. The analysis mainly uses the Program of Ship Salvage Engineering (POSSE) software and the standard Ship Motion Program (SMP) to model a stochastic sea state, simulate the LCU's loading conditions, and predict the craft's dynamic responses in certain sea state conditions. The LCU's static transverse stability is derived by the POSSE software in terms of righting arm diagrams for different loading conditions, while the SMP software determines the dynamic transverse stability. The SMP analysis is based on seakeeping theory, using sea spectra model techniques to determine the LCU's roll angle dynamic responses.

Based on these simulation results, the study evaluates the currently used stability criteria and arrives at new dynamic stability recommendations and improved operational limits. These may be further refined by using hull appendage implementations in follow-on studies.

THIS PAGE INTENTIONALLY LEFT BLANK

TABLE OF CONTENTS

THIS PAGE INTENTIONALLY LEFT BLANK

LIST OF FIGURES

LIST OF TABLES

LIST OF ACRONYMS AND ABBREVIATIONS

A	Ship's Projected Area above Water Line
A_{ij}	Matrix of Mass Forces of the Wave Exciting Forces Determination System
A_n	Amplitude of the n-th Wave Component
A_o	Wave Amplitude
AP	Ship's Afterward Draft
B_{ij}	Matrix of Damping Forces of the Wave Exciting Forces Determination System
BL	Base Line
C	Fluid Closed Curve
C_{ij}	Matrix of Hydrostatic Forces of the Wave Exciting Forces Determination System
CL	Center Line
F	Centrifugal Force on Ship due to Ship Turning
F_i	Sea Wave Exciting Forces
FP	Ship's Forward Draft
ft	Foot
ft/s	Foot per Second
ft/s^2	Foot per Second Squared
G	Ship's Initial Center of Gravity
G'	Ship's Center of Gravity after Weight Added
G''	Ship's Center of Gravity after Lateral Weight Motion
GG''	Lateral Distance between G' and G''
GM_t	Transverse Metacentric Height
GZ	Ship's Righting Arm
GZ'	Corrected Ship's Righting Arm for Added Weight
GZ''	Corrected Ship's Righting Arm for Moved Weight
g	Gravity Acceleration

HA	Ship's Heeling Arm
HA_i	Heeling Arm at Heeling Angle θ=0º for the Topside Icing Wind Condition
HA_k	Heeling Arm at Heeling Angle θ=0º for the Wind Condition without Ice
H_u	Visually Observed Significant Sea Wave Height
$H_{1/3}$	Wave Spectrum Significant Height
h	Vertical Distance from Base Line to the Position of Added Weight
h_k	Distance from the Ship's Half Draft to the Projected Area Centroid
hp	Horse Power
JONSWAP	Joint North Sea Wave Project
Kg	Kilogram
KG	Vertical Distance between Ship's Base Line and Ship's Initial Center of Gravity
KG'	Vertical Distance between Ship's Base Line and Ship's new Center of Gravity due to Added Weight
KM_t	Distance between Keel and Transverse Metacentric Height
KW	10^3 Watts
k	Number of Waves per Unit Space (Wavenumber)
k_n	Wavenumber of n-th Wave Component
L	Lateral Distance of between Moved Weight Position and Ship's Center of Gravity
LCB	Longitudinal Position of Ship's Center of Buoyancy
LCF	Longitudinal Position of Ship's Center of Flotation
LCG	Longitudinal Position of Ship's Center of Gravity
LCG_W	Longitudinal Distance Between Ship's Forward Perpendicular and Additional Weight Center of Gravity
LCU	Landing Craft Utility

l	Distance from the Centroid of Ship's Projected Area and the Centroid of the Underwater Hull Profile in m
lb	Pound
M_{ij}	Matrix of Mass Elements of the Wave Exciting Forces Determination System
MS	Mid-ship Draft
MT	Metric Tone
m_o	Total Spectral Energy
m	Meter
m^2	Square meter
m/s	Meters per Second
m/s^2	Meters per Second Squared
n	Vertical Displacement of Sea Water Free Surface
n_3	Ship's Heave Displacement
n_5	Ship's Pitch Angle
$p(\xi)$	Rayleigh Distribution Probability Function
POSSE	Program of Ship Salvage Engineering
p_k	Wind Pressure Above Sea Surface
R	Radius of Ship Turn
RAO	Response Amplitude Operator
$\|RAO(\omega)\|^2$	Transfer Function
rad	Radian
$S(\omega)$	Spectral Energy Density
Sec	Second
Sec^2	Second Squared
SMP	Ship Motion Program
$S_R(\omega)$	Ship Response Spectrum
TCG	Transverse Distance between Center Line and Ship's Center of Gravity

TCG_W	Transverse Distance between Ship's Center Line and Additional Weight Center of Gravity
T_m	Wave Spectrum Modal Period
T_u	Visually Observed Sea Wave period
T_z	Wave Spectrum Average Period
T_u	Visually Observed Sea Wave period
t	Time
u	Magnitude of X-Axis Fluid Velocity Component
V	Fluid Control Volume
VCG	Distance between Keel and Ship's Center of Gravity
VCG_W	Vertical Distance between Keel and Additional Weight Center of Gravity
V_i	Maximum wind velocity, for the Assumed Thickness of the Ship Accumulated Ice
V_k	Wind Velocity
V_s	Ship's Linear Velocity
v	Magnitude of Y-Axis Fluid Velocity Component
W	Added or Moved Weight on Ship
W_g	Total Weight of Ship's Passengers
WHA	Wind-generated Heeling Arm
w	Magnitude of Z-Axis Fluid Velocity Component
x	Sea Wave Propagation Direction
x_L	Distance Measured in Ship's Longitudinal axis

LIST OF SYMBOLS

α	Wave Spectra Constant (8.1×10^{-3})
α_p	Distance between Group of Passengers' Center of Gravity and Ship's Center of Gravity
α_s	Distance between Ship's Center of Gravity and Ship's Half Draft
β_J	JONSWAP Spectrum Constant
β_p	Pierson-Moskowitz Spectrum Constant
γ	JONSWAP Wave Spectrum Peak Factor
$\Gamma(\lambda)$	Gamma Probability Function
Δ	Ship's Displacement
$\Delta\omega$	Small Frequency Band
ζ	Bretschneider, JONSWAP, and Ochi-Hubble Spectra Wave Significant Height
θ	Ship's Heeling Angle
λ	Ochi-Hubble Wave Spectrum Shape Parameter
λ_w	Wavelength
ξ	Normalized Wave Amplitude
ξ_{VA}	Ship's Absolute Heave Displacement
ρ	Mass Density
σ	JONSWAP Wave Spectrum Constant
Φ	Exact Differential Function
ω	Sea Wave Angular Frequency
ω_e	Ship's Response Motion Frequency
ω_m	Wave Spectrum Modal Frequency
ω_p	Wave Peak Frequency
ω_z	Wave Spectrum Average Frequency
$(^o)$	Degrees
∇	Differential Operator

$[D_{ij}]^{-1}$	Inverse Matrix of the Wave Exciting Forces Determination System
$d\bar{r}$	Differential Position Vector
$\bar{h}_o$	Wave Spectrum Mean Amplitude
$\bar{H}$	Wave Spectrum Average Height
n_j	Ship's Response Displacement
$\dot{n}_j$	Ship's Response Velocity
$\ddot{n}_j$	Ship's Response Acceleration
$\bar{n}$	Ship's Response Amplitude
$\bar{r}$	Position Vector
$\Re$	Real Number
$\bar{u}_P$	Wave planar Velocity Component towards X-Axis Direction
$\bar{U}$	Fluid Velocity Vector
$\bar{w}_P$	Wave Planar Velocity Component towards Z-Axis Direction

ACKNOWLEDGMENTS

First, I would like to thank the Hellenic Navy for giving me the opportunity to study at this highly distinguished academic institution in the United States of America. I am deeply grateful to the Hellenic Navy for investing in me and offering this unique and once-in-a-life-time experience.

I would also like to thank my thesis advisor, Professor Fotis Papoulias, and co-advisor, Professor Jarema Didoszak, for their continuous and robust support of my research. Their generosity in always providing me with the right directions and critical advice taught me how to recognize the point wherein the significant question lies. They guided me in a scientific and professional manner, contributing decisively to my thesis accomplishment.

Finally, and most significantly, I would like to express my gratitude to my family for their support and encouragement throughout all these years of study, and especially during the completion of this thesis.

THIS PAGE INTENTIONALLY LEFT BLANK

I. INTRODUCTION

A. MOTIVATION

A basic concern of naval architecture is vessel stability.[1] Generally, emphasis is given to transverse stability, which refers to a vessel's ability to return to equilibrium position when the applied external forces generate moments acting around the centerline axis of the vessel. Longitudinal stability, on the other hand, expresses a ship's ability to resist trim; that is, the difference between forward and afterward drafts.

Ship stability is influenced by many factors including displacement, load distribution, wind speed, underwater volume, sea state conditions, turning angle, and speed. Those factors, expressed as numerical parameters, contribute to the generation of the ship's stability curves. Stability curves describe the ship's transverse stability over a wide range of heeling angles and provide information about the required righting arm and moments in order to return the ship to the initial equilibrium state when it has been disturbed by a particular heeling angle.

These stability curves are used to derive the stability criteria of a ship for a particular set of parameters associated with curves, such as the heeling angle, the righting arm, and the area under the curves, which are expressed in terms of mathematical limitations of parameter values. Stability criteria can provide a ship with an operational guide. Compliance with such criteria ensures a ship's positive stability (i.e., the ship's ability to restore itself to its initial position), in contrast to negative stability, which refers to the ship's tendency to overturn.

Built in 1970 by the U.S. Navy, the Landing Craft Utility (LCU) is a small displacement craft used in amphibious operations to transport troops and military equipment, such as wheeled vehicles and tanks, to shore. Carried and launched by amphibious assault ships, its primary objective is to land military equipment and

1 The ability to return to an equilibrium state when subjected to external loads that are then removed.

personnel. This research used the LCU 1644 model. Jane’s by IHS Markit describes some basic characteristics of the craft are as follows:

General Characteristics

- Length (Overall): 41.1 m
- Length (Between Perpendiculars): 40.84 m
- Beam: 8.8 m
- Depth 2.44 m
- Maximum Speed: 5.66 m/s (11 knots)
- Maximum Range: 2,222.4 Km (1200 Nautical Miles)
- Economic Speed: 4.12 m/s (8 knots)
- Maximum Load: 127 Metric Tones
- Crew Members: 16
- Propulsion system: 4 Detroit 6-71 diesels 519.007 KW (696 hp) [1]

Stability criteria currently used for the LCU are mainly based on the “*Procedures Manual for Stability Analysis of U.S. Navy Small Craft, 1977* [2].” This manual provides a transverse dynamic stability analysis for small displacement vessels. This analysis is a partially empirical procedure, uses the stability curves, and provides stability criteria by focusing on the ship restoring moment. The ship restoring moment is the moment produced by the misalignment of the gravity and buoyancy forces’ acting points and contributes to the ship righting to the initial equilibrium position.

This analysis assumes open ocean transits associated with high wind velocities; the majority of LCU missions, however, occur in coastal water with lower wind velocities. This fact then raises the question of whether or not the currently used stability criteria are in fact optimal for use with the LCU and its costal missions and associated loading conditions. More specifically, these criteria may be overly conservative, resulting in a negative impact on LCU operational limitations. Specific stability criteria for the LCU missions are not currently documented.

B. OBJECTIVES AND OUTLINE

The main objective of this research is to investigate the suitability of stability criteria currently used for the LCU by performing a rigorous analysis. This analysis examines the intact stability of the craft during coastal missions. More specifically, this analysis focuses on LCU performance in short-range coastal transits from amphibious assault ships to the beach carrying different equipment loads and personnel. A further objective is to contribute to a guideline for the entire LCU fleet based on the conditions and characteristics of its typical coastal missions. Chapter II presents the currently used stability criteria for the LCU according to the manual mentioned previously, as well as the basic static stability theory. Chapter III discusses seakeeping and dynamic stability theory, and presents the most popular and useful sea wave spectra for these kinds of analyses. Chapter IV describes the software used to determine the ship's static and dynamic responses. Chapter V presents the simulation results, with an emphasis on the operational trade space of the LCU. Chapter VI presents the conclusions and recommendations on the ship's stability, and discusses future work that could follow the current research.

C. ASSUMPTIONS AND TASKS

This research is conducted using three general, high-level assumptions for the LCU stability analysis:

- The ship's center of gravity does not change as the angle of heel increases or decreases.
- The ship's center of buoyancy is always defined as the geometric centroid of the ship's underwater hull area.
- The shape of the ship's underwater hull area will continue to change as the angle of heel increases or decreases.

This thesis research focuses on the following tasks:

- Categorization of the currently used LCU stability criteria
- Simulation of the stochastic nature of the sea state environment by using the appropriate software

- Establishment of problem boundaries by selecting the values for crucial parameters in the modeling software
- Determination of the ship's static stability and dynamic responses
- Evaluation of the LCU's static and dynamic stability on the basis of the obtained simulation results
- Development of Operational Recommendations for the LCU during usual coastal water missions

II. BACKGROUND—CURRENT STABILITY CRITERIA FOR THE LCU AND STATIC STABILITY THEORY

A. WIND ACTION AND ROLLING

Wind beams influence the transverse stability of a ship by producing a wind-generated heeling arm. This heeling arm is derived from wind force and is applied to the ship's exposed surfaces, which produces a heeling moment. This results in a heeling angle and the craft undergoes inclination, which disturbs its initial transverse stability.

Generally, the transverse stability of a ship is described by the righting arm curves. These curves are designed for the ship's specific parameters of displacement and vertical position of ship's center of gravity, resulting in the righting arm (GZ) against the heeling angle (θ). These curves provide a measure of the ship's ability to withstand capsizing under certain conditions.

The wind-produced heeling arm and heeling moment are dependent on the wind pressure applied to ship's exposed area. The wind pressure is a function of wind velocity, and this velocity is regarded to increase as a function of the height from the sea surface. The ship's projected area is not uniform, and an assumption of a combination of many simple rectangular areas is made [2]. Then, an equivalent rectangular area is used. Furthermore, in order to compute the wind pressure on the projected ship's surface, a standard rule is used to calculate wind velocity. According to this rule, wind velocity is measured at a distance of 10 meters (m) from the sea surface [2]. A typical wind velocity profile is shown in Figure 1. The wind pressure on the ship's projected area is described in [2] as:

$$p_k = 0.004\left(V_k\right)^2 . \quad (1)$$

p_k: Wind pressure in lb/ft^2

V_k: Wind velocity in knots

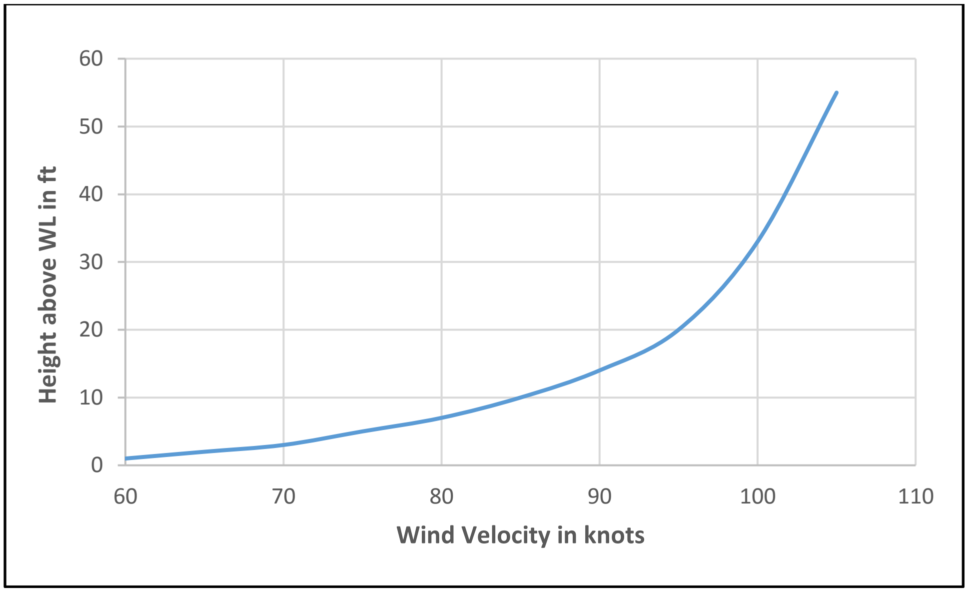

Figure 1. Wind Velocity Profile above the Water Line. Adapted from [2].

The produced wind heeling arm is a function of the aggregate wind pressure, the projected area, the ship displacement, and the centroid of the projected area height. As described in [2]:

$$HA = \frac{p_k A h_k}{\Delta}, \tag{2}$$

HA: Heeling arm in ft.

p_k: Wind pressure in lb/ft^2

A: Ship projected area above water line ft.^{2}

h_k: Distance from the half draft to the projected area centroid in ft.

Δ: Ship displacement in lbs.

According to the previous analysis, in order to have sufficient stability, a ship must meet the stability criteria as illustrated in Figure 2:

1. The heeling arm (HA) at the point of intersection of the two curves (righting arm curve and wind heeling arm curve), point C, must not exceed the 0.6 of the maximum righting arm (RA Max) [2], [3].

2. The area A_1 (the area between the two curves) should be equal to or greater than the area $1.4x(A_2)$ [2], [3].

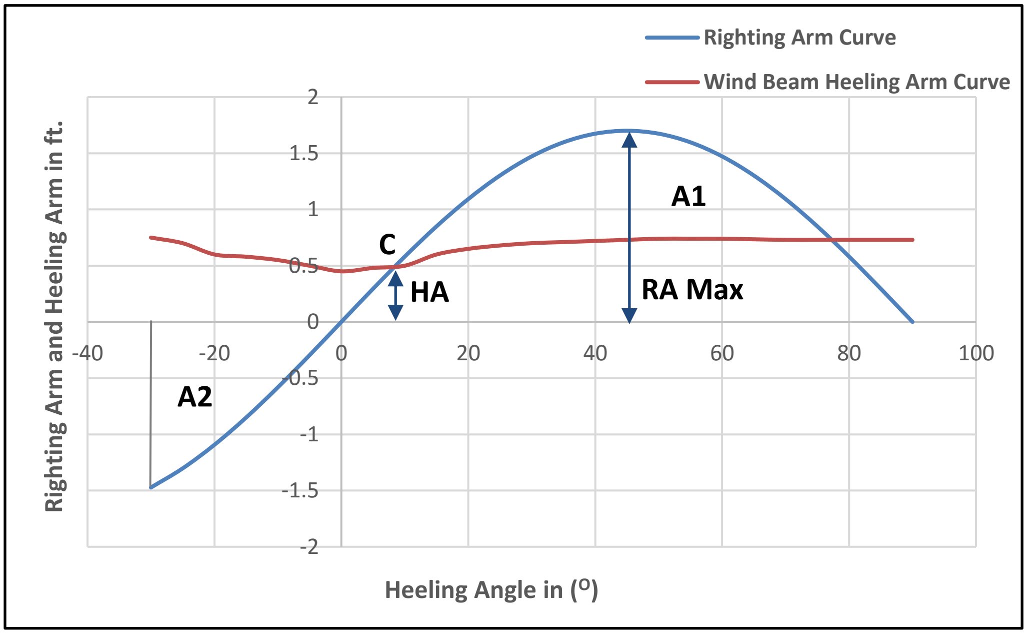

Figure 2. Righting Arm and Wind Heeling Arm Curves. Adapted from [2].

B. LIFTING HEAVY WEIGHTS OVER THE SIDE

In the case when a lifted weight is not contained in the initial displacement of the ship, the righting arm curve is no longer valid. Therefore, this curve requires correction based on the new displacement conditions. If the lifted weight is connected to the ship in a way that permits free movement, it is considered to be attached to the base of the boom and always acts downward [2]. As weight lifting affects both the total ship displacement (if the weight is added) and the position of the center of gravity (G), the required correction should take into account the new final position of that point (G'). The initial righting arm curve of the ship, $GZ(\theta)$, connects the righting arm (GZ) with the heeling angle (θ). After the weight lifting, these curves require corrections corresponding to the ship's new center of gravity. These corrections take place in two sequential, yet distinct steps:

First, we assume that the weight added in the vertical line passes from the ship's original center of gravity (VCG). The VCG parameter is the vertical distance between the lower keel point K (base line) and the ship's center of gravity, point G. The additional weight (W) placed at a height (h) from the base line results in the position change of the ship's center of gravity toward this vertical line. The new position is given by the formula as noted in [2]:

$$KG' = \frac{(\Delta KG + Wh)}{\Delta + W}, \tag{3}$$

KG: Vertical distance between base line and initial center of gravity in ft.

KG': Vertical distance between base line and new center of gravity in ft.

h: Vertical distance from the base line to the position the weight added in ft.

Δ: Ship displacement in lbs.

W: Added weight in lbs.

Then, the corrected/adjusted righting arm corresponds to one of the following:

If $KG < h$ the new righting arm is as explained in [2]:

$$GZ'(\theta) = GZ(\theta) + GG' \sin\theta, \tag{4}$$

If $KG > h$ the new righting arm is as explained in [2]:

$$GZ'(\theta) = GZ(\theta) - GG' \sin\theta, \tag{5}$$

Second, the weight (W) is moved from the ship's center line by a lateral distance L. This movement results in a shift of the ship's center of gravity to a new position given by the relationship, as described in [2]:

$$G'G'' = \frac{WL}{\Delta + W}\,, \tag{6}$$

$G'G''$: Lateral distance between the G' position and the final location of center of gravity G'' in ft.

Δ : Ship displacement in lbs.

W : Moved weight in lbs.

L : Lateral distance between the G' position and the location of the added weight in ft.

The final corrected/adjusted righting arm is as explained in [2]:

$$GZ''(\theta) = GZ'(\theta) + G'G''\cos\theta\,. \tag{7}$$

Based on the previous analysis, as shown in Figure 3, the criteria that must be satisfied for stability are as follows:

1. The heeling angle at the point of intersection of the two curves (righting arm curve and weight over side curve), point C, must be equal to or lower than 15 degrees [2], [3].
2. The heeling arm (HA) at point C must not exceed the 0.6 of the maximum righting arm (RA Max) [2], [3].
3. The area representing the reverse dynamic stability of the craft (the area between the two curves) must be equal to or greater than 40 percent of the total area under the curve of the righting arm [2], [3].

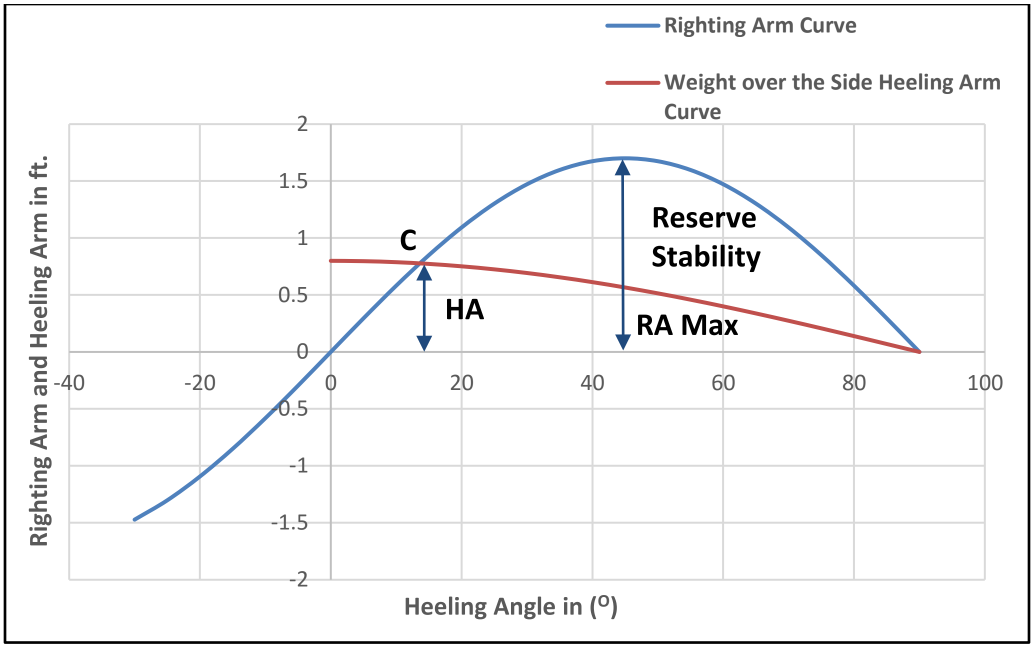

Figure 3. Righting Arm and Weight over the Side Heeling Arm Curves. Adapted from [2].

C. CROWDING OF PASSENGERS TO ONE SIDE

The crowding of passengers to one side of a ship affects the transverse stability of the ship by producing a heeling arm, which changes the ship's initial righting arm and alters its stability. For this heeling arm analysis, the assumptions made are the passenger contact areas, individual passenger's weight, and the locations of the total weight. According to these, each passenger stands over a 2 foot square (0.186 m^2) area and weighs 165 pounds (74.84 Kg) on average, and the entire group of passengers is located on one side of the craft [2]. The heeling arm produced is given by the formula as explained in [2]:

$$HA = \frac{W_g \alpha_P \cos\theta}{\Delta}, \tag{8}$$

HA: Heeling arm in ft.

W_g: Total weight of passengers in lbs.

α_P: Distance between the group passengers' center of gravity and the ship's center line in ft.

Δ: Ship displacement in lbs.

θ: Heeling angle in degrees (º)

According to the previous considerations, as shown in Figure 4, the criteria that should be met for adequate stability are:

1. The heeling angle at the point of intersection of the two curves (righting arm curve and crowding of passengers to one side curve), point C, must be equal to or less than 15 degrees [2], [3].
2. The heeling arm (HA) at point C must not exceed 0.6 of the maximum righting arm (RA Max) [2], [3].
3. The area representing the reverse dynamic stability of the craft (the area between the two curves) must be equal to or greater than 40 percent of the total area under the curve of the righting arm [2], [3].

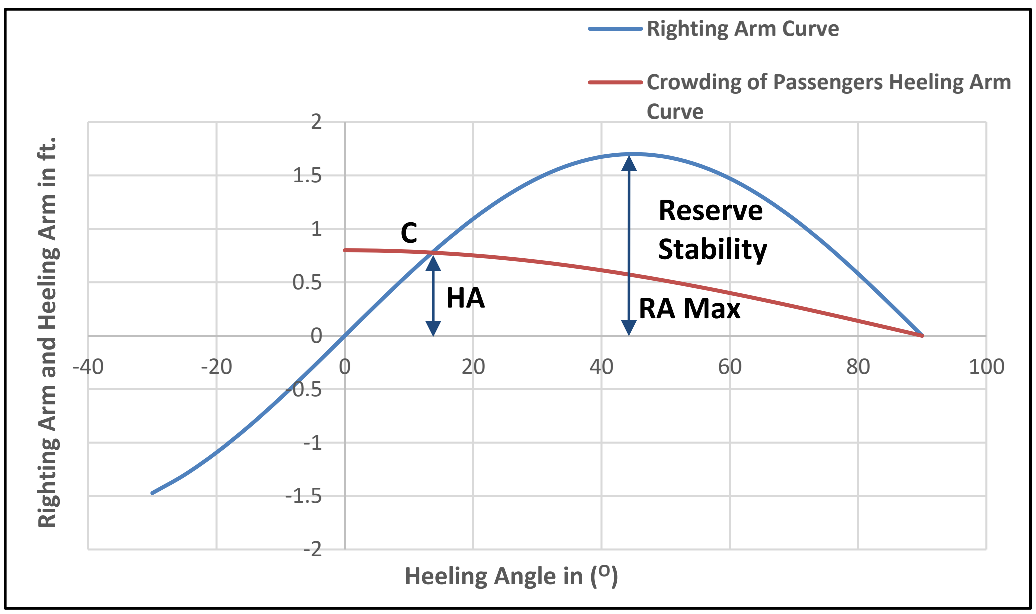

Figure 4. Righting Arm and Crowding of Passengers Heeling Arm Curves. Adapted from [2].

D. HIGH-SPEED TURNING

When a ship makes a turn at high speed, centrifugal force arises and acts on the ship toward the outside. The magnitude of this force is expressed by the formula, as noted in [2]:

$$F = \frac{\Delta V_S^{\,2}}{gR}, \tag{9}$$

Δ : Ship displacement in lbs.

V_S : Ship linear velocity in ft/s

g : Gravity acceleration = 32.174 ft/s^2

R : Radius of turn in ft.

In an equilibrium state of the forces, a side resistance develops that is equal and opposite to centrifugal force [2]. This resistance creates a moment that consequently produces a heeling arm. The lever of this moment is considered to be the distance between the ship's center of gravity (G) and the application point of the side resistance in the submerged part of the ship, which, by convention, is chosen half way along the draft [2]. This lever measured in feet is symbolized as a_S. Then, the heeling arm of the high-speed ship turning is yielded by the expression, as explained in [2]:

$$HA = \frac{V_S^{\,2} \alpha_S \cos\theta}{gR}, \tag{10}$$

θ: Heeling angle in degrees (º)

V_S : Ship linear velocity in ft/s

g : Gravity acceleration = 32.174 ft/s^2

R : Radius of turn in ft.

In cases of high-speed turning, the criteria for adequate ship stability according to Figure 5 are as follows:

1. The heeling angle at the point of intersection of the two curves (righting arm curve and high-speed turning heeling arm curve), point

C, must be equal to or less than 10 degrees for a new ship and 15 degrees for a ship in service [2], [3].

2. The heeling arm (HA) at the point C must not exceed the 0.6 of the maximum righting arm (RA Max) [2], [3].

3. The area representing the reverse dynamic stability of the craft (the area between the two curves) must be equal to or greater than 40 percent of the total area under the curve of the righting arm [2], [3].

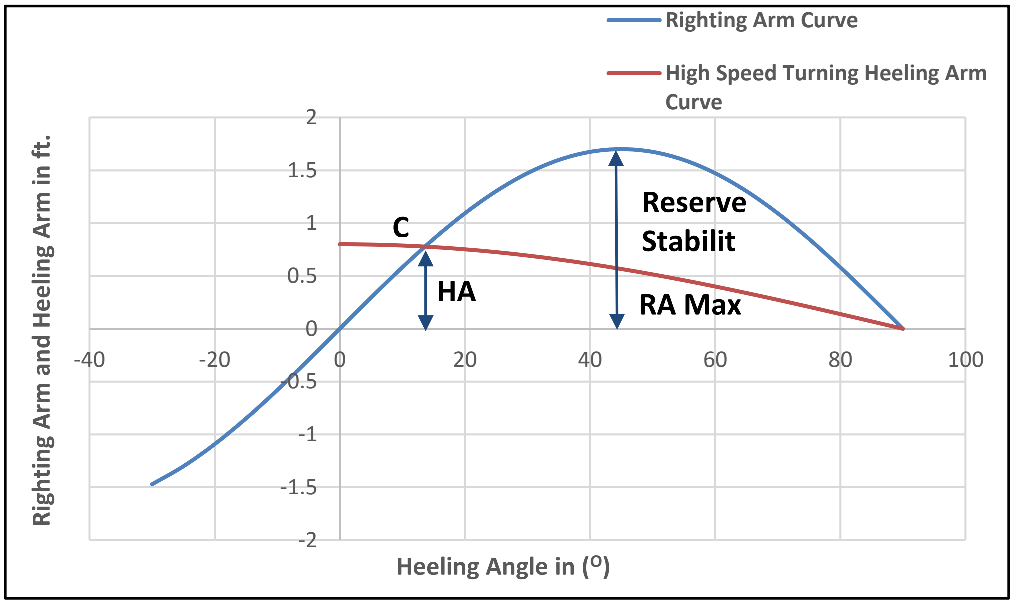

Figure 5. Righting Arm and High Speed Turning Heeling Arm Curves. Adapted from [2].

E. TOPSIDE ICING

Ice accumulation on a ship depends on various factors such as velocity, surface texture, location, and surface inclination. Generally, the analyses assume a standard thickness of accumulated ice on the weather deck. If the thickness is not specifically determined, then it is taken as 3 inches (0.0762 m) and 6 inches (0.1524 m), and this research examines both cases [2]. Ice accumulation on masts and other fittings is assumed to be 0 inches [2].

Topside icing affects a ship's stability by increasing its displacement and raising the center of gravity. For the calculations, ice density is assumed to be 56.7 lbs/ft^3 (908.25 Kg/m^3) [2]. Analysis of topside icing stability criteria is closely related to wind beam effects on the ship's stability. The topside icing effect is studied as an adjustment of the wind beam effect. This is an adjustment of the wind heeling arm curve due to the equivalent wind velocity. The equivalent wind velocity is yielded by the formula, as described in [2]:

$$V_i = V_k \left(\frac{HA_i}{HA_k} \right)^{1/2}, \tag{11}$$

V_i : Maximum wind velocity, for the assumed ice layer thickness, in knots

HA_i : Heeling arm at heeling angle $\theta=0^o$ for the topside icing wind condition

HA_k : Heeling arm at heeling angle $\theta=0^o$ for the wind condition without ice

V_k : Wind Velocity without ice in knots

After the determination of the equivalent wind velocity, the analysis uses relationships (1) and (2) to determine the heeling arm produced by the topside icing effect. Stability is sufficient if all the criteria of wind beam and rolling case, referred to previously, are met according to Figure 6 [2].

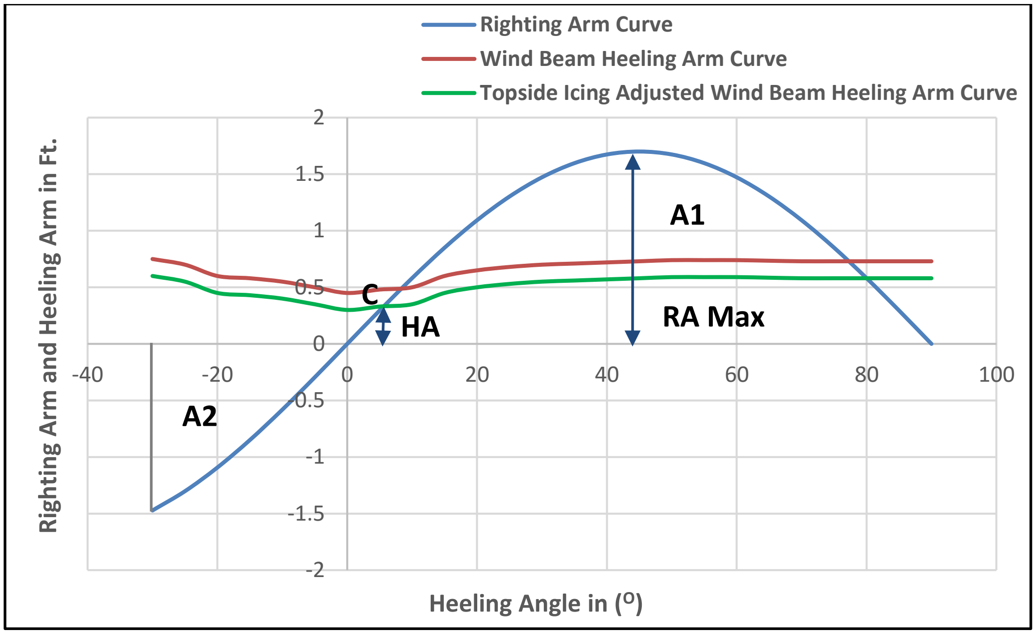

Figure 6. Righting Arm and Topside Icing Adjusted Wind Beam Heeling Arm Curves. Adapted from [2].

Additionally, in the topside icing condition, the analysis uses a combined approach, which takes into consideration both the maximum acceptable ice thickness and the maximum acceptable wind velocity:

1. The maximum acceptable thickness for an ice layer is specified by the wind conditions in the area of interest [2].
2. The maximum acceptable wind velocity is specified by the assumed thickness of the ice layer [2].
3. If ice accumulations or wind velocities are predicted to be higher than the maximum set values, the craft safety is no longer secured and depends on the decision to depart [2].

THIS PAGE INTENTIONALLY LEFT BLANK

III. SEAKEEPING AND DYNAMIC STABILITY THEORY

A. BASIC FLUID MECHANICS ASSUMPTIONS

Seakeeping is the dynamic response and motional behavior of the ship on sea waves. To study seakeeping, we consider only the surface sea waves, which are characterized by time periods of some seconds [4]. One basic tool of this study is the potential flow theory, which describes the fluid properties under two main assumptions: the conservation of mass and the irrotational flow [4].

Conservation of mass requires that fluid mass flowing in a control volume (V) should be equal with the increase of the mass in this volume. This concept is expressed by the relationship as described in [4]:

$$\frac{\partial \rho}{\partial t} + \nabla \cdot \left(\rho \overline{U} \right) = 0 . \tag{12}$$

By assuming the fluid density ρ to be constant (incompressible flow), we get the volume-continuity equation from [4]:

$$\nabla \cdot \overline{U} = 0 , \tag{13}$$

$\overline{U}$: The velocity vector of fluid $\overline{U} = u \cdot \overline{i} + v \cdot \overline{j} + w \cdot \overline{k}$, (14)

∇ : The operator $\nabla = \frac{\partial}{\partial x} \overline{i} + \frac{\partial}{\partial y} \overline{j} + \frac{\partial}{\partial z} \overline{k}$, (15)

from which the final continuity equation is derived, as explained in [4]:

$$\frac{\partial u}{\partial x} + \frac{\partial v}{\partial y} + \frac{\partial w}{\partial z} = 0 . \tag{16}$$

Irrotational flow requires no circulation of the fluid in a closed curve C . That discipline is mathematically described by the equation, as noted in [4]:

$$\int_C \overline{U} \cdot d\overline{r} = 0 , \tag{17}$$

C : Closed curve

$\bar{r}$: Position vector

$d\bar{r} = \bar{i}dx + \bar{j}dy + \bar{k}dz$

Since the integral is the same in any path of integration, the velocity vector can be described by the expression of exact differential of the function (Φ), which is a scalar magnitude [4]. The velocity potential is identified as follows, according to [4]:

$$\bar{U} = \nabla\Phi \, . \tag{18}$$

Combining Equations (13) and (16), we take the Laplace equation, as noted in [4]:

$$\nabla^2\Phi = \frac{\partial^2\Phi}{\partial x^2} + \frac{\partial^2\Phi}{\partial y^2} + \frac{\partial^2\Phi}{\partial z^2} = 0 \, . \tag{19}$$

B. SEA WAVE NATURE

1. Regular Waves

To identify the motion of the free surface of seawater, we consider a two-dimensional wave in the x-z plane, as shown in Figure 7. This type of wave is called a regular wave and has a simple sinusoidal form [4]. The propagation direction of the wave is the x-axis, and the vertical motion of any point in the free surface is measured in the z-axis and is given by the formula, as described in [4]:

$$n(x,t) = A_O \cos(kx - \omega t) \, , \tag{20}$$

n : Vertical displacement of seawater free surface in m

ω : Angular frequency in rad/sec

x : Wave propagation direction

t : Time in sec

k : Number of waves per unit space ($k = 2\pi / \lambda_W$)

λ_W : Wavelength in m

A_O : Wave amplitude in m

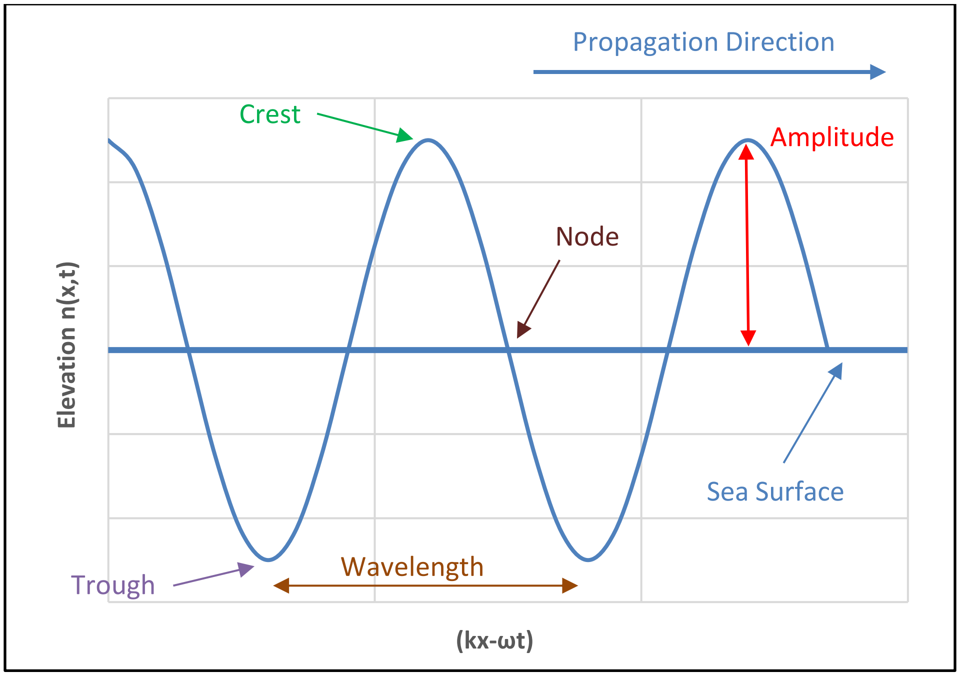

Figure 7. Sinusoidal Form of Regular Free Surface Wave in x-z Plane.

The wave number k is linked with the angular frequency by the dispersion equation, as explained in [4]:

$$k = \frac{\omega^2}{g}. \tag{21}$$

A wave moves with planar velocity, which has two components, horizontal $\overline{u}_P$, and vertical $\overline{w}_P$. The horizontal velocity component reaches the maximum value at the points of crests and troughs, while the vertical velocity component takes maximum values at the points of nodes [4].

2. Irregular Waves

In general conditions, we have waves with different amplitudes A_n and wavenumbers k_n, which are characterized as irregular or random waves [4]. Irregular waves can be described as a large number of superimposed regular waves [4]. Subsequently, the irregular motion of a ship can be described by its superposition of responses to regular waves. If we consider n-Number of regular waves, then the motion equation of irregular seaway is as described in [4]:

$$n(x,t) = \sum_{n=1}^{N} \Re\left\{ A_n \exp(-ik_n x + i\omega t) \right\}. \tag{22}$$

3. Waves Features

Sea waves have features that define their form and size. A wave crest is the highest part of the wave cycle above the water level, where the free sea surface displacement is at its maximum. Based on this feature, waves are characterized as long- and short-crested. Real seas are most likely characterized by short-crested rather than long-crested waves. The lowest part of a wave, the trough, is located between two crests. At this part, the free sea surface has the maximum displacement below the water level. The fetch is the horizontal distance over a free surface area where the wind acts in a constant direction and creates waves [4]. The fetch is a critical factor that affects the waves' size. An increase in the fetch results in the generation of increased wave height. In the case where sea wave spectra have reached a steady state condition with maximum wave size, independent of the fetch and the time within the wind has been applied on the sea surface, then the sea is called a fully developed sea [4]. When the sea waves are no longer exposed to the wind action field, they form a decaying sea [4].

C. SHIP DYNAMIC RESPONSES

1. Ship Motion—Degrees of Freedom

To determine a ship's motion resulting from waves' forces applied to its body, we make an assumption about the waves' nature, regarding them as the superposition of basic plane sinusoidal waves [4]. Then we can distinguish the ship's body motion in six ways: three translational and three rotational, both types with respect to the three main axes of the coordinate system (x, y, z). The three motions toward the axes' directions are called "surge," "sway," and "heave," while the three rotational motions around the axes' directions are called "roll," "pitch," and "yaw," respectively [4]. These motions are shown in Figure 8.

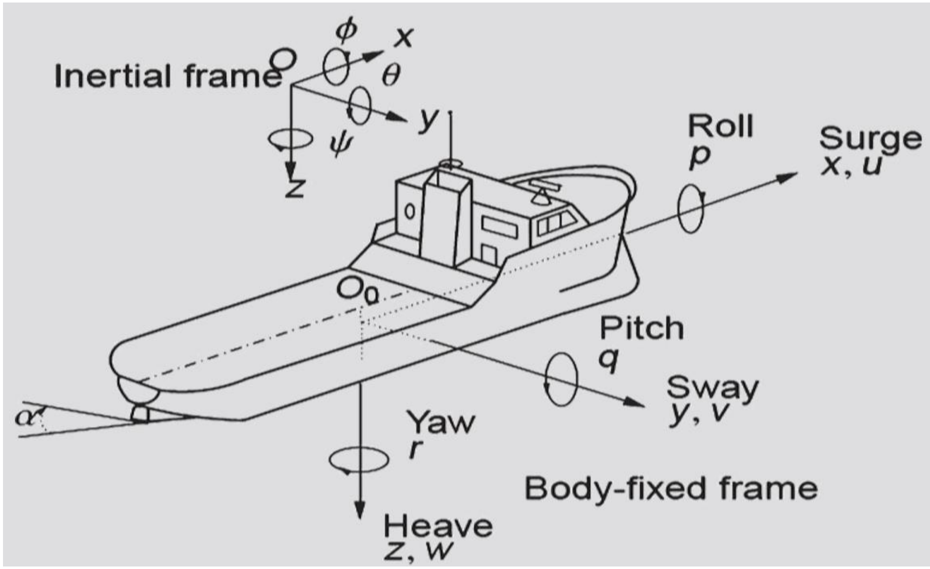

Figure 8. Degrees of Freedom of Ship Motion. Source: [5].

More specifically, the six degrees of freedom in a ship's motion are explained in *Ship Motions Program*:

Surge: The fore and aft rigid motion of the vessel in waves.

Sway: The ship's rigid-body lateral motion of the vessel in waves.

Heave: The vertical rigid-body motion of the vessel in waves.

Roll: The rigid-body rotational motion of the vessel in waves about the longitudinal axis.

Pitch: The rigid-body rotational motion of the vessel about the mid-ship axis.

Yaw: The rigid-body rotational motion of the vessel in waves about the vertical axis [7].

The determination of the ship's motion in those six ways requires the calculation of the harmonic responses of ship in terms of displacement (n_j), velocity ($\dot{n}_j$), and acceleration ($\ddot{n}_j$) as a result of the wave's applied forces, known as exciting forces [4]. The harmonic responses are given by these equations, as described in [4]:

$$n_j(t) = \bar{n}\exp(i\omega_e t)\ ,\ \ j = 1-6\ , \tag{23}$$

$$\dot{n}_j(t) = i\omega_e\bar{n}\exp(i\omega_e t)\ ,\ \ j = 1-6\ , \tag{24}$$

$$\ddot{n}_j(t) = -\omega_e^{\ 2}\bar{n}\exp(i\omega_e t)\ ,\ \ j = 1-6\ , \tag{25}$$

where $\bar{n}$ is the harm1onic response amplitude and ω_e refers to the ship motion frequency when the ship possesses nonzero linear velocity V_S, as noted in [4] :

$$\omega_e = \omega + \frac{\omega^2}{g}V_S\ . \tag{26}$$

A ship's motions are linked to the forces applied on the ship body as expressed by a set of six equations in the frequency domain, as explained in [4]:

$$\sum_{j=1}^{6} n_j[-\omega_e^2(M_{ij} + A_{ij}) + i\omega_e B_{ij} + C_{ij}] = A_O F_i\ , \tag{27}$$

F_i : The force per wave unit amplitude (exciting forces)

A_O : Wave amplitude

M_{ij} : Matrix of mass elements

A_{ij} : Matrix of force components in the i motion per unit of acceleration in the j motion (add mass forces)

B_{ij} : Matrix of force components in the i motion per unit of velocity in the j motion (damping forces)

C_{ij} : Matrix of restored forces and moments by the hydrostatic buoyancy effect on the ship (hydrostatic forces)

The solution of the equations (27) gives the six ways of ship motion as follows, according to [4]:

$$n_j = A_O\sum_{j=1}^{N}[D_{ij}]^{-1}F_i\ ,\ \ N = 1-6\ , \tag{28}$$

$[D_{ij}]^{-1}$: The system appropriate inverse matrix

An important magnitude derived by this equation is the Response Amplitude Operator (RAO), which relates the amplitude of the ship's motion to the amplitude of the incidental wave [4]. In other words, RAO indicates how much ship motion displacement is produced per unit of excitation force, and is given by the formula noted in [4]:

$$RAO = \frac{n_j}{A_O} = \sum_{j=1}^{N} [D_{ij}]^{-1} F_i \, , \; N = 1 - 6 \, . \tag{29}$$

2. Exciting Forces Coupling Effect

When applied concurrently on the ship's body, waves' exciting forces create combined effects on the ship's motion responses, known as coupling effects. For example, if the ship body undergoes heave and pitch due to applied exciting forces and the displacements related to those motion are n_3 and n_5, respectively, then we have to take into consideration both heave and pitch displacements to determine the absolute vertical displacement (ξ_{VA}) of a point sited in the distance x_L along the ship hull's length [4]. We can do this using the equation described in [4]:

$$\xi_{VA} = n_3 \pm x_L n_5 \, . \tag{30}$$

D. WAVES DESCRIPTION AND STATISTICAL ANALYSIS

Surface sea waves are characterized by the random nature of their height and phase. This randomness is due to the wind motion variations and the long distances at which the waves are propagating [4]. Therefore, the study of those waves becomes complicated, especially if we need to take into consideration all the different waves acting on a ship body. For that reason, the effective study of waves requires a probabilistic approach. For this probabilistic study to be feasible and sufficient, we must introduce some necessary assumptions about the waves' characteristics in space and time. The first assumption regards the wave as stationary, which means its statistical properties are the same for a few hours, so the wave does not change over time [4]. The second assumption is that the wave is homogeneous, which requires the statistical properties of the wave to be constant in a small sea area, so the wave does not change in space [4]. The third assumption is the ergodic wave, which means that the properties obtained by the study of a wave sample (sampling process) are the same as those of the whole wave [4].

Thus, to study random waves, we perform a Fourier analysis for each wave component (different amplitudes and frequencies) and plot the energy of these components against the frequency. The energy content of all wave components put in the same frequency diagram gives the seaway spectrum in the frequency domain. A plot of the seaway spectrum shows the total energy contained in the seaway, as well as the distribution of this energy in the frequency range [4]. The spectral density $S(\omega)$ in the frequency domain ω is shown in Figure 9.

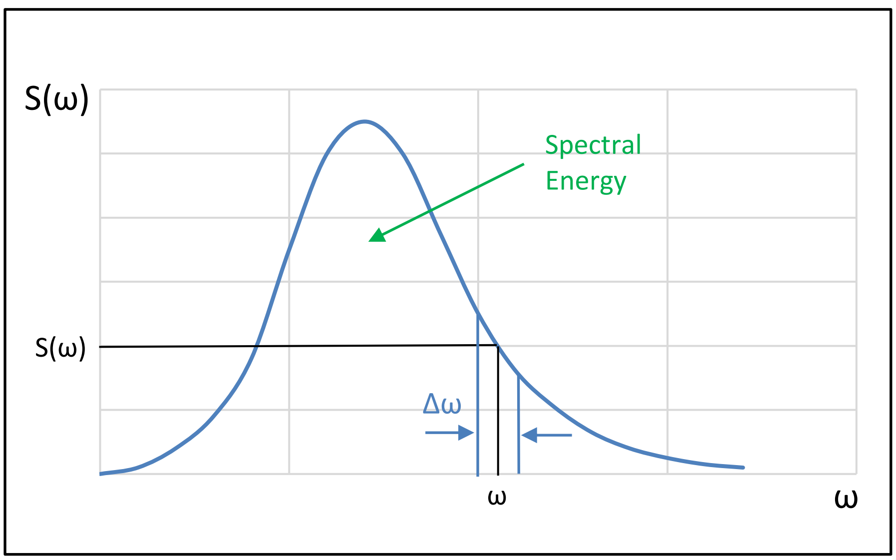

Figure 9. Spectral Density as Function of Frequency. Adapted from [4].

The wave energy is proportional to the mean amplitude squared [4]. In a very small frequency band $\Delta\omega$ the wave mean amplitude is related to the spectral density by the equation, as explained in [4]:

$$\bar{h}_o^2 = S(\omega)\Delta(\omega)\,. \tag{31}$$

Using the aforementioned assumptions about the wave nature, this equation can be extended to the whole examined sea area by the relationship as noted in [4]:

$$\bar{h}_o^2(\omega) = \int_0^\infty S(\omega)d\omega \,. \tag{32}$$

After obtaining the wave's mean high using the spectral density, it is necessary to identify the distribution of the wave heights around the mean value. To do that, we assume that seaway is divided into narrow bandwidths of waves, which carry the sea spectra energy. Then, we conduct statistical analysis for those waves in order to determine their significant values [4]. This statistical analysis uses Rayleigh distribution, which we assume waves follow. The function of probability density of this statistical distribution is given by the formula explained in [4], [6]:

$$p(\xi) = \xi \exp(-\xi^2 / 2) \,. \tag{33}$$

This is a normalized function, since the variable ξ is normalized with respect to the total spectrum energy m_o [4]. We also call m_o the "zero moment," which is the $S(\omega)$ integration for all the frequencies of the spectrum and is equal to the spectrum's total energy, as explained in [4]:

$$m_o = \int_0^\infty S(\omega)d(\omega) \,. \tag{34}$$

The variable ξ expresses the normalized wave amplitude and is given by the equation noted in [4]:

$$\xi = \frac{\mathrm{A}_O}{\sqrt{m_o}} \,. \tag{35}$$

Using the probability density function, we can derive two useful magnitudes related to the wave heights: the average height and the significant height. Note that the wave height is twice the wave amplitude A_O [4]. The average wave height is given by the relationship, as described in [4]:

$$\bar{H} = 2\int_0^\infty Ap(\xi)d\xi = 2.5(m_o)^{1/2}. \tag{36}$$

The significant height represents the average value of 30% of the highest waves and is derived by the expression, as noted in [4]:

$$H_{1/3} = 4(m_o)^{1/2}. \tag{37}$$

Some other significant parameters for the wave spectra description are the average frequency and the modal frequency. The average frequency, ω_z, gives the number of times the wave passes from zero amplitude toward positive direction [4], and the modal frequency, ω_m, represents the frequency value when wave spectrum reaches its maximum value [4]. Since sea spectrum is a probability distribution function, modal frequency represents the most possible values in the frequency distribution. Consequently, the average and modal periods are derived by the formulas, as explained in [4]:

$$T_z = \frac{2\pi}{\omega_z}, \tag{38}$$

$$T_m = \frac{2\pi}{\omega_m}. \tag{39}$$

By describing the wave spectra with significant heights and average periods, we simplify the calculations and enhance the model-predicting capabilities, as compared to the cases where we base the predictions on parameters such as wind velocity [4]. Furthermore, significant heights and average periods are more consistent with the empirical observations associated with those values.

E. SEA SPECTRA MODELS

To model random, wind-generated waves, we use wave spectra that are functions of a wave's parameters and express the wave's spectral energy against the wave's frequency. The function parameters vary with each model's assumptions and characteristics. Those parameters depend on some physical magnitudes, such as the wind speed and the time during which the wind is acting on the sea surface [4]. Typical wave spectra of this category are discussed in the following subsections.

1. Pierson-Moskowitz Spectrum Model

A very common and useful spectrum model often used to identify spectral density of long-crested waves is the Pierson-Moskowitz. This is a one-parameter spectrum, which is appropriate to describe the wave's energy distribution in fully developed seas [4]. The Pierson-Moskowitz spectrum formulation is given here, as described in [4], [6]:

$$S(\omega) = \frac{ag}{\omega^5}\exp[-\beta_P\left(\frac{g}{V_K\omega}\right)^4], \tag{40}$$

$S(\omega)$: Spectral energy in m^2sec

$a = 8.1\times10^{-3}$

$\beta_P = 0.74$

g : Gravity acceleration = 9.81 m/s^2

ω : Wave frequency in rad/sec

V_K : Wind speed in m/s

Using the wave spectrum formula, the significant height and modal frequency of the Pierson-Moskowitz model are derived:

Significant height of the wave as explained in [4]:

$$H_{1/3} = 4(m_o)^{1/2} = 0.2092\frac{{V_K}^2}{g}, \tag{41}$$

Modal frequency of the spectrum as explained in [4]:

$$\omega_m = 0.877\frac{g}{V_K}. \tag{42}$$

The Pierson-Moskowitz spectrum model is more appropriate in oceanographic studies, which are characterized by long periods of steady winds

[4]. A typical diagram of this model for fully developed sea and different significant heights from $H_{1/3}$ = 1 to 10 meters is shown in Figure 10.

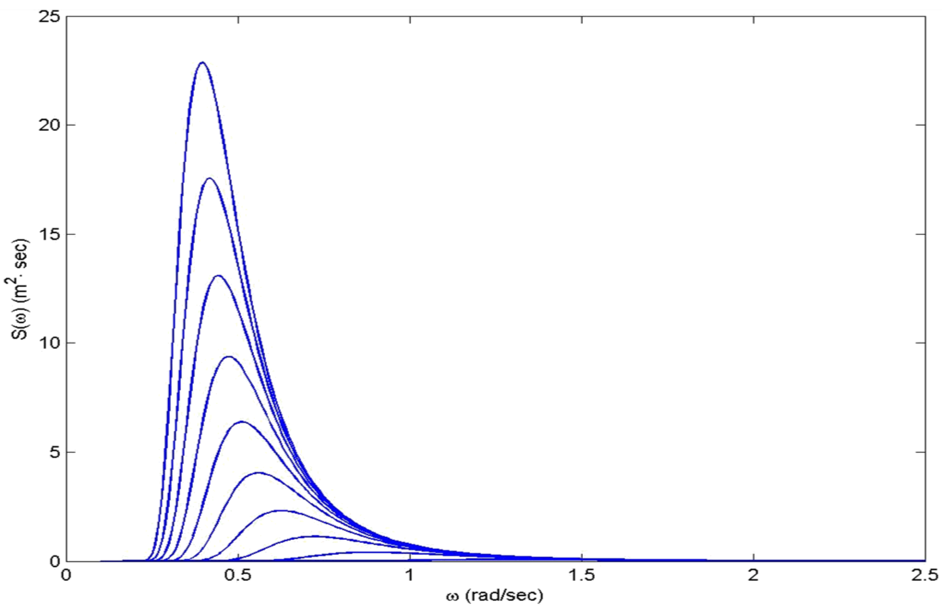

Figure 10. Pierson-Moskowitz Wave Spectrum ($H_{1/3}$=1 to 10 m)

2. Bretschneider Spectrum Model

To model sea wave spectra, the Bretschneider spectrum model is used as well. This is a two-parameter model: the significant wave height and the modal frequency represent developing to decaying seas [4]. The model provides results that are very close to the visual observation [4]. This model is expressed by the formula described in [8], [9]:

$$S(\omega) = \frac{1.25}{4} \frac{\omega_m^4}{\omega^5} \zeta^2 e^{-1.25\left(\frac{\omega_m}{\omega}\right)^4}, \tag{43}$$

$S(\omega)$: Spectral energy in m^2sec

ω : Wave frequency in rad/sec

ω_m : Modal frequency in rad/sec

ζ : Significant wave height in m

The zero moment of the spectrum is as explained [8]:

$$m_o = \int_0^\infty S(\omega) d(\omega) = \left(\frac{\zeta}{4}\right)^2 . \tag{44}$$

Then, using the previous expression the significant parameters of the model can be defined:

Significant height of the wave, as explained in [8]:

$$H_{1/3} = 4(m_o)^{1/2} = \zeta , \tag{45}$$

Modal frequency of the spectrum, as explained in [8]:

$$\omega_m = 0.4\sqrt{\frac{g}{\zeta}} . \tag{46}$$

Experimental data have shown that the Bretschneider spectrum model parameters' predictions can be related with the visual observations for the significant wave height H_υ and zero point period T_υ (the time between two consecutive zero spectra points) by the empirical relations as noted in [4], [6]:

$$H_{1/3} = 1.68 H_u^{0.75} , \tag{47}$$

$$\omega_m = \frac{5.44}{T_u^{0.96}} . \tag{48}$$

The Bretschneider model is also appropriate for seas with changing wind conditions [4]. An example of the Bretschneider spectrum for fixed modal period and varying significant wave heights from 1 to 10 meters is provided by Figure 11.

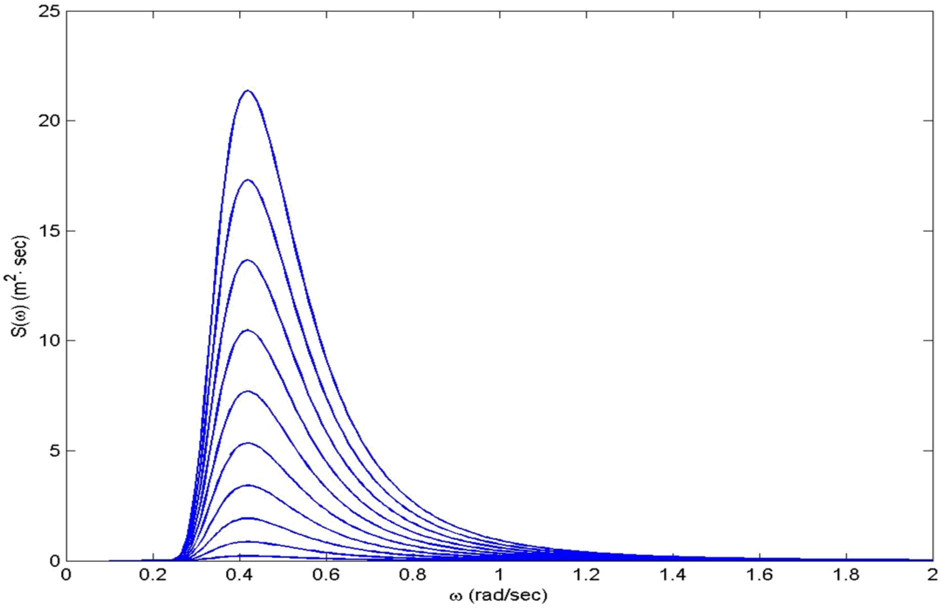

Figure 11. Bretschneider Wave Spectrum ($H_{1/3}$=1 to 10 m)

3. JONSWAP Spectrum Model

The Joint North Sea Wave Project (JONSWAP) is a two-parameter wave spectrum model defined by the wind speed and the fetch, and widely used in offshore industry [4]. It is equivalent to the Pierson-Moskowitz model for limited fetch wave conditions and is very effective for representing non-fully developed seas characterized by limited fetch waves [4]. It is developed based on data from the JONSWAP Observations and is capable of modeling single-peaked wave spectra. The formulation of JONSWAP spectrum is similar to that of Pierson-Moskowitz, and is supplemented by the peak amplitude factor γ, which is a function of wave frequency [9]. Therefore, the Pierson-Moskowitz spectrum model can be seen as a variant of the JONSWAP. With the appropriate adjustments of the peak factor, the JONSWAP spectrum can cover a variety of other spectra, such as the Bretschneider spectrum and swells. The mathematical form of the JONSWAP spectrum is given by the formula as described in [8]:

$$S(\omega) = \frac{ag^2}{\omega^5}\exp[-\beta_J \frac{\omega_p^4}{\omega^4}]\gamma^r , \tag{49}$$

$$r = \exp[\frac{-(\omega - \omega_p)^2}{2\sigma^2 \omega_p^2}], \tag{50}$$

$S(\omega)$: Spectral energy in m^{2}sec

$a = 8.1 \times 10^{-3}$

$\beta_J = 1.25$

g : Gravity acceleration = 9.81 m/s^2

ω : Wave frequency in rad/sec

ω_p : Peak wave frequency in rad/sec

$\gamma = 3.3$ (Peak factor)

$\sigma = 0.07, \omega \le \omega_p$

$\sigma = 0.09, \omega > \omega_p$

A graphical presentation of the JONSWAP spectrum for certain fetch and varying wind speeds from 1 to 30 meters per second is given in Figure 12.

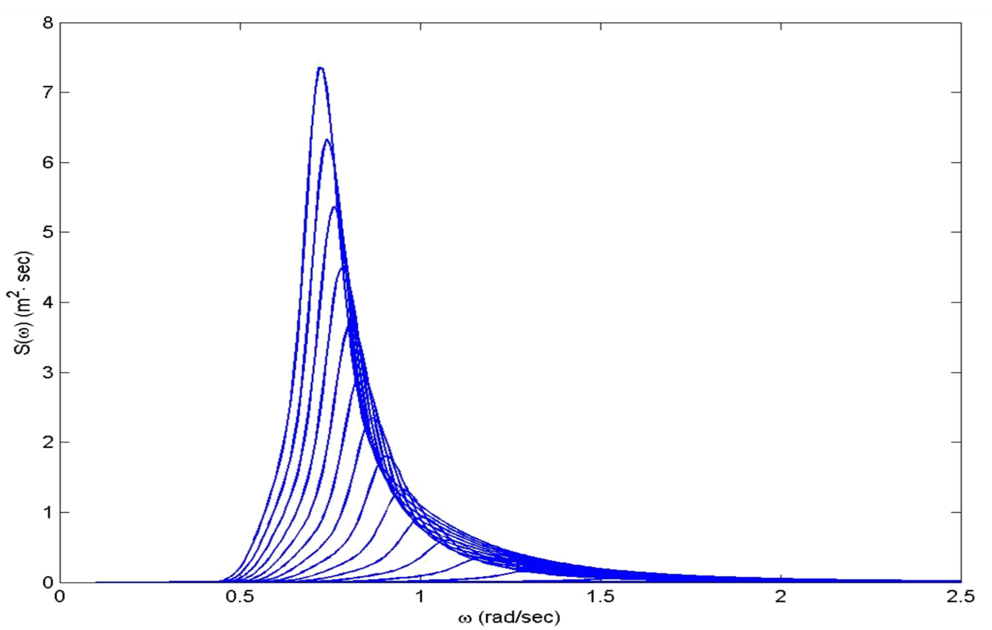

Figure 12. JONSWAP Wave Spectrum (V_k=1 to 30 m/s)

4. Ochi-Hubble Spectrum Model

The Ochi-Hubble is a six-parameter spectrum derived by superimposing two simple three-parameter spectra, each of which is an extension of the Bretschneider spectrum [10]. Controlled by significant height and the modal frequency like the Bretschneider spectrum, the Ochi-Hubble spectrum has a third consideration, the shape parameter [4]. This spectrum is very useful in cases where the experimental data require a more accurate fitting with the spectra models [4]. The reason for that is that this spectrum incorporates one more parameter; hence, it provides more flexible description of the sea waves. More specifically, this spectrum is more appropriate in describing two-peaked waves and combined sea states that include both swell and local wind-generated waves [10]. By superimposing two three-parameter Ochi spectra, one for the swell and the other for the local wind wave, the model ends up with a combined six-parameter wave spectrum [10]. These characteristics enhance the model's capability to fit with more complex actual wave spectra.

The critical extra parameter of this spectrum is the shape parameter, which, mathematically, is controlled by the variable λ.Technically, this variable determines the width of the spectra and usually takes values in the range of 0 to 10 ft. (0 to 3.048 m) [10]. The larger the λ parameter, the sharper the spectral shape and the higher the peak. The formulation of this spectra is as described in [9], [10]:

$$S(\omega) = \frac{1}{4}\frac{\left(\frac{4\lambda+1}{4}\omega_m^4\right)^{\lambda}}{\Gamma(\lambda)}\frac{\zeta^2}{\omega^{4\lambda+1}}e^{-\left(\frac{4\lambda+1}{4}\right)\left(\frac{\omega_m}{\omega}\right)^4}, \tag{51}$$

$S(\omega)$: Spectral energy in m^2sec

ω : Wave frequency in rad/sec

ω_m : Modal frequency in rad/sec

ζ : Significant wave height in m

λ : Shape parameter

$\Gamma(\lambda)$: Gamma probability function

An example of the six-parameter Ochi-Hubble wave spectra for certain significant wave height, modal frequency, and varying shape parameters from 0 to 1 ft. is given in Figure 13.

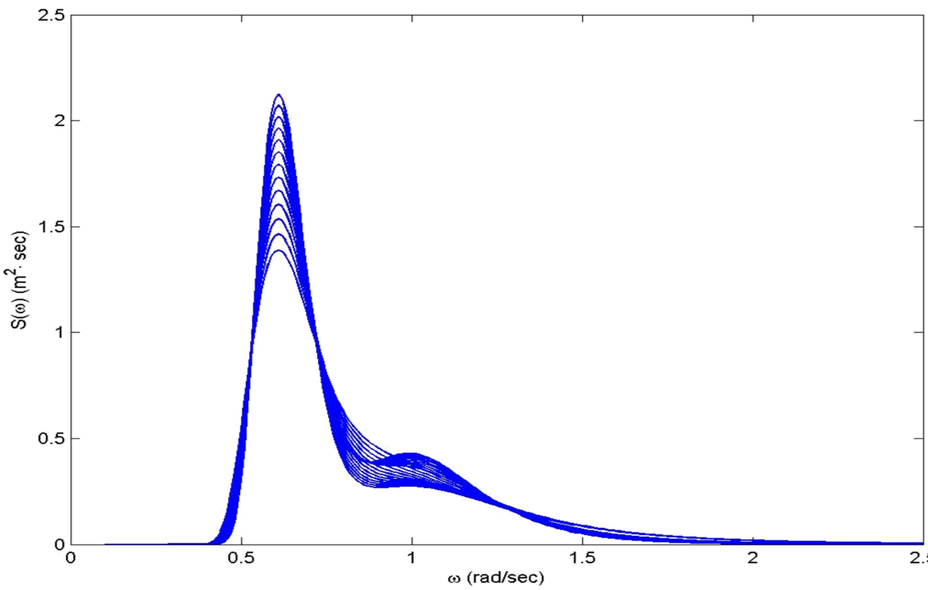

Figure 13. Ochi-Hubble Wave Spectrum (λ = 0 to 1 ft)

F. SHIP MOTION IN SEAWAY

After selecting the model for the seaway spectrum, we can proceed to the identification of the ship's motion spectrum. Ship motion occurs in response to the wave motion. Statistical properties of ship response spectra are the same as those of the wave spectra, so once we determine wave spectrum we can determine the ship response spectrum [4]. More specifically, the ship response spectrum $S_R(\omega)$ corresponds to the seaway spectrum $S(\omega)$ by the square of RAO, which is a function of frequency ω, as described in [4]:

$$S_R(\omega) = |RAO(\omega)|^2 \, S(\omega) \,. \tag{52}$$

The function $|RAO(\omega)|^2$, or transfer function, facilitates the translation from the seaway spectrum to the ship response spectrum and yields quite accurate results for both regular and irregular waves [4].

G. SHIP DESIGNING FOR SEAKEEPING

Ship designing and selection of stability criteria have to take into consideration seakeeping behavior. These seakeeping considerations are divided into three main domains: habitability, operability, and survivability [4]. Habitability ensures proper seakeeping conditions for the crew in order to avoid the reduction of its performance onboard; operability is the ability of the system ship-crew to perform its designated mission under a certain environment; and survivability is the ability of the ship to withstand an environment of extreme conditions [4]. All those domains are highly affected by seakeeping parameters such as the values of ship displacement, velocities, and accelerations in the six degrees of motion mentioned earlier.

Thus, to determine the dynamic stability criteria for a ship, we first need to identify its operational environment, which is described by the sea spectrum. According to the previous analysis, we only need to select the significant height of the waves and the modal period. Then, it is necessary to establish the operational seakeeping requirements that maximize the ship’s operability in the particular mission. After that, we set limiting values for the seakeeping parameters so that the seakeeping requirements can be satisfied. For example, we set limiting values for the roll and pitch in terms of maximum values.

The next step is to produce diagrams that describe the ship’s seakeeping performance in terms of parameter values, such as roll angle versus heading angles. Finally, once we have set our acceptable parameters’ values, we can evaluate the seakeeping performance and determine the ship’s operational limits.

IV. STANDARD SHIP MOTION PROGRAM

A. INTRODUCTION

The Standard Ship Motion Program (SMP) provides simulations and predictions of a ship's motions in terms of displacement, velocity, and acceleration when the ship is subjected to a modeled sea environment. This environment is described by seaway parameters that are incorporated in the program. The program is capable of providing ship's motion results for both regular and irregular sea waves by utilizing the appropriate wave spectra [11]. Aside from the ship's absolute body motions, this program yields relative motion results for certain locations of the ship, as well as the generated bending moments in those locations [11]. All these results can be obtained for a ship's various speed and heading values.

B. CAPABILITIES

More specifically, as described in *Ship Motions Program* [7] and *SMP95: Standard Ship Motions Program User Manual* [11], the program is capable of delivering results as follows:

- Rigid body motions: These are the motion responses of the ship in terms of displacement, velocity, and acceleration for the six degrees of freedom.
- Motions at a point: These are the motion responses at specific points of the ship in terms of displacement, velocity, and acceleration in the longitudinal, transverse, and vertical directions.
- Relative motions at a point: These include the motion responses at specific points of the ship in terms of displacement, velocity, and acceleration in the longitudinal, transverse, and vertical directions. These motion responses are relative to certain ship locations.
- Structural loads: These are the vertical bending moments in every ship station due to the wave-exciting forces.

- Rigid body Slamming Motions: Probability and frequency of slamming and submerging at the points where relative motions are determined.

C. ASSUMPTIONS

To generate the ship's motion responses, the program incorporates assumptions associated with ship geometry, sea state conditions, and ship stability parameters. Once a ship hull model is imported in terms of offset coordinates, the program uses interpolation to create a smoother fit to offset points [7]. The coordinate system origin is located at the point of intersection between the base line (BL), forward perpendicular, and center line (CL) [7]. The X axis coordinate is then measured as positive from the forward to the afterward perpendicular [7]. Therefore, the ship stations are measured by assigning the number 0 to the forward perpendicular station and the number 20 to the afterward perpendicular station [7]. The Y axis is measured from the CL with positive values to the port [7]. The Z axis is measured from the BL with positive Z upwards [7]. Additionally, the program assumes hull symmetry at the center line [7]. The program also uses default values for water mass density (1,025.820 kg/m^3), acceleration of gravity (9.806 m/s^2), and kinematic viscosity (1.19E-06 m^2/s^2) [7].

Program outputs have by default certain conventional sea headings. The SMP considers 0 degrees as head seas, 90 degrees as starboard seas, and 180 degrees as following seas [7]. By default, the program uses the two parameters of the Bretschneider sea spectrum model, but JONSWAP and Ochi-Hubble spectra are also available. For POSSE imported files, the program initially sets the ship drafts equal to the half depth [7]. Based on the imported ship model, SMP calculates its own GM value [7]; if this value is negative, the program crashes [7]. To avoid this inconvenience, the we must select the option "adjust KG at runtime to make SMP GM=GMt" in advance [7]. The SMP treats weights as lumped weights applied on each ship station in order to have the same loading condition as the POSSE program [7]. Consequently, the SMP treats the KG as the vertical position of the center of the entire ship lumped weight [7].

D. STRUCTURE

The SMP consists of two distinct processes: the pre-processor part, which accepts the input values, and the post-processor part, which provides the program outputs. The SMP contains two subprograms: the SMP Regular Waves (SMPRGW), which executes the regular wave computations, and the SMP Irregular Waves (SMPIRGW), which performs the irregular wave calculations [11]. The SMP models sea waves by incorporating the default two-parameter Bretschneider spectrum, the three-parameter JONSWAP spectrum, and the six-parameter Ochi-Hubble spectrum. The program uses the parameters of significant wave height and modal period in order to define the spectra outputs. All these spectra can be used to provide results for both long- and short-crested irregular seas.

Based on the selected sea wave spectrum, the program generates the RAO and the Transfer Functions (TF). These are all statistical values and are derived by the Rayleigh probability distribution, which the program incorporates [7]. Then, once these statistical values are derived by the selected spectra models, they are applicable for the SMP to generate all of a ship's response RAOs. Vertical ship response RAOs—such as heave, surge, and pitch—are linear and independent of the sea state [11]. Lateral ship response RAOs—such as sway, roll and yaw—are non-linear and dependent on the sea state [11]. The basic high-level equation that describes what the SMP executes in order to predict the ship motions is as described in [7]:

$$\textit{(Sea Spectra) x (Transfer Function) = (Ship Response Spectra)}. \quad (53)$$

Schematically, the corresponding logical sequence of these SMP steps is shown in Figure 14.

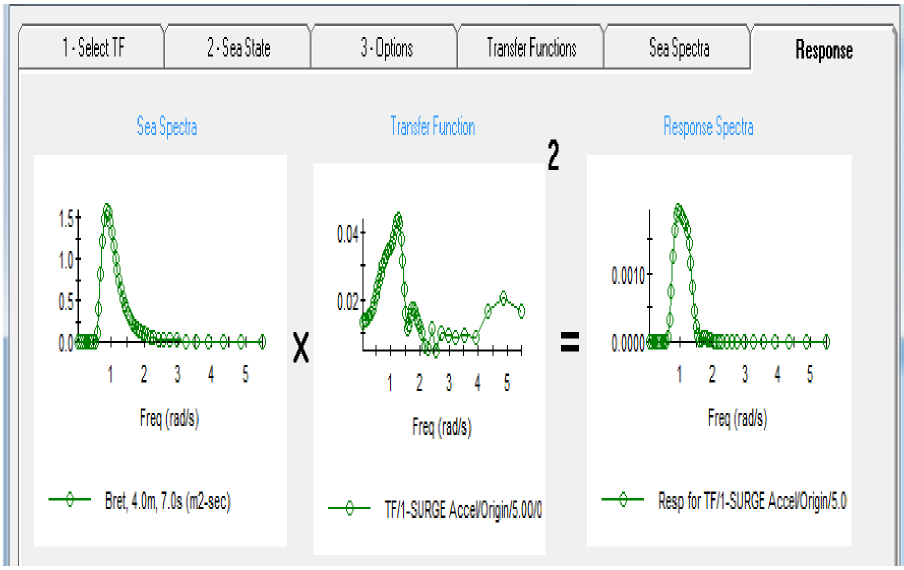

Figure 14. SMP Ship's Responses Calculator

E. INPUTS

Residing in the pre-processor part of the SMP, the program inputs are categorized into eight major data divisions: the general, hull form, appendages, loading, sea state, responses, motion points, and relative points. Those data divisions are shown in Figure 15.

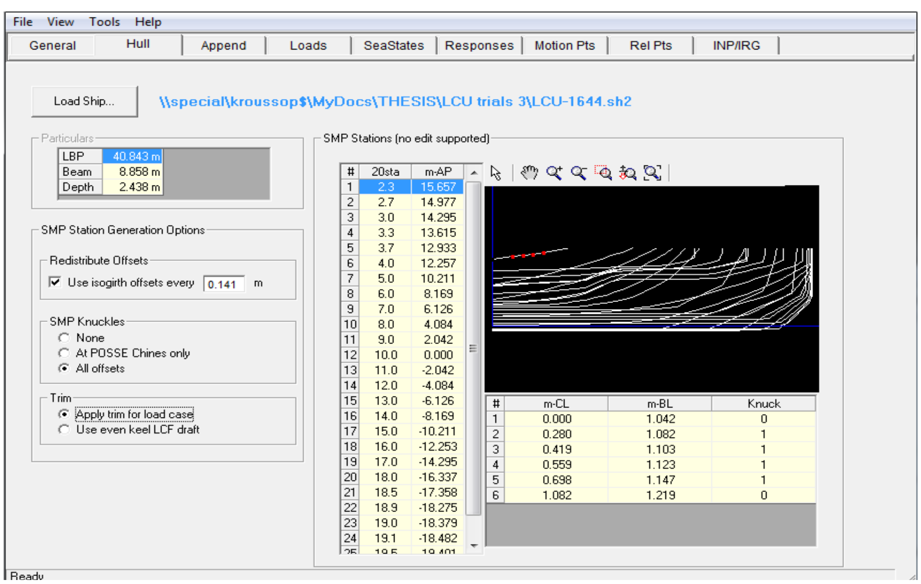

Figure 15. SMP Data Input Modules

In the general data, we can primarily select ship speeds. Multiple speeds can be input and separated by commas. In the hull data, the program accepts the loading of an imported POSSE ship file. This file contains ship hull offsets and, once the loading is completed, the SMP defines the hull geometry. Certain values of this geometry, such as Length, Beam, and Depth, cannot be changed [7]. In the appendages data inputs, a variety of additions like rudders, stability fins, propellers, sonar domes, and others can be modeled and imported into the ship's hull [7]. In the loading data, the SMP defines the current loading conditions of the ship and provides the parameters for the selection of different loading cases.

The SMP defines its own GM for the calculations and takes into account the free surface correction [7]. To ensure that the GM calculated by the SMP is greater than 0 and also the same as the one from the POSSE model, we should select the option "adjust KG at runtime to make SMP GM=GMt" during the input process [7]. In the sea state input section, the program offers the selection of the wave spectrum and the parameters of significant wave height and modal wave period associated with each selected spectrum. We can set multiple modal period values for each specific, significant height. In the responses module, the program requires us to select the statistic for the SMP response output. In the motion points division, we define the points for the motion outputs, such as displacement or velocity, at a specific point. In the relative points division, the program permits the determination of the points for the relative motion output such as the slamming of the bow.

F. OUTPUTS

The SMP produces a large number of output files, as well as visualized ship motion results [11]. These results, located in the post-processing part of the SMP, are divided into five modules: motion transfer function, load transfer function, events, responses, and load extreme, as shown in Figure 16.

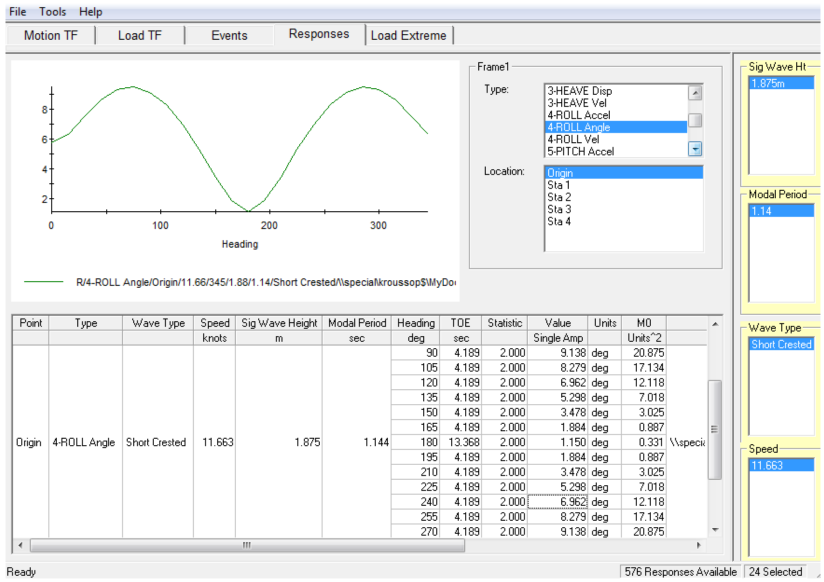

Figure 16. SMP Output Modules

The Motion-TF tab provides the transfer function for the six degrees of motion in terms of displacement, velocity, and acceleration [7]. These results are generated from the RAO output file that the SMP produces [7]. We can obtain these transfer functions for different ship speeds and headings. The Load-TF tab provides the load RAO results, which are generated in the SMP output file and give the loading conditions in every ship station as a result of the application of the selected wave spectra [7]. The Events module tab provides the probability of slamming or submerging of the ship in certain sea state conditions [7]. The Responses tab provides the ship body responses spectra against ship headings for the six degrees of freedom. These responses are obtained in terms of displacement, velocity, and acceleration, and for certain values of significant wave height, modal period, and wave type (long- or short-crested). The SMP permits the observation of ship responses for different ship speeds. The Load Extreme module tab yields the maximum vertical bending moments for each station of the ship, due to wave loading in graphical and tabular form. These loads are dependent on the parameters of significant wave height and ship time exposure in the wave [7]. The SMP also provides the POSSE equivalent static wave height, which generates the same loading results [7]. These bending moment results can be observed for different values of ship speed and headings.

G. POSSE INTEGRATION

1. Capabilities

Incorporating SMP, a Towing analysis program (Tow), and a Rapid analysis program (Rapid), POSSE software provides support for salvage response engineers planning free-floating or stranded ship operations [12]. Based on offsets as its main input, POSSE software predicts intact and salvage ships' static stability strengths [12]. The program creates and utilizes the ship model as defined by the hull and compartments, including stations and tanks. It uses the same assumptions as the SMP [12]. POSSE capabilities include performing structural calculations and outflow analyses of flooding, stranding, tide cycles, dry-dock, and heavy lifts [12]. These capabilities are used for determination of the ship's post-damage structural properties, evaluation of the ship's ultimate strength and static stability, and deriving the ship's standing, dry-dock, ballasting, and heavy lift plans.

2. Static Stability

The POSSE program allows changing the ship's loading conditions by providing the options of weight additions and adjustments of various tank capacities.[2] This capability facilitates analyses of multiple operational scenarios and loading cases, as well as evaluation of the ship's associated static stability.

In order to evaluate the ship's static stability, the program calculates the righting arm (GZ) curves corresponding to various loading conditions. After performing the required adjustments for added weight and free-surface effects, the program develops the GZ curve against ship's rolling angle θ; this curve corresponds to each particular ship's displacement. If the program embeds certain

2 E.g., oil, fuel, water, and ballast water

GZ criteria,[3] it compares them to the resulting GZ curves and provides individual assessment for static stability of the ship in terms “pass” or “fail.”

3. Integration

The SMP is integrated with the POSSE and, once the pre-processing SMP runs the POSSE-modeled input ship file, the POSSE provides the static stability results for the particular ship. Meanwhile the post-processing part of the SMP provides the dynamic stability results. Ship loading conditions could be modified in the POSSE and the resulting modeled ship file can then be imported to the SMP for obtaining the dynamic stability corresponding to the changed loading conditions.

3 These criteria include wind action and rolling, lifting heavy weights over the side, crowding of passengers to one side, high speed turning, and topside icing.

V. SIMULATION RESULTS

A. LOADING CASES

We decided to conduct stability simulations for three significant loading cases, which corresponded to some of the most common operational conditions of the LCU. Based on the LCU's displacement, these cases are the lightship, lightship carrying half the cargo deadweight, and lightship carrying a full cargo deadweight load.

1. Lightship

In this case, we modeled the craft in order to simulate the lightship's displacement, which includes diesel oil, fresh water, ballast water, and the 16-member crew. To create this condition, we loaded the craft model into the POSSE software.[4] We made the general assumption of loading the ship's tanks to about 85% of their maximum capacities, which is a realistic representation of the LCU's typical operational conditions. Located on each side about mid-ship in the longitudinal direction, the LCU has two diesel oil tanks with capacities of 7 (port) and 8 (starboard) metric tons (MT). To ensure the ship's heeling angle is closer to 0 degrees, we loaded the port diesel tank to 70% of capacity, and the starboard diesel tank to 100% of capacity. The diesel oil tank loading condition is presented in Figure 17.

[4] This model includes only the hull geometry of the ship; therefore, the additional loads have to be imported manually.

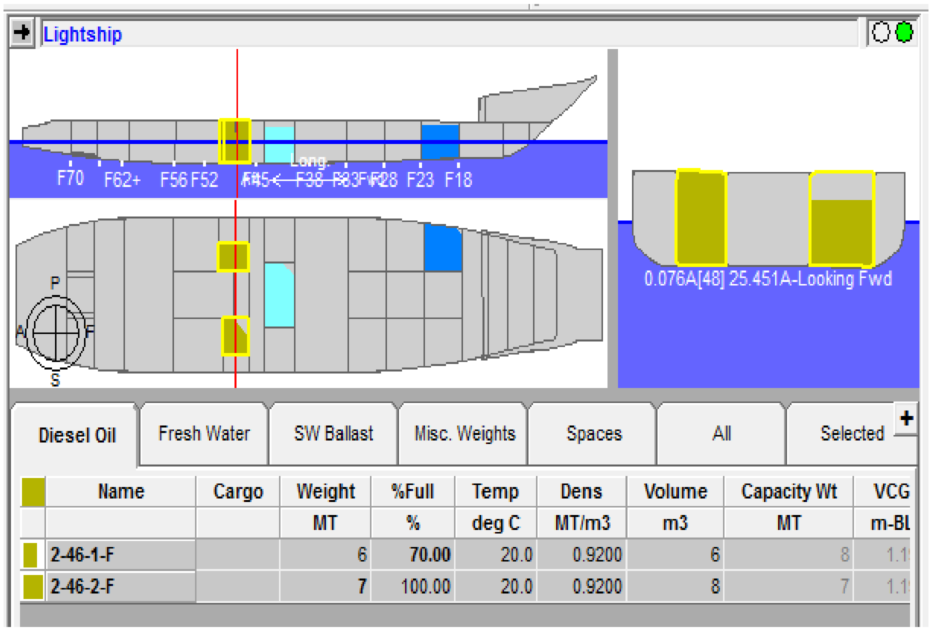

Figure 17. LCU Diesel Oil Tanks Loading Condition

The LCU has one fresh water tank located at mid-ship and at centerline, with a capacity of 19 MT. We loaded this tank to 85% of maximum capacity, which equals 16 MT. This loading condition appears in Figure 18.

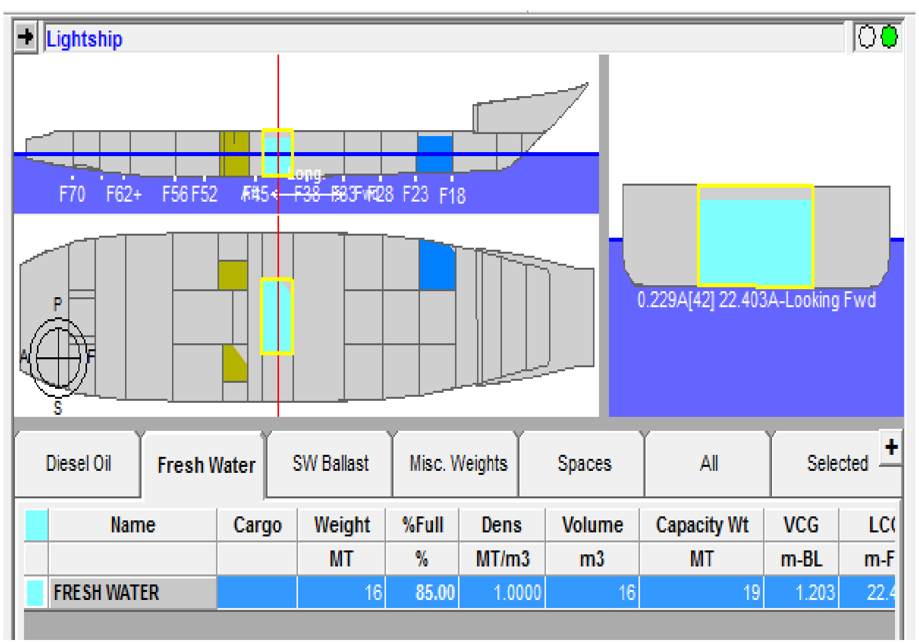

Figure 18. LCU Fresh Water Tank Loading Condition

The LCU has four ballast tanks. Three of them are located close to the ship's bow: one each on the port and on the starboard side with individual capacities of 13 MT, and one at mid-ship with a capacity of 14 MT. The fourth tank is located near the stern and the ship's center line with a capacity of 10 MT. To compensate for the ship's heeling angle, we only loaded the forward port ballast tank to 85% of its maximum capacity (11 MT). The ballast tank loading condition is shown in Figure 19.

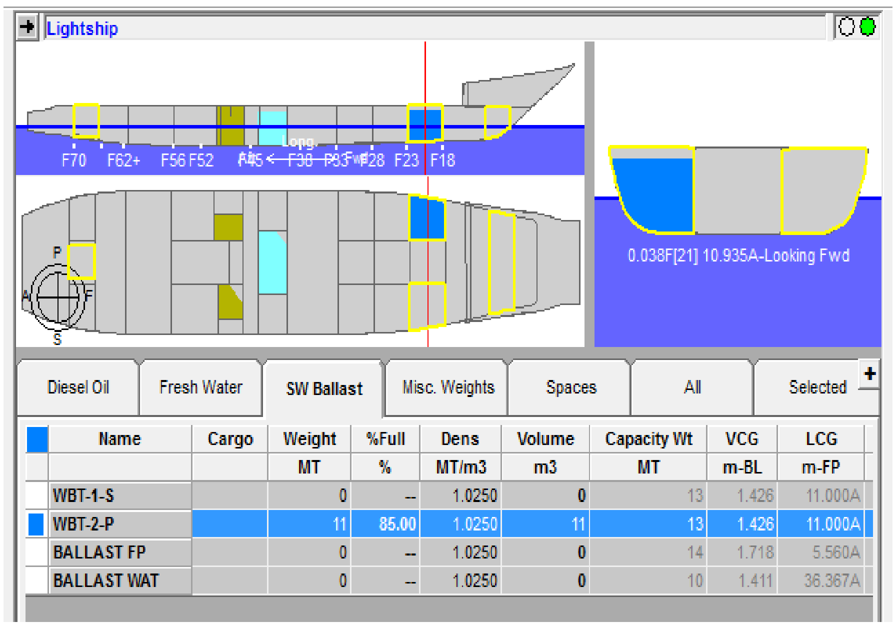

Figure 19. LCU Ballast Tanks Loading Condition

The LCU operates with a 16-member crew. Under the assumption that each individual weighs about 75 kg, the total added weight was 1.2 MT. POSSE treated this load as lumped load and allowed the user to decide its location. We made assumptions about the crew lumped load location in terms of LCG_W, TCG_W, and VCG_W. We chose to locate the crew lumped load 20.422 m after forward perpendicular (LCG_W) and 3 m to port with respect to the center line (TCG_W). Making the assumption that the center of gravity for the group of crew members stands 1.2 m above the ground and knowing the distance between ship's keel and deck to be 2.44 m, we selected the vertical location of the crew load to be 3.64 m with respect to ship’s base line (VCG_W). The crew load condition is shown in Figure 20.

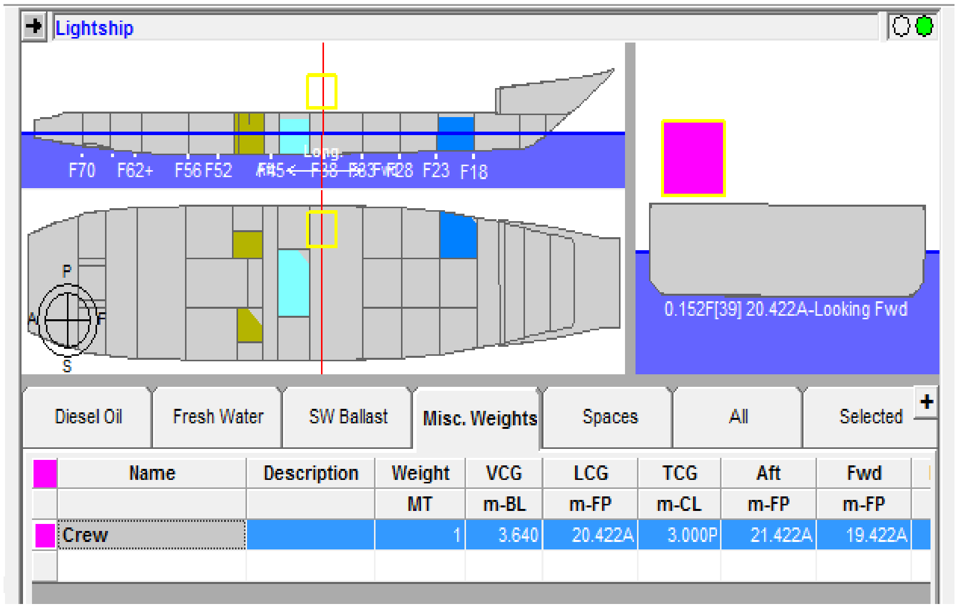

Figure 20. Crew Loading Condition

The lightship loading case resulted in the following ship’s stability characteristics:

- Total ship’s Displacement (Δ): 257 MT
- Forward Draft (FP) : 1.193 m
- Afterward Draft (AP): 1.078 m
- Mid-ship Draft (MS): 1.136 m
- Trim: 0.115 m forward
- GM_t: 5.423 m
- VCG: 1.639 m
- LCG: 22.654 m afterward from forward perpendicular
- TCG: 0.028 m starboard from center line
- LCF: 23.645 m afterward from forward perpendicular
- LCB: 22.948 m afterward from forward perpendicular
- Heeling Angle (θ) : 0.31 degrees to starboard

2. LCU Carrying Half Cargo Deadweight Load

The next relevant loading case is the LCU carrying half the cargo deadweight load. The cargo load is modeled as a geometric volume that has a length of approximately 10 m, a width of 3.5 m, a height of 2.5 m, and a weight of 57.15 MT. We assume that the center of gravity of this volume is located in the middle of the length and width, and at one-third of its height (0.813 m). We put the representative volume 25 m after forward perpendicular (LCG_W=25 m), 3.25 m above ship's base line (VCG_W), and at the ship's center line (TCG_W = 0 m). The half cargo deadweight loading case is then the lightship case with the added lumped mass at the location described previously. This loading case is shown in Figure 21.

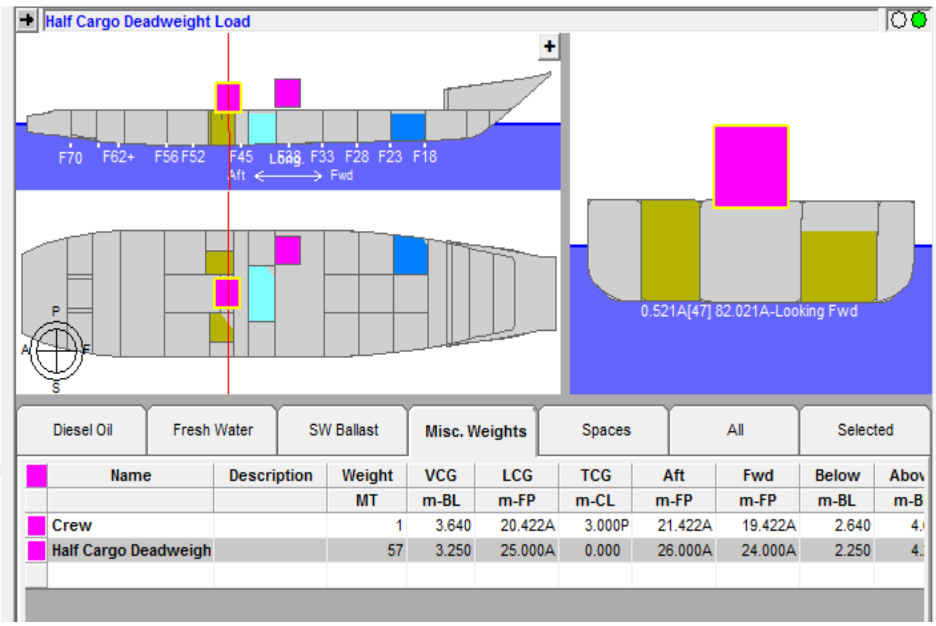

Name	Description	Weight	VCG	LCG	TCG	Aft	Fwd	Below	Abov
		MT	m-BL	m-FP	m-CL	m-FP	m-FP	m-BL	m-B
Crew		1	3.640	20.422A	3.000P	21.422A	19.422A	2.640	4.
Half Cargo Deadweigh		57	3.250	25.000A	0.000	26.000A	24.000A	2.250	4.

Figure 21. Lightship with Half Cargo Deadweight Loading Condition

The Lightship with half cargo deadweight loading case results in the following ship's stability characteristics:

- Δ: 314 MT
- FP: 1.314 m
- AP: 1.325 m
- MS: 1.320 m
- Trim: 0.011 m afterward
- GM_t: 4.124 m
- VCG: 1.933 m
- LCG: 23.081 m afterward from forward perpendicular
- TCG: 0.023 m starboard from center line
- LCF: 23.399 m afterward from forward perpendicular
- LCB: 23.056 m afterward from forward perpendicular
- θ: 0.32 degrees to the starboard

3. LCU Carrying Full Cargo Deadweight Load

The third loading case examined in this study is the LCU carrying a full cargo deadweight load. According to the dimensions, weight, and the assumption referred to previously used regarding typical equipment transported aboard the LCU, we selected to arrange both cargo volumes one behind the other on the ship's center line. The front lumped weight is located 17 m after ship's forward perpendicular (LCG_W) and at the center line (TCG_W = 0 m), while the second is positioned further behind, having its lumped weight 32 m after forward perpendicular and at the center line (TCG_W = 0 m). Both of these representative masses' centers of gravity are located 3.25 m above the ship's baseline (VCG_W). This loading case is presented in Figure 22.

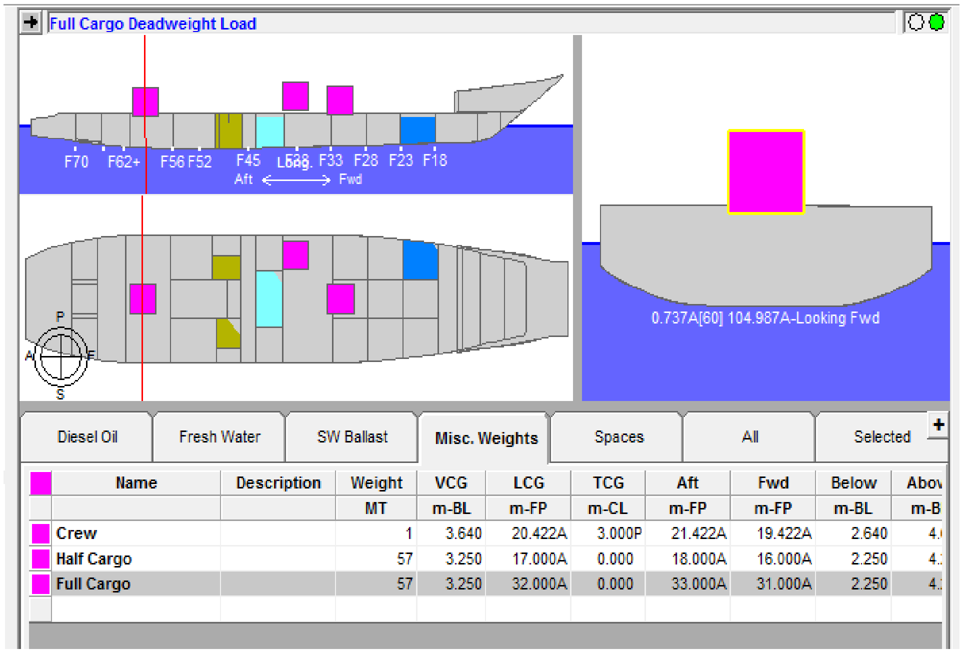

Figure 22. Lightship with Full Cargo Deadweight Loading Condition

The full cargo deadweight loading case results in the following ship's stability characteristics:

- Δ: 371 MT
- FP: 1.474 m
- AP: 1.541 m
- MS: 1.507 m
- Trim: 0.067 m afterward
- GM_t: 3.252 m
- VCG: 2.136 m
- LCG: 23.223 m afterward from forward perpendicular
- TCG: 0.020 m starboard from center line
- LCF: 23.192 m afterward from forward perpendicular
- LCB: 23.093 m afterward from forward perpendicular
- θ: 0.35 degrees to starboard

B. STATIC STABILITY RESULTS

1. Boundary Conditions

The study of the LCU's static stability focuses on the ship's wind-rolling stability because it is the most important aspect of stability for the coastal missions the LCU performs. Wind-rolling stability is based on the resulting rolling angles of the ship when it is subjected to wind forces, as described in detail in the following subsection, "Lightship Wind-Rolling Stability." To model the wind-rolling stability, we imported the appropriate ship file into the POSSE software. We further imported the particular loading case of the ship and derived the ship's GZ curve. Then, we compared this curve to the specific wind-stability criterion for wind rolling. For that case, we selected the U.S. Navy wind-rolling criterion, which is incorporated in the software. This criterion is the same as that described in chapter II, and hence requires the satisfaction of the same relationships in terms of heeling arm and reserve area. However, the criterion needs tailoring in order to correspond to the desirable sea state condition we need to obtain the results. These adjustments take place in terms of the wind velocity, which is the main parameter in the software options. For this case, we selected to study LCU wind-rolling stability for the sea states 2, 4, and 6. These sea state conditions correspond to wind velocities of 4.37, 9.77, and 19.29 meters per second (m/s) as shown in Table 1.

Table1. Wind Velocity and Significant Wave Height for Sea States 2, 4, and 6. Adapted from [9].

Sea State	2	4	6
Wind Velocity (m/s)	4.37 (8.49 Knots)	9.77 (18.99 Knots)	19.29 (37.49 Knots)
Significant Wave Height ($H_{1/3}$) (m)	0.3	1.875	5

After changing the wind-rolling stability criterion in POSSE, we ran the software for all the loading conditions (lightship, lightship carrying half the cargo deadweight, and lightship carrying a full cargo deadweight load.) and all of the aforementioned sea states, which represent the most appropriate trade space for the LCU coastal transits. To obtain precise results, we modified the ship's wind projected area by making assumptions on its profile surface. We created this profile area in the POSSE software, taking into account the real ship drawings and, especially, the worst case scenario with the maximum projected area. The ship's wind profile, which was used for the calculations, is shown in Figure 23. As we can observe the total projected area is 1,624.98 ft^2 (150.97 m^2).

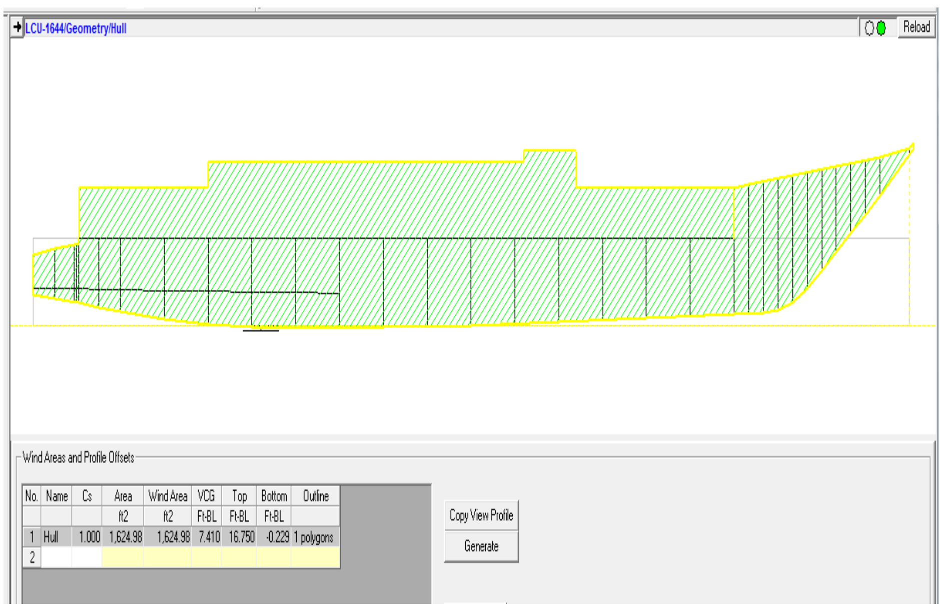

Figure 23. LCU Wind Profile

The selected boundary values for each main parameter, which define the LCU static stability trade space, are summarized in Table 2.

Table 2. LCU Static Stability Parameters' Boundary Values

Loading condition	Sea State
Lightship	2
Half Cargo Deadweight	4
Full Cargo Deadweight	6

2. Lightship Wind-Rolling Stability

After the software run, we obtained the simulation results for the lightship loading case. The wind-rolling GZ curve for sea state 2 is shown in Figure 24. The LCU meets both the criteria for the righting arm and the reserve area.

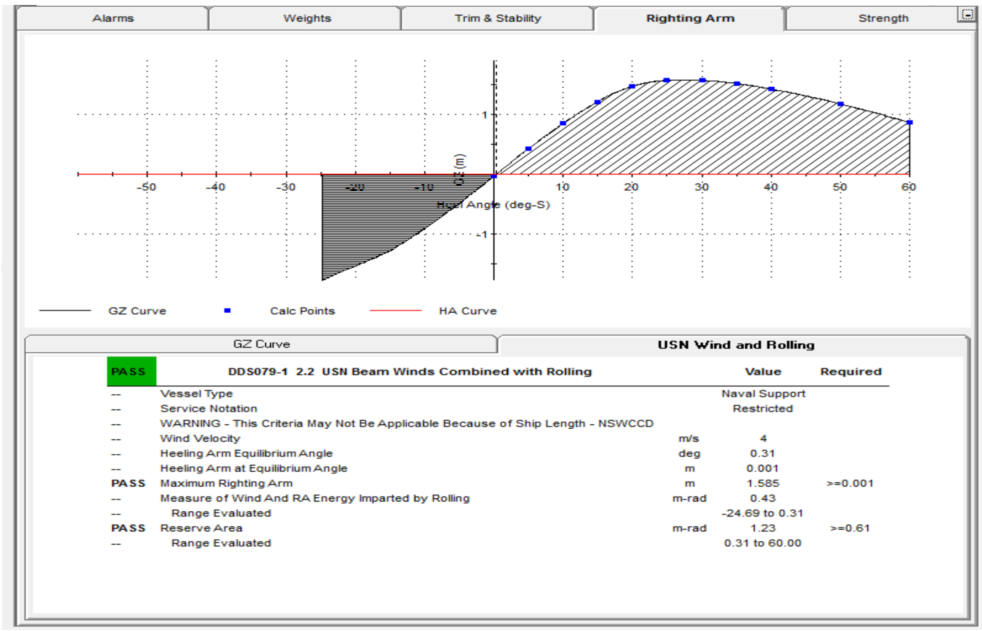

Figure 24. Wind-Rolling Stability for LCU Lightship in Sea State 2

The wind-rolling GZ curve for sea state 4 is presented in Figure 25. The LCU meets the wind-rolling criteria for this case.

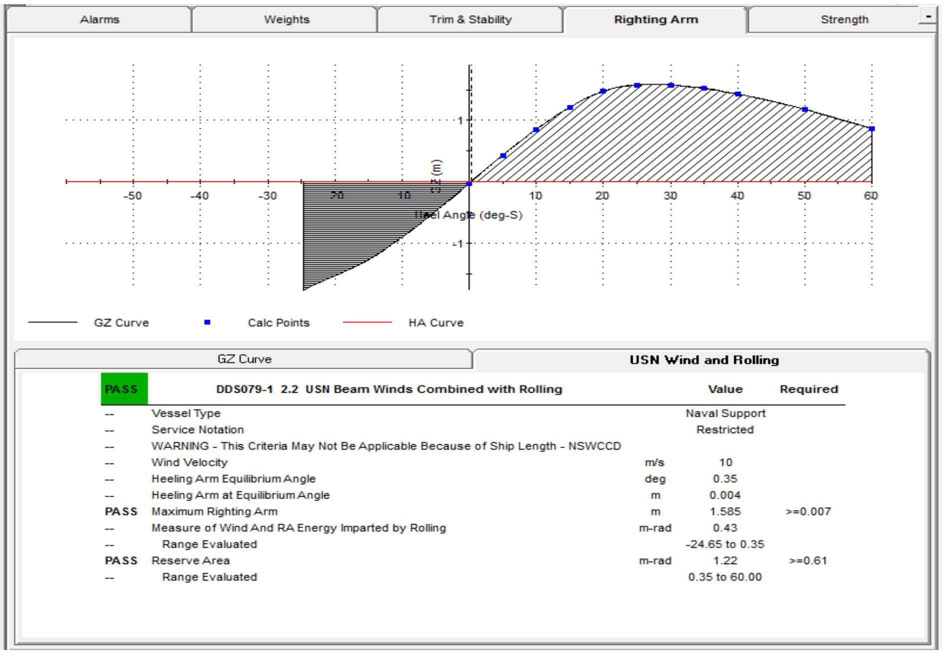

Figure 25. Wind-Rolling Stability for LCU Lightship in Sea State 4

The wind-rolling GZ curve results for sea state 6 are provided in Figure 26, which shows that the wind-rolling criteria are satisfied for that case.

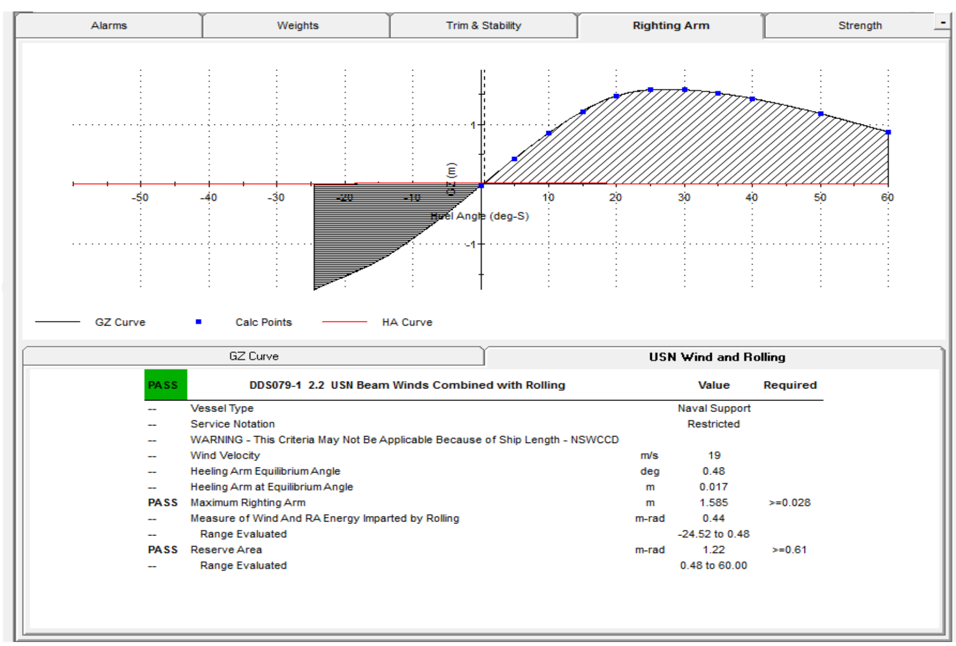

Figure 26. Wind-Rolling Stability for LCU Lightship in Sea State 6

3. LCU with Half Cargo Deadweight Wind-Rolling Stability

For the loading case of half the cargo deadweight, POSSE results show the LCU passes the wind-rolling criterion for all the sea state conditions. The LCU's performance in sea state 2 is shown in Figure 27.

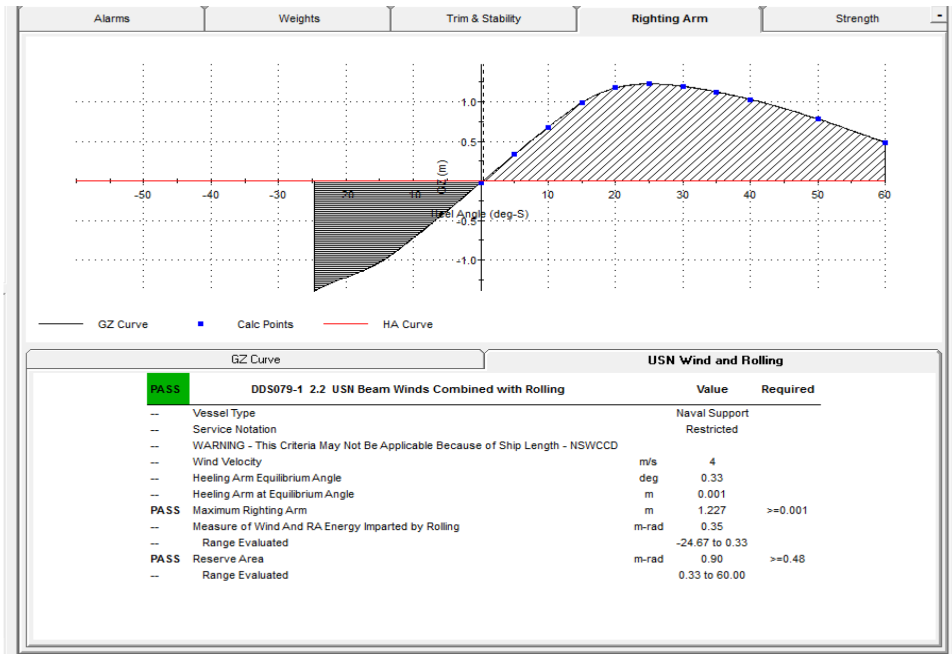

Figure 27. Wind-Rolling Stability for LCU Carrying Half Cargo Deadweight in Sea State 2

Similarly, the wind-rolling criteria results for sea state 4 is presented in Figure 28.

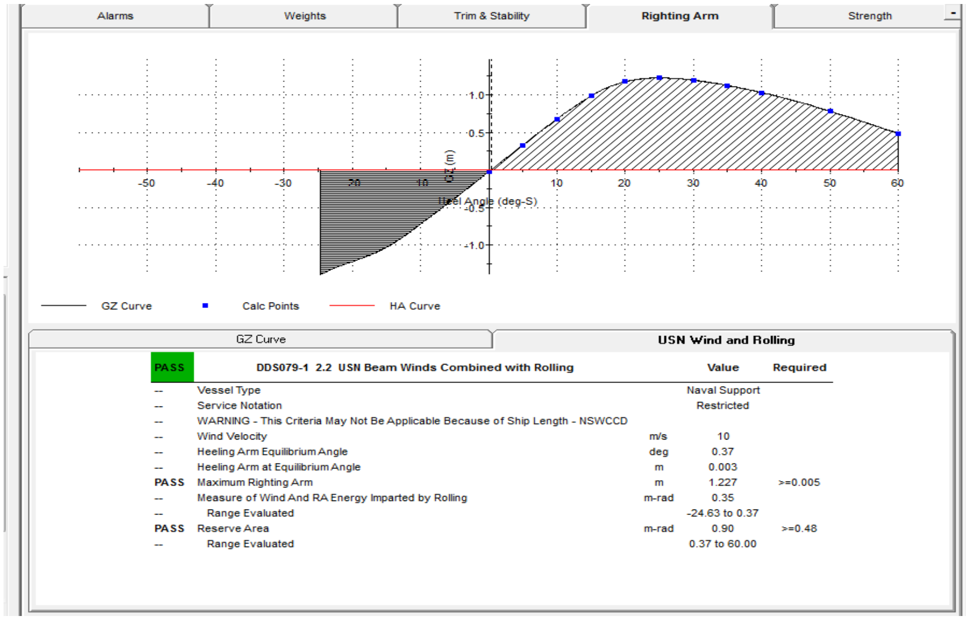

Figure 28. Wind-Rolling Stability for LCU Carrying Half Cargo Deadweight in Sea State 4

Additionally, the LCU with half the cargo deadweight loading case satisfies the wind-rolling criteria for sea state 6, as Figure 29 indicates.

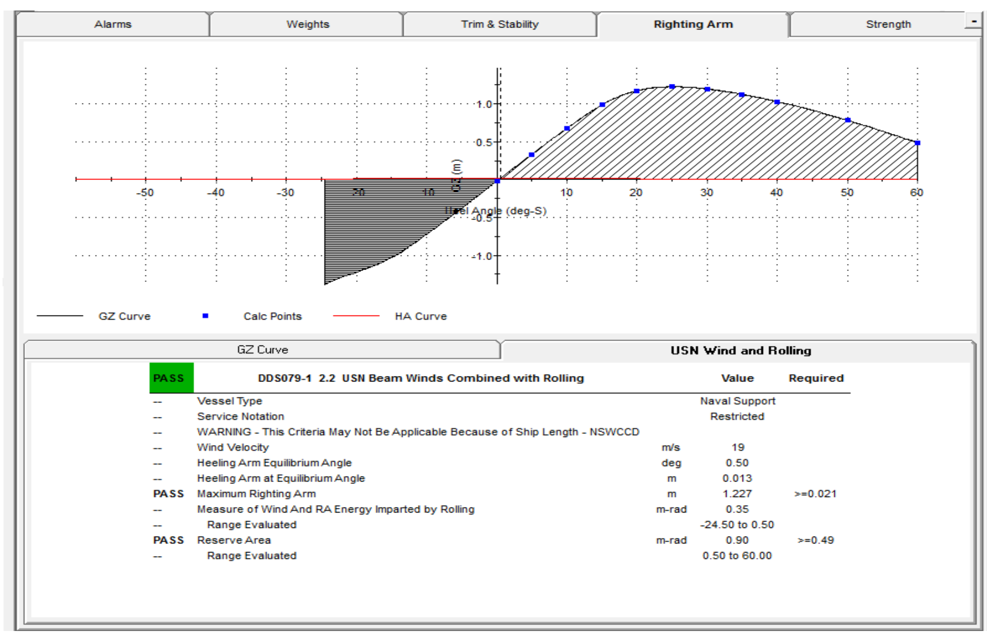

Figure 29. Wind-Rolling Stability for LCU Carrying Half Cargo Deadweight in Sea State 6

4. LCU with Full Cargo Deadweight Wind-Rolling Stability

The third case examines the LCU's static stability for the full cargo deadweight loading case. This case is studied for the same sea state conditions 2, 4, and 6. The derived results for sea state 2 show that the LCU's static stability is adequate in terms of wind-rolling criterion. The results are shown in Figure 30.

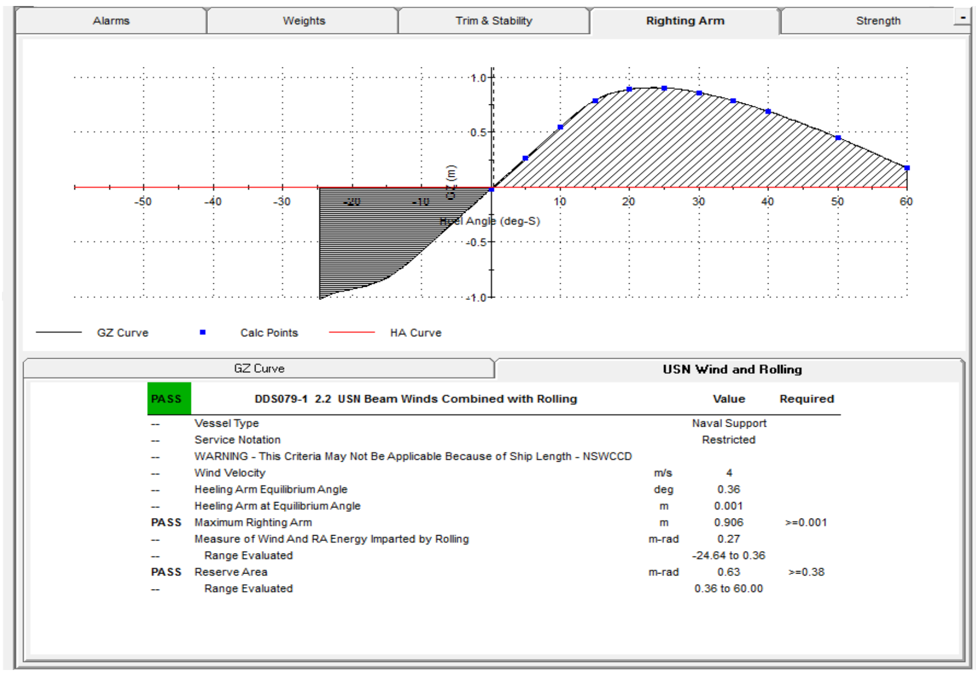

Figure 30. Wind-Rolling Stability for LCU Carrying Full Cargo Deadweight in Sea State 2

The LCU with full cargo deadweight loading case also satisfies the wind-rolling criterion for sea state 4, as displayed in Figure 31.

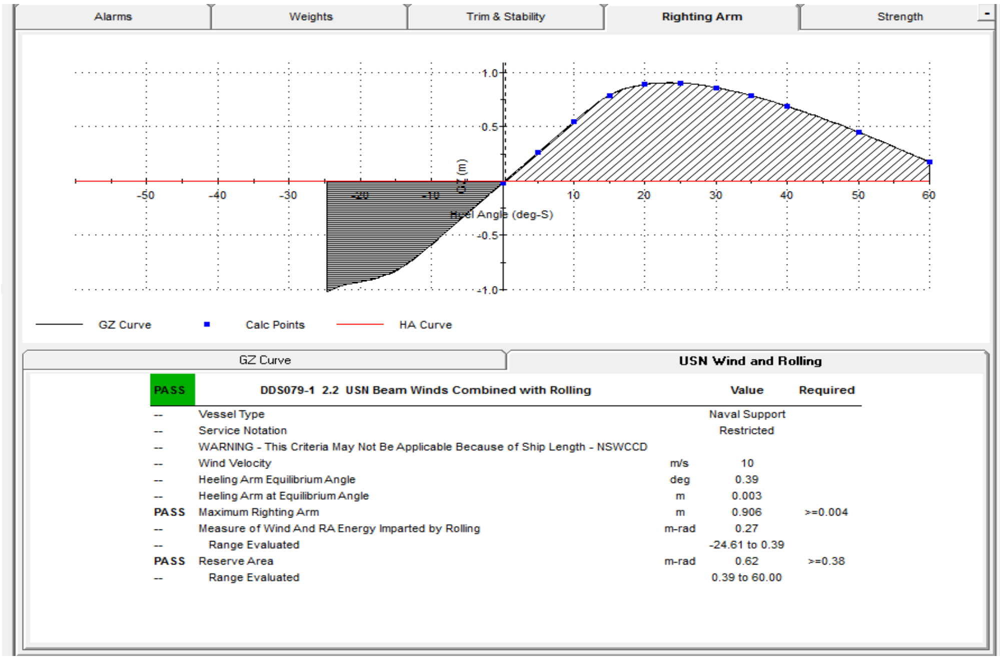

Figure 31. Wind-Rolling Stability for LCU Carrying Full Cargo Deadweight in Sea State 4

In sea state 6, the LCU with full cargo deadweight loading case demonstrates adequate wind-rolling stability, as provided by Figure 32.

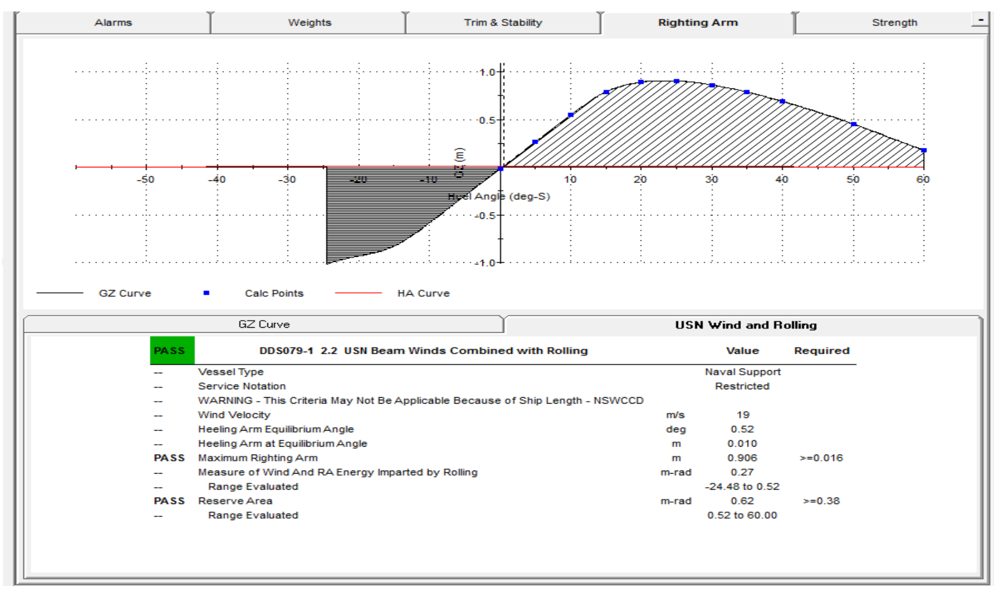

Figure 32. Wind-Rolling Stability for LCU Carrying Full Cargo Deadweight in Sea State 6

5. Analytical Determination of Static Stability Equilibrium

Given the POSSE wind-rolling static stability outcomes for all the LCU loading cases in the selected sea states, we also applied an analytic method in order to verify the static stability equilibrium results. This method is based on the equation that provides the wind-generated heeling arm as a function of wind speed, the ship's projected area, the distance between the centroids of the ship's projected area and underwater hull profile, the ship's displacement, and the heeling angle. The mathematical expression of this equation is as described in [13]:

$$WHA = \frac{0.0171 V_k^2 Al \cos^2\theta}{1000\Delta} \tag{54}$$

WHA: Heeling arm in m

V_k: Wind velocity in knots

A: Ship's projected area above water line m^2

l: Distance from the centroid of ship's projected area and the centroid of the underwater hull profile in m

θ: Heeling angle in degrees (^{o})

Δ: Ship's displacement in MT

In the wind-rolling static stability equilibrium, the wind-generated heeling arm WHA is equal to the ship-developed righting arm GZ. For low values of heeling angle, an approximation of the ship's righting arm is provided by the equation as explained in [13]:

$$GZ(\theta) = GM_t \sin\theta, \tag{55}$$

where GM_t is the ship's metacentric height corresponding to its loading condition.

By combining Equations (55) and (56), we can determine the equilibrium heeling angle for any combination of values between metacentric height GM and wind velocity. Likewise, we can define the equilibrium metacentric height for any combination of heeling angles and wind velocities. We developed a MATLAB code to identify the areas of values where the equilibrium heeling angle sits. We chose the intervals of the critical parameters to represent both the selected operation environment in terms of wind velocity and the POSSE outcomes in terms of generated metacentric heights. More specifically, we selected the wind velocity to vary from 0 to 60 knots and the ship's metacentric height to vary from 1 to 6 meters.

We developed diagrams that show the static stability reaches an equilibrium state with the combinations of values of wind velocity, metacentric height, and heeling angle. We conducted the analysis by creating two equilibrium diagrams for each loading condition; those diagrams include all the cases of operational trade space of the LCU referred to in Table 1. The diagrams show that, in all cases, the results derived by POSSE are consistent with those obtained by the analytical method. In this particular trade space, the heeling angle took values within the interval of 0.2 to 0.5 degrees, which verifies the validity of the POSSE calculations. The two different ways to display these results for each LCU loading case are provided by Figures 33 to 38.

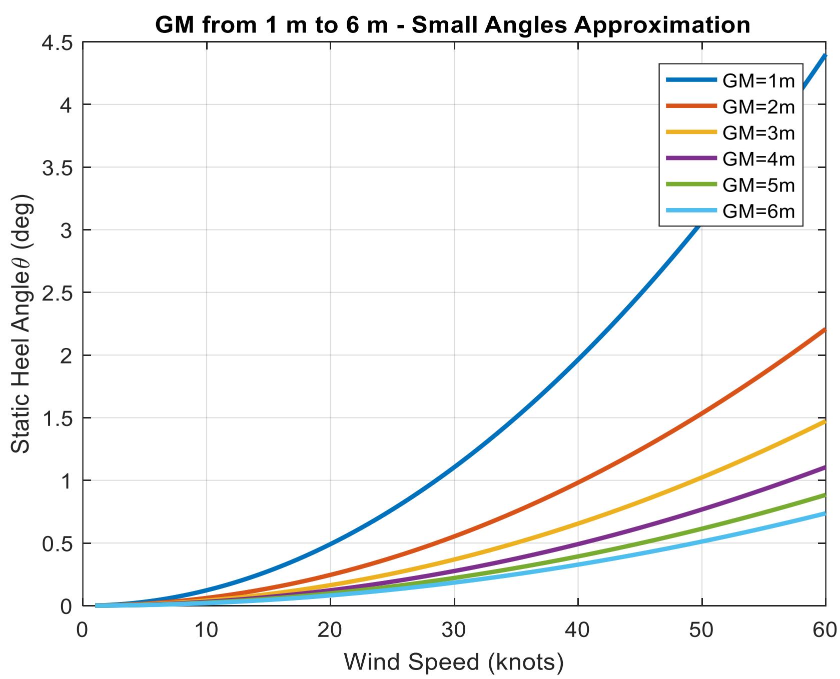

Figure 33. Heeling Angle versus Wind Speed Wind-Rolling Static Stability Equilibrium Curves for LCU Lightship

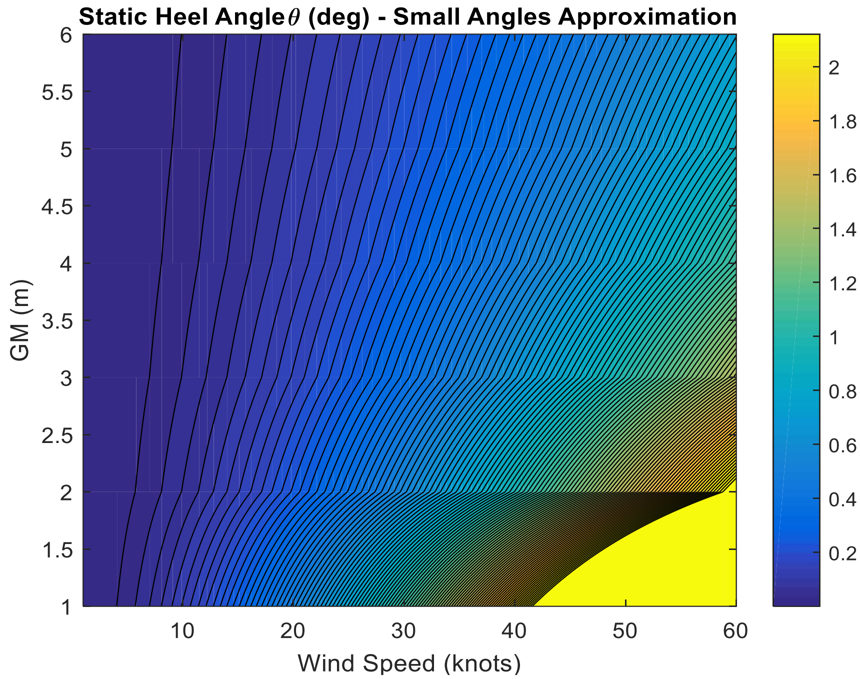

Figure 34. Metacentric Height versus Wind Speed Wind-Rolling Static Stability Equilibrium Curves for LCU Lightship

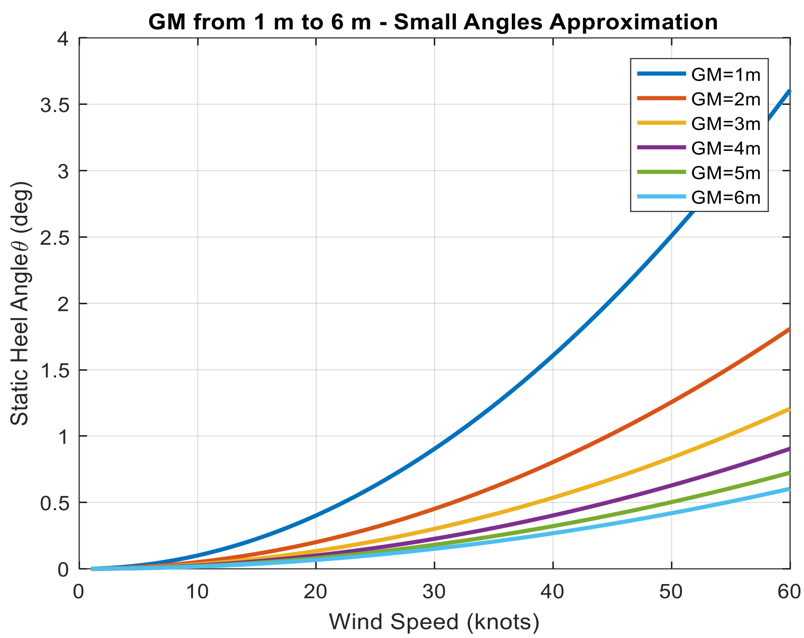

Figure 35. Heeling Angle versus Wind Speed Wind-Rolling Static Stability Equilibrium Curves for LCU Carrying Half Cargo Deadweight

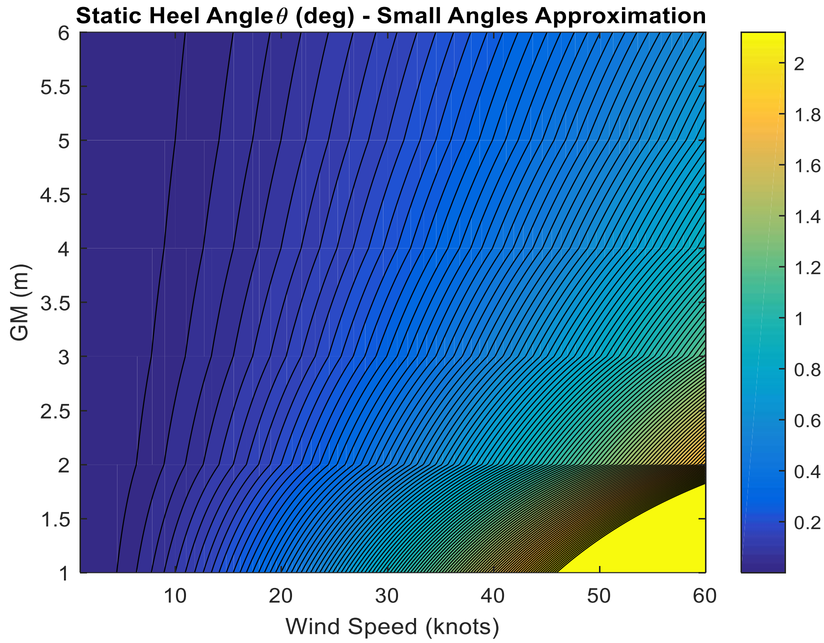

Figure 36. Metacentric Height versus Wind Speed Wind-Rolling Static Stability Equilibrium Curves for LCU Carrying Half Cargo Deadweight

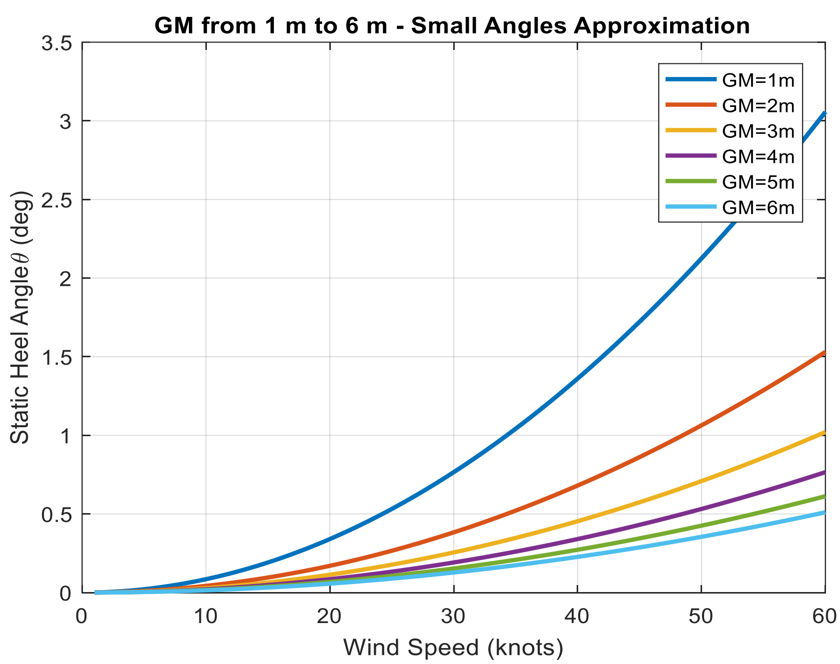

Figure 37. Heeling Angle versus Wind Speed Wind-Rolling Static Stability Equilibrium Curves for LCU Carrying Full Cargo Deadweight

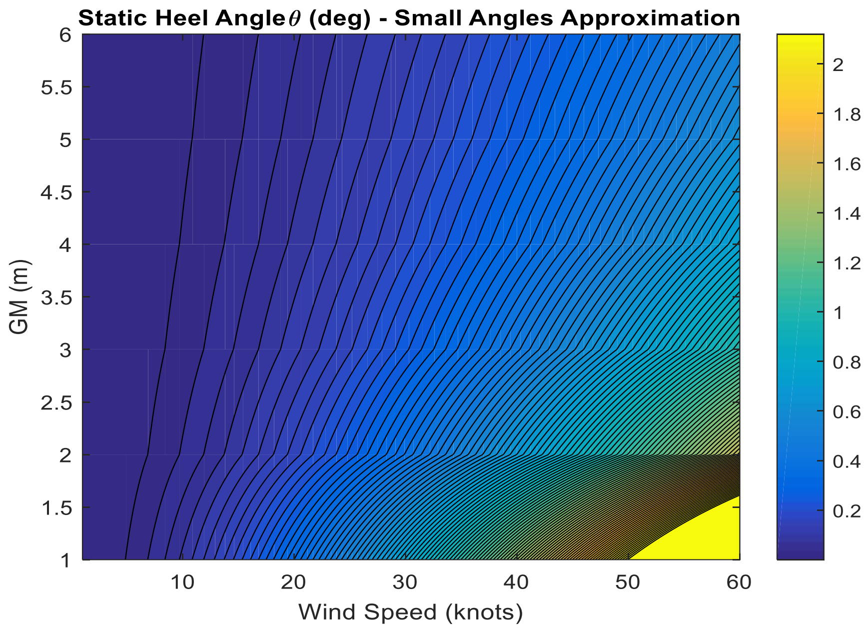

Figure 38. Metacentric Height versus Wind Speed Wind-Rolling Static Stability Equilibrium Curves for LCU Carrying Full Cargo Deadweight

The heeling angle values at the wind-rolling static stability equilibrium for the various loading cases and sea state conditions are summarized in Table 3.

Table 3. Wind-Rolling Static Stability Equilibrium Heeling Angles

Wind-Rolling Static Stability Equilibrium			
Loading Case	**Sea State**	**Heeling Angle (Degrees)**	
		POSSE Results	**Analytical Determination Results**
Lightship	2	0.31	0.22
	4	0.35	0.31
	6	0.48	0.43
Lightship with Half Cargo Deadweight	2	0.33	0.24
	4	0.37	0.36
	6	0.50	0.47
Lightship with Full Cargo Deadweight	2	0.36	0.30
	4	0.39	0.37
	6	0.52	0.49

C. DYNAMIC STABILITY RESULTS

1. Boundary Conditions

Because the LCU satisfies the most significant static stability criterion, study of its stability should extend into investigating this craft's dynamic stability. As discussed in detail in Chapter III, dynamic stability is based on the ship's body responses to the six degrees of freedom when subjected to the random waves' exciting forces. Those responses are derived from the SMP in terms of displacement, velocity, and acceleration of all the degrees of freedom of ship motions. To obtain these responses, we imported the LCU model into the SMP. Maintaining the consistency with the previous calculations, we also imported the three examined loading cases: the LCU lightship, LCU lightship carrying half the cargo deadweight, LCU lightship carrying a full cargo deadweight. Additionally, we selected the appropriate wave spectra in order to model the sea wave conditions. Available SMP wave spectra are the Bretschneider, the JONSWAP, and the Ochi-Hubble models.

For our case of a short coastal mission, the most appropriate wave spectrum is the six-parameter Ochi-Hubble model, which provides the most probable ship responses. To conduct a more global study of LCU dynamic stability, we also used the Bretschneider wave spectrum model. We did not use the JONSWAP spectrum because it has many similarities to the Bretschneider model and is more appropriate for open seas. The Ochi-Hubble spectrum model has, by default, a single modal period of 1.14 sec. The Bretschneider spectrum model has, by default, five values of modal periods Tm (7, 9, 11, 13, 15 sec). We conducted the basic analysis using the default Ochi-Hubble, and the moderate Bretschneider case, in which the modal period equals 11 sec. We also conducted an analysis for the extreme modal period values of 7 and 15 sec.[5]

The trade space of the dynamic stability study is the same as that for static stability; therefore, we examined the LCU responses for the sea states 2, 4, and

[5] Results are provided in the appendix.

6. These sea states are modeled in the SMP by selecting the significant wave height of the wave spectrum that corresponds to each sea state. According to Table 1, the significant wave heights for the sea states 2, 4, and 6 are 0.3, 1.875, and 5 m, respectively. We also decided to conduct an analysis for the most critical values of the LCU's operational speed range; for this we picked the values 0, 2, 4, and 6 m/s. We conducted the analysis using the short-wave spectra variation due to the fact that, for coastal waters, the seaway is more realistically modeled using the short-crested waves. The selected boundary values for each main parameter, which define the LCU's dynamic stability trade space, are summarized in Table 4.

Table 4. LCU Dynamic Stability Parameters' Boundary Values

<table>
<tr><th>Loading Condition</th><th>Sea State</th><th>Ship Speed (m/s)</th><th>Wave Type</th><th>Wave Spectrum</th><th>Bretschneider Spectrum Modal Period Tm (sec)</th></tr>
<tr><td rowspan="2">Lightship</td><td rowspan="2">2</td><td>0</td><td rowspan="7">Short-Crested</td><td rowspan="3">Ochi-Hubble</td><td rowspan="2">7</td></tr>
<tr><td rowspan="3">2</td></tr>
<tr><td rowspan="3">Lightship with Half Cargo Deadweight</td><td rowspan="3">4</td><td rowspan="3">11</td></tr>
<tr><td rowspan="4">Bretschneider</td></tr>
<tr><td rowspan="2">4</td></tr>
<tr><td rowspan="2">Lightship with Full Cargo Deadweight</td><td rowspan="2">6</td><td rowspan="2">15</td></tr>
<tr><td>6</td></tr>
</table>

2. Dynamic Stability—LCU Lightship

We focused on studying the LCU's roll angles because our objective was to evaluate the intact dynamic stability of the LCU from all the SMP-derived responses for the ship. The SMP provides the ship's roll angles against the sea heading, calculating the rolling angle for every 15 degrees of increment in heading angle within the range of 0 to 360 degrees.

The results we obtained showed symmetrical heeling angle values between the heading ranges of 0 to 180 degrees and 180 to 360 degrees. Therefore, we present the plots heeling angle versus heading angle for the heading range of 0 to 180 degrees. The resulting conclusions derived for the plots are valid for the heading ranges 180 to 360 degrees. For example, if the LCU demonstrates maximum heeling angle at sea headings of 90 or 120 degrees, that means it undergoes the same heeling inclination at (360–90) 270 or (360–120) 240 degrees, respectively, and so forth.

By applying all the boundary conditions described previously, we derived the LCU roll angle responses for the Ochi-Hubble wave spectrum shown in Table 5. The plots of the ship's heeling angle against sea heading (provided in Figure 39) describe roll angle responses for all the combinations of sea states and ship's speeds.

Table 5. Roll Angle Responses in Ochi-Hubble Short-Crested Sea Waves for LCU Lightship

Sea Heading (Degrees)	LCU Heeling Angle (Degrees)											
	Sea State 2				Sea State 4				Sea State 6			
	Vs=0 m/s	Vs=2 m/s	Vs=4 m/s	Vs=6 m/s	Vs=0 m/s	Vs=2 m/s	Vs=4 m/s	Vs=6 m/s	Vs=0 m/s	Vs=2 m/s	Vs=4 m/s	Vs=6 m/s
0	0.34	0.44	0.58	0.66	1.96	2.54	3.33	3.85	4.51	5.76	7.52	8.81
15	0.40	0.51	0.64	0.72	2.32	2.90	3.66	4.18	5.31	6.55	8.24	9.52
30	0.54	0.64	0.77	0.85	3.10	3.67	4.38	4.90	7.03	8.24	9.81	11.06
45	0.69	0.78	0.89	0.97	3.92	4.44	5.10	5.59	8.82	9.93	11.37	12.56
60	0.81	0.89	0.98	1.06	4.59	5.03	5.59	6.05	10.26	11.20	12.46	13.56
75	0.89	0.94	1.02	1.08	5.03	5.34	5.79	6.18	11.19	11.89	12.90	13.83
90	0.91	0.94	0.99	1.04	5.18	5.35	5.65	5.95	11.52	11.92	12.61	13.33
105	0.89	0.89	0.91	0.94	5.03	5.04	5.19	5.38	11.21	11.28	11.63	12.09
120	0.81	0.78	0.78	0.79	4.60	4.46	4.45	4.53	10.29	10.03	10.03	10.24
135	0.69	0.64	0.61	0.61	3.93	3.65	3.52	3.51	8.85	8.30	8.00	7.97
150	0.55	0.48	0.44	0.42	3.12	2.75	2.53	2.44	7.07	6.30	5.81	5.61
165	0.41	0.33	0.29	0.27	2.34	1.93	1.68	1.57	5.36	4.47	3.92	3.66
180	0.34	0.27	0.22	0.20	1.98	1.55	1.31	1.20	4.57	3.64	3.10	2.85

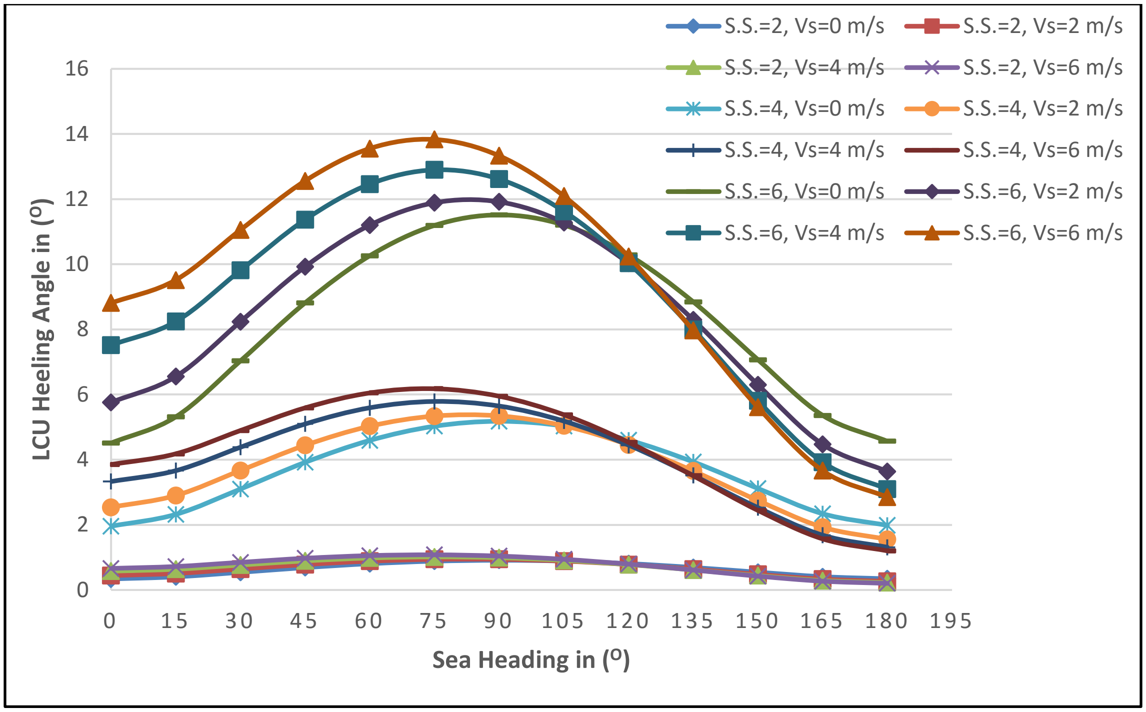

Figure 39. Heeling Angle versus Sea Heading in Ochi-Hubble Short-Crested Waves for LCU Lightship

Additionally, the LCU lightship's dynamic stability is examined using the Bretschneider short-crested wave spectrum with a modal period of 11 sec. The values of the roll angles against sea heading are shown in Table 6, while the plots of the heeling angles versus the sea heading are presented in Figure 40.

Table 6. Roll Angle Responses in Bretschneider (Tm = 11 sec) Short-Crested Sea Waves for LCU Lightship

Sea Heading (Degrees)	LCU Heeling Angle (Degrees)											
	Sea State 2				Sea State 4				Sea State 6			
	Vs=0 m/s	Vs=2 m/s	Vs=4 m/s	Vs=6 m/s	Vs=0 m/s	Vs=2 m/s	Vs=4 m/s	Vs=6 m/s	Vs=0 m/s	Vs=2 m/s	Vs=4 m/s	Vs=6 m/s
0	0.25	0.31	0.40	0.47	1.55	1.92	2.47	2.96	4.13	5.11	6.57	7.87
15	0.29	0.34	0.43	0.51	1.78	2.15	2.68	3.17	4.74	5.72	7.13	8.41
30	0.37	0.43	0.51	0.58	2.30	2.66	3.16	3.62	6.11	7.06	8.37	9.59
45	0.46	0.51	0.58	0.65	2.86	3.19	3.64	4.07	7.56	8.43	9.63	10.78
60	0.53	0.58	0.64	0.70	3.32	3.60	3.98	4.37	8.76	9.49	10.53	11.56
75	0.58	0.61	0.66	0.71	3.63	3.82	4.12	4.44	9.53	10.06	10.89	11.75
90	0.60	0.61	0.65	0.68	3.73	3.83	4.03	4.27	9.80	10.09	10.65	11.30
105	0.58	0.58	0.60	0.62	3.63	3.63	3.71	3.86	9.54	9.57	9.83	10.25
120	0.53	0.52	0.52	0.52	3.33	3.23	3.21	3.27	8.78	8.54	8.53	8.70
135	0.46	0.43	0.41	0.41	2.87	2.69	2.59	2.57	7.58	7.13	6.88	6.84
150	0.37	0.33	0.31	0.30	2.31	2.08	1.93	1.86	6.13	5.52	5.13	4.96
165	0.29	0.25	0.22	0.21	1.80	1.54	1.37	1.30	4.78	4.09	3.66	3.45
180	0.25	0.21	0.18	0.17	1.56	1.30	1.14	1.07	4.17	3.47	3.05	2.85

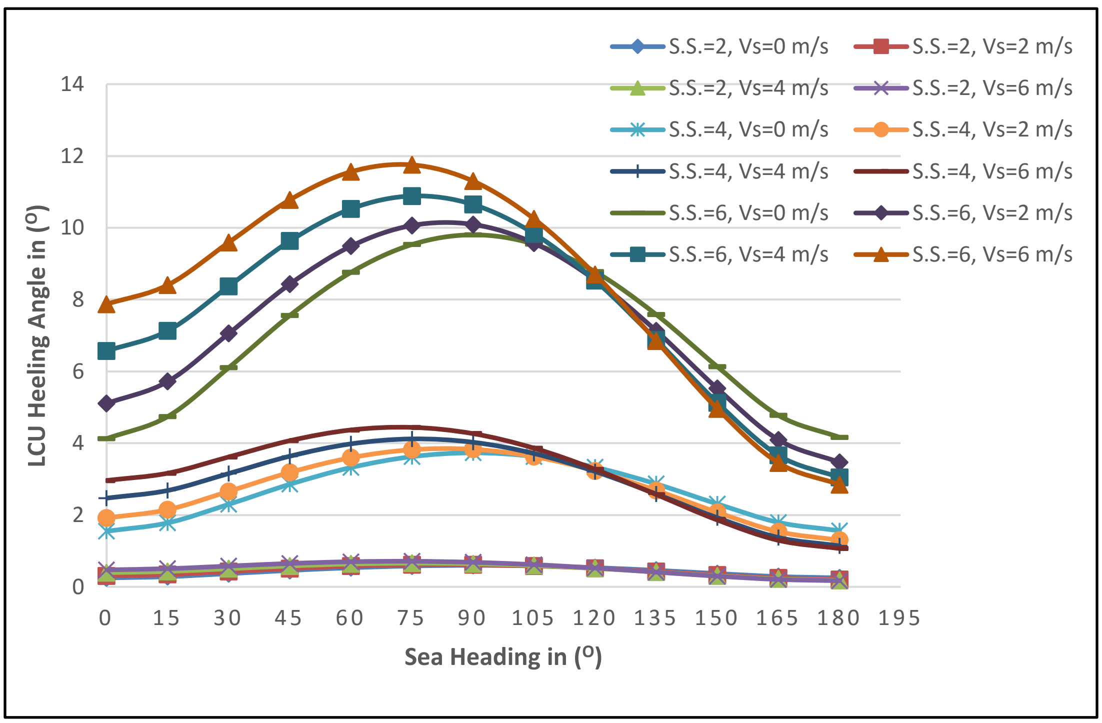

Figure 40. Heeling Angle versus Sea Heading in Bretschneider (Tm = 11 sec) Short-Crested Waves for LCU Lightship

3. Dynamic Stability—LCU with Half Cargo Deadweight

As described previously, the LCU roll angle responses for the loading case in which the ship carries half the maximum cargo deadweight are derived by importing this loading condition into SMP and setting the parameters of sea state, ship speed, and wave spectrum. Likewise, these responses are generated by both the Ochi-Hubble and the Bretschneider wave spectra models. Table 7 provides the LCU ship's heeling angles for all the combinations of sea states and wave speeds, while Figure 41 presents the plots of the ship's heeling angles versus the sea heading for the Ochi-Hubble wave spectrum.

Table 7. Roll Angle Responses in Ochi-Hubble Short-Crested Sea Waves for LCU Carrying Half Cargo Deadweight

Sea Heading (Degrees)	LCU Heeling Angle (Degrees)											
	Sea State 2				Sea State 4				Sea State 6			
	Vs=0 m/s	Vs=2 m/s	Vs=4 m/s	Vs=6 m/s	Vs=0 m/s	Vs=2 m/s	Vs=4 m/s	Vs=6 m/s	Vs=0 m/s	Vs=2 m/s	Vs=4 m/s	Vs=6 m/s
0	0.40	0.57	0.74	0.84	2.28	3.23	4.29	4.93	5.16	7.14	9.54	11.20
15	0.49	0.65	0.82	0.92	2.77	3.68	4.71	5.34	6.18	8.09	10.40	12.04
30	0.67	0.83	0.99	1.08	3.77	4.65	5.62	6.23	8.25	10.04	12.24	13.86
45	0.86	1.00	1.15	1.24	4.80	5.60	6.49	7.09	10.28	11.95	14.02	15.62
60	1.01	1.13	1.26	1.34	5.62	6.29	7.08	7.63	11.89	13.35	15.23	16.73
75	1.11	1.20	1.30	1.36	6.15	6.64	7.28	7.75	12.90	14.06	15.66	16.96
90	1.15	1.19	1.26	1.31	6.33	6.62	7.07	7.42	13.25	14.03	15.23	16.26
105	1.12	1.12	1.15	1.17	6.15	6.22	6.45	6.67	12.91	13.26	13.99	14.66
120	1.02	0.98	0.97	0.98	5.64	5.47	5.48	5.57	11.91	11.79	12.00	12.31
135	0.86	0.79	0.75	0.74	4.82	4.44	4.27	4.23	10.31	9.74	9.48	9.44
150	0.68	0.58	0.52	0.50	3.80	3.27	2.97	2.84	8.30	7.33	6.71	6.44
165	0.50	0.38	0.32	0.29	2.81	2.19	1.83	1.68	6.27	5.03	4.24	3.89
180	0.41	0.29	0.22	0.20	2.34	1.68	1.31	1.16	5.28	3.92	3.10	2.75

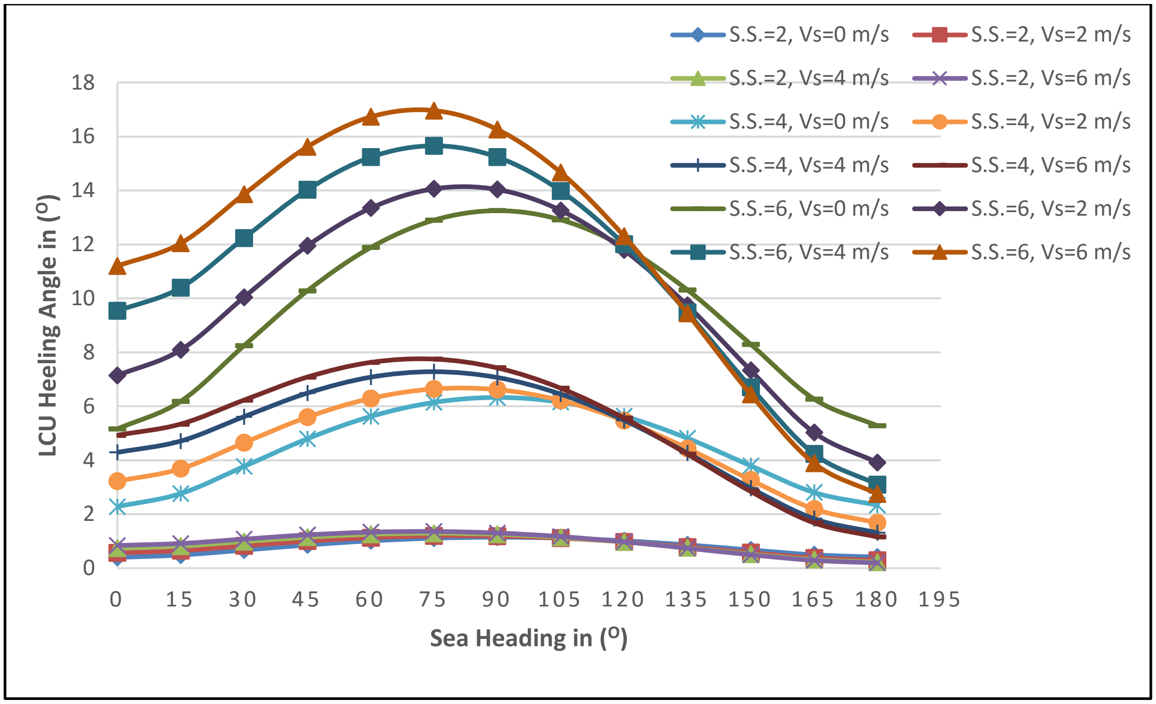

Figure 41. Heeling Angle versus Sea Heading in Ochi-Hubble Short-Crested Waves for LCU Carrying Half Cargo Deadweight

Similarly, the LCU heeling angle responses for the Bretschneider spectrum and the corresponding plots are shown in Table 8 and Figure 42, respectively.

Table 8. Roll Angle Responses in Bretschneider (Tm = 11 sec) Short-Crested Sea Waves for LCU Carrying Half Cargo Deadweight

Sea Heading (Degrees)	LCU Heeling Angle (Degrees)											
	Sea State 2				Sea State 4				Sea State 6			
	Vs=0 m/s	Vs=2 m/s	Vs=4 m/s	Vs=6 m/s	Vs=0 m/s	Vs=2 m/s	Vs=4 m/s	Vs=6 m/s	Vs=0 m/s	Vs=2 m/s	Vs=4 m/s	Vs=6 m/s
0	0.28	0.38	0.51	0.62	1.72	2.34	3.16	3.88	4.57	6.16	8.30	10.17
15	0.33	0.42	0.55	0.66	2.03	2.62	3.42	4.13	5.35	6.90	8.96	10.79
30	0.43	0.52	0.64	0.75	2.68	3.25	4.00	4.67	7.00	8.46	10.40	12.16
45	0.54	0.63	0.74	0.84	3.36	3.89	4.57	5.20	8.68	10.02	11.83	13.50
60	0.64	0.71	0.80	0.89	3.93	4.37	4.96	5.53	10.02	11.18	12.80	14.33
75	0.70	0.75	0.82	0.90	4.30	4.62	5.09	5.57	10.88	11.78	13.12	14.43
90	0.72	0.74	0.79	0.85	4.42	4.60	4.93	5.29	11.17	11.75	12.73	13.75
105	0.70	0.70	0.72	0.76	4.30	4.33	4.49	4.72	10.88	11.10	11.67	12.33
120	0.64	0.62	0.62	0.63	3.94	3.82	3.84	3.92	10.04	9.87	10.01	10.31
135	0.55	0.50	0.48	0.48	3.38	3.13	3.01	2.99	8.70	8.18	7.94	7.92
150	0.43	0.38	0.35	0.33	2.69	2.36	2.16	2.07	7.04	6.23	5.73	5.51
165	0.33	0.27	0.23	0.21	2.05	1.67	1.44	1.34	5.41	4.44	3.83	3.56
180	0.28	0.22	0.18	0.17	1.75	1.36	1.13	1.03	4.65	3.63	3.01	2.75

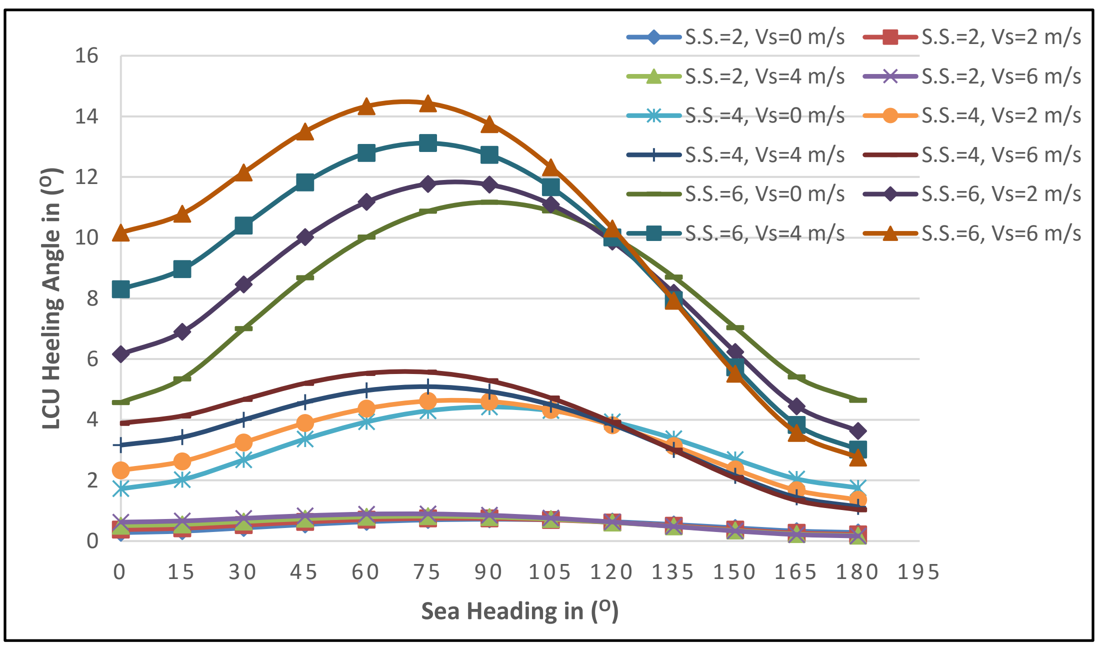

Figure 42. Heeling Angle versus Sea Heading in Bretschneider (Tm = 11 sec) Short-Crested Waves for LCU Carrying Half Cargo Deadweight

4. Dynamic Stability—LCU with Full Cargo Deadweight

By importing the full cargo deadweight loading condition, we obtained the LCU heeling angle responses for the sea states and ship's speed as described in Table 3. Similar to the previous cases, we derived results using both the Ochi-Hubble and the Bretschneider spectra models. The heeling angles values for the sea-heading angles in the Ochi-Hubble spectra model are provided in Table 9 and the corresponding plots are shown in Figure 43.

Table 9. Roll Angle Responses in Ochi-Hubble Short-Crested Sea Waves for LCU Carrying Full Cargo Deadweight

Sea Heading (Degrees)	LCU Heeling Angle (Degrees)											
	Sea State 2				Sea State 4				Sea State 6			
	Vs=0 m/s	Vs=2 m/s	Vs=4 m/s	Vs=6 m/s	Vs=0 m/s	Vs=2 m/s	Vs=4 m/s	Vs=6 m/s	Vs=0 m/s	Vs=2 m/s	Vs=4 m/s	Vs=6 m/s
0	0.49	0.73	0.89	0.99	2.73	4.09	5.12	5.76	5.99	8.72	11.23	13.00
15	0.61	0.83	0.98	1.09	3.35	4.62	5.62	6.33	7.19	9.71	12.18	14.08
30	0.85	1.05	1.18	1.32	4.60	5.75	6.69	7.51	9.46	11.78	14.22	16.32
45	1.09	1.27	1.38	1.52	5.82	6.85	7.71	8.59	11.61	13.80	16.19	18.39
60	1.28	1.43	1.52	1.66	6.76	7.64	8.40	9.29	13.27	15.25	17.50	19.70
75	1.41	1.51	1.57	1.70	7.35	8.03	8.65	9.48	14.31	15.97	17.96	20.02
90	1.45	1.51	1.53	1.64	7.55	8.00	8.42	9.14	14.66	15.93	17.51	19.29
105	1.41	1.41	1.39	1.48	7.36	7.54	7.72	8.28	14.32	15.11	16.15	17.54
120	1.29	1.24	1.18	1.24	6.78	6.68	6.60	6.96	13.30	13.54	13.96	14.87
135	1.09	1.00	0.92	0.94	5.85	5.48	5.16	5.30	11.66	11.32	11.10	11.48
150	0.85	0.73	0.63	0.61	4.65	4.06	3.57	3.48	9.54	8.67	7.89	7.73
165	0.62	0.48	0.37	0.33	3.42	2.68	2.13	1.88	7.32	5.96	4.84	4.31
180	0.51	0.35	0.24	0.19	2.83	1.99	1.41	1.15	6.17	4.53	3.30	2.75

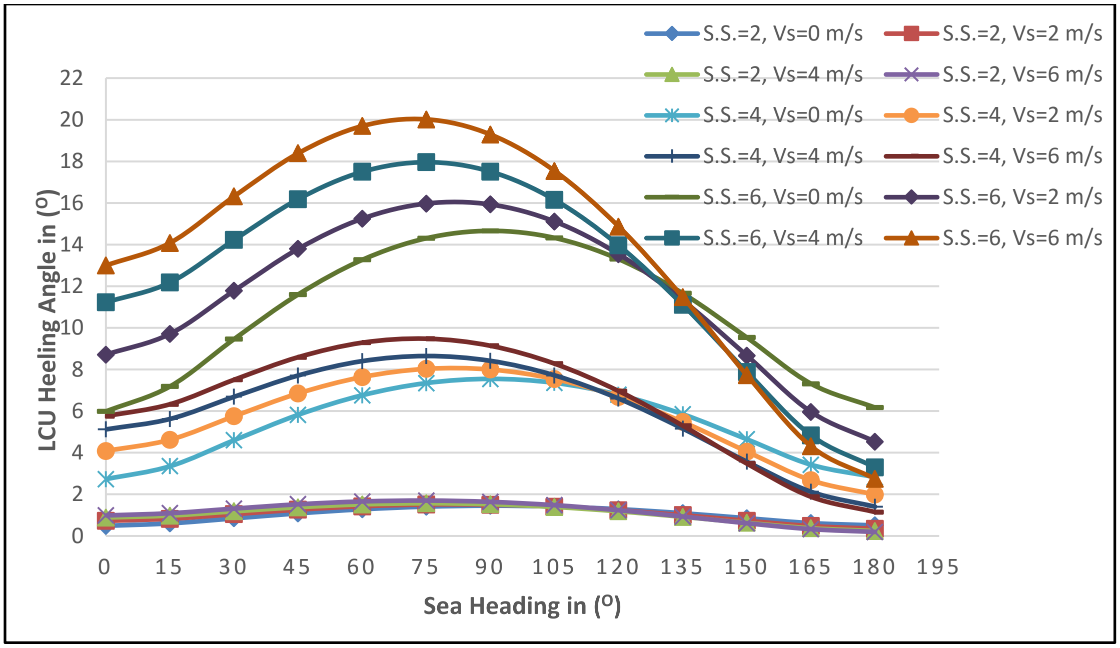

Figure 43. Heeling Angle versus Sea Heading in Ochi-Hubble Short-Crested Waves for LCU Carrying Full Cargo Deadweight

Likewise, the LCU heeling angle responses for the Bretschneider spectrum and the corresponding plots are shown in the Table 10 and Figure 44, respectively.

Table 10. Roll Angle Responses in Bretschneider (Tm = 11 sec) Short-Crested Sea Waves for LCU Carrying Full Cargo Deadweight

Sea Heading (Degrees)	LCU Heeling Angle (Degrees)											
	Sea State 2				Sea State 4				Sea State 6			
	Vs=0 m/s	Vs=2 m/s	Vs=4 m/s	Vs=6 m/s	Vs=0 m/s	Vs=2 m/s	Vs=4 m/s	Vs=6 m/s	Vs=0 m/s	Vs=2 m/s	Vs=4 m/s	Vs=6 m/s
0	0.32	0.48	0.63	0.78	1.98	2.93	3.92	4.8	5.185	7.52	10	12.3
15	0.39	0.53	0.68	0.83	2.37	3.27	4.22	5.13	6.136	8.32	10.8	13.1
30	0.52	0.66	0.79	0.95	3.19	4.02	4.9	5.84	8.025	10	12.3	14.7
45	0.67	0.78	0.9	1.06	4.03	4.77	5.56	6.51	9.845	11.7	13.9	16.3
60	0.78	0.88	0.98	1.13	4.71	5.33	6.01	6.92	11.26	12.9	14.9	17.2
75	0.86	0.93	1	1.13	5.14	5.61	6.14	6.96	12.16	13.5	15.3	17.4
90	0.88	0.92	0.96	1.08	5.28	5.58	5.92	6.61	12.47	13.4	14.8	16.6
105	0.86	0.86	0.87	0.96	5.14	5.24	5.39	5.9	12.17	12.7	13.6	14.9
120	0.78	0.76	0.74	0.79	4.72	4.62	4.57	4.89	11.29	11.4	11.6	12.5
135	0.67	0.62	0.58	0.59	4.05	3.77	3.56	3.69	9.883	9.48	9.24	9.58
150	0.53	0.46	0.4	0.39	3.22	2.82	2.5	2.45	8.084	7.27	6.6	6.48
165	0.39	0.31	0.26	0.23	2.42	1.94	1.59	1.44	6.234	5.1	4.22	3.83
180	0.33	0.24	0.19	0.16	2.04	1.52	1.17	1.02	5.316	4.02	3.11	2.73

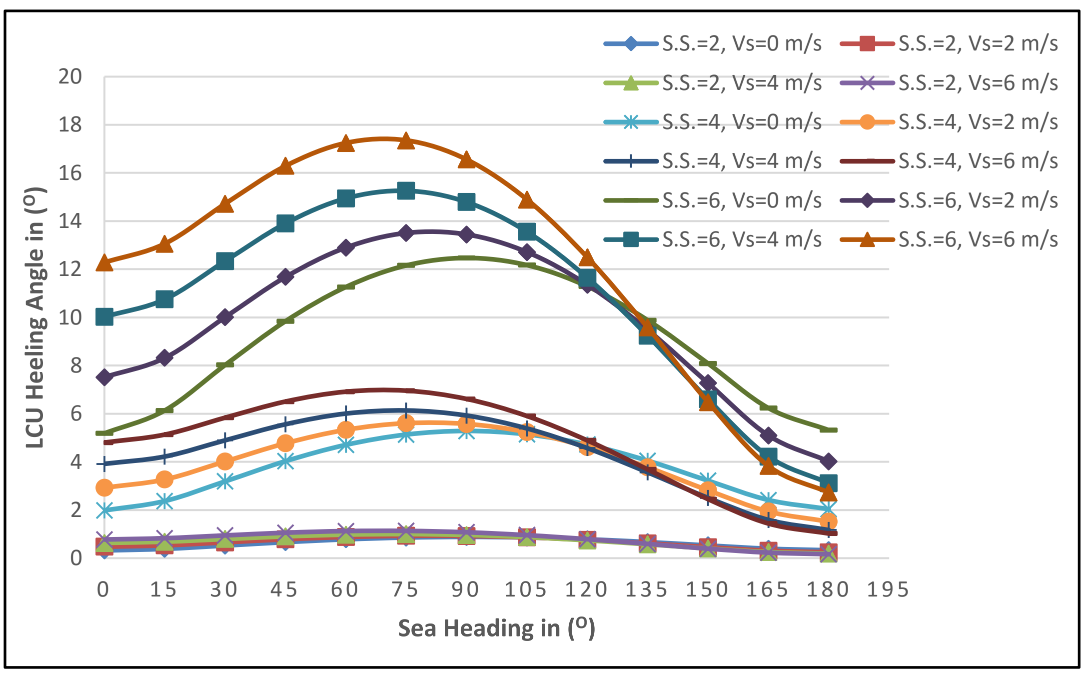

Figure 44. Heeling Angle versus Sea Heading in Bretschneider (Tm = 11 sec) Short-Crested Waves for LCU Carrying Full Cargo Deadweight

THIS PAGE INTENTIONALLY LEFT BLANK

VI. CONCLUSIONS

A. STATIC STABILITY

1. Static Stability Assessment

The static stability of the LCU was considered adequate in all loading cases. The static stability was based on the U.S. Navy's wind-rolling criterion, which was met throughout the operational trade space of the LCU. The research focused on this criterion, since it is the most significant for the operational conditions the ship experiences during short coastal missions.

2. Lightship Loading

A LCU in the lightship loading condition demonstrates adequate static stability in all sea states; the static stability evaluation is based on the satisfaction of the wind-rolling criterion. The LCU meets the minimum requirements of the reserve area as well as the maximum wind heeling arm described in Chapter I. Because the ship is subjected to relatively low wind forces during its coastal missions, the produced wind heeling arm is very low. Given the very low wind heeling arm, the ship's righting arm (GZ) is much higher than the wind heeling arm; both meet the requirements of the wind-rolling criterion. Simulations provided results of the equilibrium point of wind static stability, at which the righting arm is equal to the wind heeling arm. At this point in the sea state 2, the LCU undergoes a heeling angle of 0.31 degrees, as shown in Figure 23. The heeling angles at the equilibrium state in sea states 4 and 6 are 0.35 and 0.48 degrees, respectively, according to Figures 24 and 25. The ship develops a maximum righting arm equal to 1.585 m in all sea states in the lightship condition, which plays a critical role in ensuring the ship's adequate static stability.

3. Half Cargo Deadweight Loading

In all examined sea states, the LCU passed the wind-rolling criterion when carrying half of the maximum allowable cargo deadweight. As with the previous loading condition, the low wind-velocities corresponding to the examined sea state conditions produced very low wind heeling arms for the ship. Combined with the ship's much higher righting arm, the LCU satisfies the wind-rolling stability criterion requirements. At the equilibrium point in sea states 2, 4, and 6, the ship develops a heeling angle equal to 0.33, 0.37, and 0.50 degrees, as demonstrated in Figures 26, 27, and 28, respectively. In this loading case, the ship develops a righting arm of 1.277 m, which is large enough to return the ship to the initial position, and contributes to its adequate static stability.

4. Full Cargo Deadweight Loading

In the most significant loading case, an LCU with a full cargo deadweight load has adequate static stability in all the sea states of our study, satisfying both reserve area and heeling arm requirements. In this case, the produced wind heeling arm remains very low due to the low wind velocities of these sea states. In almost all heeling angles, the ship's righting arm is higher than the wind heeling arm and provides the capability for the ship to return to the equilibrium state. At the equilibrium point's state in sea states 2, 4, and 6, the LCU heeling angle takes values of 0.36, 0.39, and 0.52 degrees, respectively, as shown in Figures 29, 30, and 31. At the equilibrium points, the LCU also generates a maximum righting arm equal to 0.906 m. We observed that the ship's maximum righting arm was reduced as the added weight (in terms of cargo deadweight) increased, which was expected and consistent with our theory.

B. DYNAMIC STABILITY

1. General Observations

In both the Ochi-Hubble and the Bretschneider spectra models and in all loading cases, the plots of the LCU's heeling angle against sea heading demonstrate common features. The LCU undergoes non-zero heeling angles in a sea heading equal to 0 degrees. The heeling angle increases as the sea heading increases from 0 to 75, and from180 to 285, then deceases as the sea heading takes values within the range of 75 to 180, and 285 to 360 degrees. The LCU is subjected to higher heeling angles while traveling in heading seas (sea with the heading in the area of 0 degrees) than while traveling in following seas (when the sea heading is in the area of 180 degrees). The ship undergoes the highest heeling angles while traveling in sea headings within the ranges of either 60 to 90 or 270 to 300 degrees. For the lightship, lightship with half cargo deadweight and lightship with full cargo deadweight loading cases, those heeling angles' maximum values occur in sea state 6 and are 14, 17, and 20 degrees, shown by the plots in Figures 39, 41, and 43 in all loading cases, respectively. The results obtained from the two spectra are very similar. Since the Ochi-Hubble spectrum is more probable, we derived the conclusions based on this spectrum.

Due to this similarity, these conclusions are also applicable to the Bretschneider spectrum with a modal frequency of 11 seconds. Using the Bretschneider spectrum for modal frequencies equal to 7 and 15 seconds, the simulation results[6] of the LCU's roll responses, provide patterns of heeling angle against sea heading very similar to those generated by the Ochi-Hubble spectrum model.

2. Ship Speed Effects

Ship speed is one of the main parameters of the dynamic stability analysis. According to the heeling angle versus sea heading diagrams, we observe that ship speed influences the ship's heeling angle by following certain patterns. For the lightship loading and lightship with half cargo deadweight loading conditions and sea states above 2, the increase in ship speed causes a heeling angle increase for sea headings from 0 to 120 and from 240 to 360 degrees, while causing a heeling angle decrease for sea headings from 120 to 240 degrees. For an LCU with full cargo deadweight and sea states above 2, the ship speed influence is similar; however, the heeling angle increases for sea headings from 0 to 135 and from 225 to 360 degrees, and decreases for sea headings from 135 to 225 degrees. As we can clearly observe in the plots in the sea heading area around

[6] As indicated in the appendix

120 and 240 degrees, the ship speed change does not have any influence on the change of ship-generated heeling angles for any given sea state. As the LCU approaches this region of sea heading, the ship speed change has decreasing influence on the heeling angles' change. As the LCU moves away from that region, the speed change has the opposite effect.

Another significant observation is that the ship speed effect over its heeling angles is greater as the sea state deteriorates, maintaining the same pattern as described previously. Therefore, as the ship's speed changes, the heeling angle variations for all the aforementioned sea headings are greater in higher (worse) sea states. In sea state 2, this variation is negligible; in sea state 6, it is high.

3. Sea State Effects

The most obvious effect of sea states on the ship's heeling angle is that heightened sea states result in higher values of heeling angle throughout the entire range of sea headings, dividing the plots into three distinct areas corresponding to each examined sea state. Keeping the ship speed and loading condition constant, we observed that the sea state influenced both the heeling angle values and the variation of those values. In all sea states, the ship undergoes increased heeling angles for sea headings ranging from 0 to 75 degrees and from 180 to 285 degrees; it experiences decreasing heeling angles as sea headings ranging from 75 to 180 and 285 to 360 degrees. The variations in the heeling angle values are greater in higher sea states; as shown in the diagrams, the higher sea state is represented by steep curves, while the lower sea states are represented by clearly flatter curves. Moreover, as the sea state increases, the ship's speed effects (described earlier) become more intense.

4. Loading Condition Effects

Keeping the ship speed and sea state constant, we can observe that in all ranges of sea headings the LCU experiences higher heeling angles in the higher displacement loading conditions. For example, the LCU's highest values of heeling angle, which were observed in sea state 6 and in ship's speed 6 m/s, are 14, 17, and 20 degrees for the lightship, half cargo deadweight, and full cargo deadweight loading cases, respectively. Furthermore, the higher the displacement of the LCU, the more intense the ship-speed effects (discussed earlier). Therefore, for each specific ship's speed and sea state, in the full cargo deadweight loading condition, we observed more intense variations of the ship's heeling angle than in the lightship and half cargo deadweight loading conditions. Additionally, the main pattern of the heeling angle versus sea heading plots remains the same regardless the variants of the loading condition.

C. OPERATIONAL RECOMMENDATIONS FOR THE LCU

A further objective of this study is to provide practical recommendations that can be used as an operational guide for the LCU. According to the conclusions described previously, we can derive some particular directions for facilitating a safer and more effective way for the LCU to perform its coastal missions. Generally, it is recommended that the ship's operators favor following seas over heading seas when this is possible, as the ship is less susceptible to higher heeling angles in those conditions. When the ship operates in sea states 2 or lower, no specific recommendations are required since it is subjected to very low heeling angles in all loading conditions and sea headings. To mitigate the negative effect of the highest heeling angle values, it is recommended that the ship operators avoid sea headings in the regions 60 to 90, and 270 to 300 degrees, if possible, in sea states greater than 2 (when the ship experiences higher heeling angles depending on sea heading). The higher the sea state, the stronger this recommendation.

Another significant recommendation is associated with the ship's speed, combined with sea headings. Assuming that the objective of a ship's operators is to mitigate the heeling angles the ship undergoes, the study suggests certain ship speed adjustments in order to achieve this objective for various loading conditions and sea states. For the lightship and half cargo deadweight loading conditions, and in sea states 4 and 6, if the ship operates keeping sea headings 0 to 120 and

240 to 360 degrees, it is recommended the operators reduce speed or maintain ship's speed close to 4 knots (if feasible). If the LCU operates while keeping the sea heading 120 to 240 degrees, then the operators should reduce speed or maintain speed close to 11 knots, if possible. Likewise, for the full cargo deadweight loading case, if the LCU operates at a sea heading 0 to 135 or 225 to 360 degrees, it is recommended that the ship's speed be reduced or maintained close to 4 knots. The ship's speed should be increased or kept close to 11 knots in cases where the ship operates at sea headings of 135 to 225 degrees, if these are maritime allowed. All the preceding recommendations for mitigating the heeling angles that an LCU undergoes are summarized as a practical operational guide in Table 11.

Table 11. LCU Sea Heading and Speed Operational Guide (Conditions Permitting)

Given Variables \ Selected Variables		Sea Heading (Degrees)	Ship Speed (Knots)	
Lightship, and Half Cargo Deadweight Loading Cases			**Sea Heading 0–120 and 240–360**	**Sea Heading 120–240**
	Sea State 2	-	-	-
	Sea State 4	Avoid sea headings 60 – 90 and 270 – 300	Reduce or maintain speed close to 4	Increase or maintain speed close to 11
	Sea State 6	Avoid sea headings 60 – 90 and 270 – 300	Reduce or maintain speed close to 4	Increase or maintain speed close to 11
Full Cargo Deadweight Loading Case			**Sea Heading 0–135 and 225–360**	**Sea Heading 135–225**
	Sea State 2	-	-	-
	Sea State 4	Avoid sea headings 60 – 90 and 270 – 300	Reduce or maintain speed close to 4	Increase or maintain speed close to 11
	Sea State 6	Avoid sea headings 60 – 90 and 270 – 300	Reduce or maintain speed close to 4	Increase or maintain speed close to 11

The operational recommendations for the various loading conditions and sea states in Table 11 are better visualized in the polar diagrams. In these diagrams, the radial component represents the sea states (4 to 6 here), while the angular component represents the heading. Figure 45 shows the recommended actions for the LCU operators in the lightship and the half deadweight loading cases in sea states 4 and 6, for any possible sea heading. Likewise, Figure 46 provides the operational recommendations for the LCU carrying a full cargo deadweight in the same sea state conditions. Further results should refine recommended actions for regions of other sea states as well.

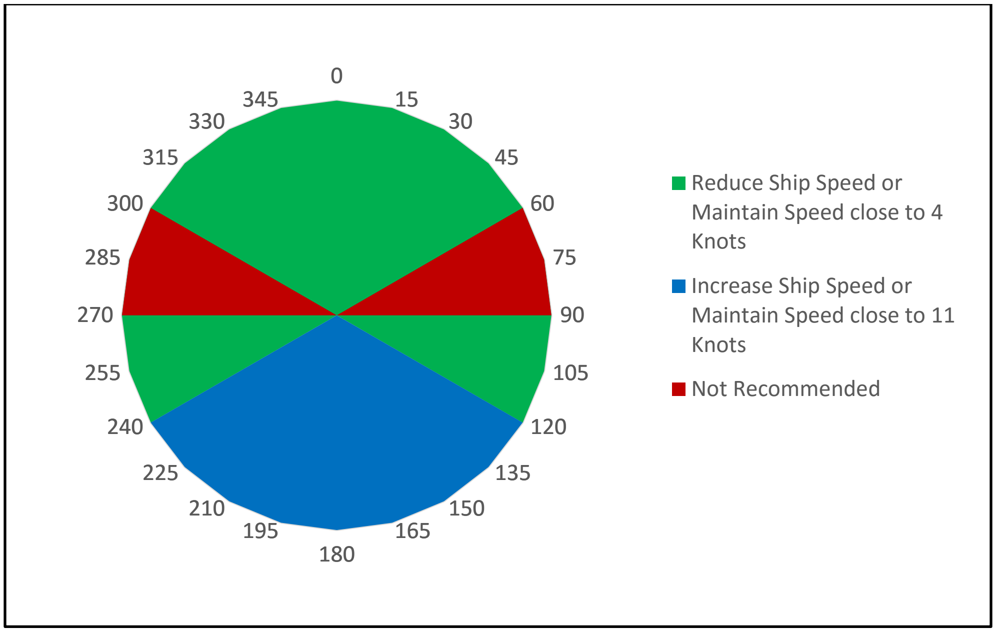

Figure 45. Sea Headings Based Operational Polar Diagram for LCU Lightship and Lightship with Half Cargo Deadweight in Sea States 4 and 6

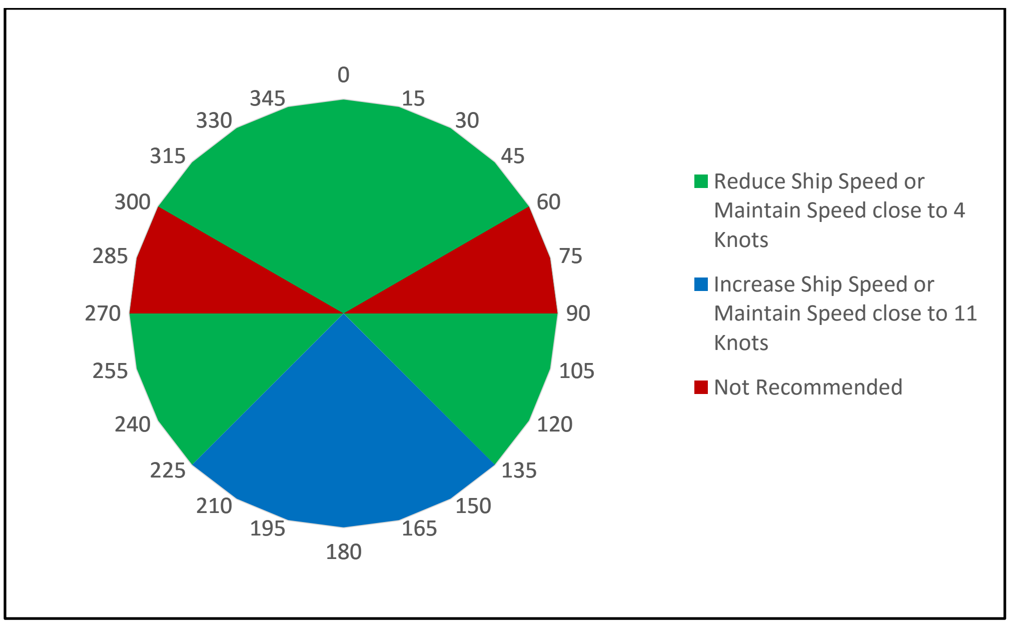

Figure 46. Sea Headings Based Operational Polar Diagram for LCU Carrying Full Cargo Deadweight in Sea States 4 and 6

D. FUTURE WORK

This study's outcomes correspond with the most likely conditions related to the usual LCU coastal missions. The research modeled these conditions, which are associated with the ship's loading cases, as well as actual coastal sea features. An LCU's stability performance has been found to be dependent on the sea state, sea heading, ship's loading condition, and speed. The research examined only the intact stability of the craft, operating within a certain set of values of the stability influencing factors, as just mentioned.

Any future work should focus on the examination of the effects of potential hull adjustments on the intact LCU dynamic responses in a similarly modeled coastal water environment. One of those adjustments could be the addition of appendages, such as passive stabilization fins in the bottom of the ship's hull. Another adjustment could be the modification of the craft tanks in order to mitigate the free surface effect. It is highly probable that these adjustments will improve the ship's dynamic responses by reducing the resulting rolling angles. Future work should keep the loading conditions and the sea environment parameters as established in this research, as they define the most realistic trade space of the LCU's usual missions.

Finally, future research could examine the damage stability of the LCU. For example, such research could examine the static and dynamic responses of the craft during a flooding event due to an enemy hit. As stated earlier, it is recommended any future research keep the same operational trade space. Such a study could contribute to an LCU survivability assessment during its usual missions.

THIS PAGE INTENTIONALLY LEFT BLANK

APPENDIX

A. MATLAB CODE FOR DETERMINATION OF THE WIND-ROLLING STATIC STABILITY EQUILIBRIUM FOR ALL LCU LOADING CASES

```
% Wind-Rolling Static Stability Equilibrium Determination Based on the Equation
% GZ(θ)= WHA(θ)

% A: Ship’s Projected Area in m^2
% D: Ship’s Displacement in MT
% L: Distance between Projected Area and Hull Profile Centroids in m
% GM: Ship’s Metacentric Height in m
% Vk: Wind Velocity in Knots
% theta: Static Stability Equilibrium Heeling Angle in Degrees


% (1) LCU Lightship Loading Case

clear all
% Variables Initialization
A1 = 151;
D1 = 257;
L1 = 2.134;
bar_scale = [0:0.02:2.134];
iGM = 0;
GMmin = 1;
GMmax = 6;
strGMmin = num2str(GMmin);
strGMmax = num2str(GMmax);
for GM = GMmin:1:GMmax;
 iGM = iGM + 1;
 GM_vector(iGM) = GM;
 iVk = 0;
 for Vk = 1:0.1:60,
  iVk = iVk + 1;
  % Coefficient of the Equation “WHA(θ)=(Coef)*(cosθ)^2”
  % WHA(θ)= [0.0171*Vk^2*A*L/(1000*D)]*(cosθ)^2
  Coef = 0.0171*Vk*Vk*A1*L1/(1000*D1);
  % Equilibrium: GM*sinθ=WHA(θ)
  C = Coef/GM;
  % Determines the Equilibrium Heeling Angle
  sin1 = (-1+sqrt(1+4*C*C))/(2*C);
  theta = 57.3*asin(sin1);
```

```
  Vk_vector(iVk) = Vk;
  theta_vector(iGM,iVk) = theta;
 end
end

figure(1)
% Provides Graphical Metacentric Height Values for Various
% Equilibrium States Given by Various Combinations of Heeling
% Angles and Wind Velocities
plot(Vk_vector,theta_vector,'LineWidth',2),grid
ylabel('Static Heel Angle\theta (deg)')
xlabel('Wind Speed (knots)')
title(['LCU-LIGHTSHIP GM from ',strGMmin,' m to ',strGMmax,' m - Small Angles Approximation'])
legend('GM=1m','GM=2m','GM=3m','GM=4m','GM=5m','GM=6m')


figure(2)

% Provides Graphical Heeling Angle Values for Various Equilibrium
% States Given by Various Combinations of Metacentric Heights and
% Wind Velocities
contourf(Vk_vector,GM_vector,theta_vector,bar_scale),colorbar
xlabel('Wind Speed (knots)'),ylabel('GM (m)')
title('LCU-LIGHTSHIP Static Heel Angle\theta (deg) - Small Angles Approximation')
shading flat


% (2) LCU with Half Cargo Deadweight Loading Case

clear all
% Variables Initialization
A2 = 151;
D2 = 314;
L2 = 2.134;
bar_scale = [0:0.02:2.134];
iGM = 0;
GMmin = 1;
GMmax = 6;
strGMmin = num2str(GMmin);
strGMmax = num2str(GMmax);
for GM = GMmin:1:GMmax;
 iGM = iGM + 1;
 GM_vector(iGM) = GM;
```

```
 iVk = 0;
 for Vk = 1:0.1:60,
  iVk = iVk + 1;
  % Coefficient of the Equation “WHA(θ)=(Coef)*(cosθ)^2”
  % WHA(θ)= [0.0171*Vk^2*A*L/(1000*D)]*(cosθ)^2
  Coef = 0.0171*Vk*Vk*A2*L2/(1000*D2);
  % Equilibrium: GM*sinθ=WHA(θ)
  C = Coef/GM;
  % Determines the Equilibrium Heeling Angle
  sin1 = (-1+sqrt(1+4*C*C))/(2*C);
  theta = 57.3*asin(sin1);
  Vk_vector(iVk) = Vk;
  theta_vector(iGM,iVk) = theta;
 end
end

figure(3)
% Provides Graphical Metacentric Height Values for Various
% Equilibrium States Given by Various Combinations of Heeling
% Angles and Wind Velocities
plot(Vk_vector,theta_vector,’LineWidth’,2),grid
ylabel(‘Static Heel Angle\theta (deg)’)
xlabel(‘Wind Speed (knots)’)
title([‘LCUHALF CARGO GM from ‘,strGMmin,’ m to ‘,strGMmax,’ m - Small Angles Approximation’])
legend(‘GM=1m’,’GM=2m’,’GM=3m’,’GM=4m’,’GM=5m’,’GM=6m’)

 figure(4)
% Provides Graphical Heeling Angle Values for Various Equilibrium
% States Given by Various Combinations of Metacentric Heights and
% Wind Velocities
contourf(Vk_vector,GM_vector,theta_vector,bar_scale),colorbar
xlabel(‘Wind Speed (knots)’),ylabel(‘GM (m)’)
title(‘LCUHALF CARGO Static Heel Angle\theta (deg) - Small Angles Approximation’)
shading flat


% (3) LCU Carrying Full Cargo Deadweight Loading Case

clear all
% Variables Initialization
A3 = 151;
D3 = 371;
L3 = 2.134;
```

```
bar_scale = [0:0.02:2.134];
iGM = 0;
GMmin = 1;
GMmax = 6;
strGMmin = num2str(GMmin);
strGMmax = num2str(GMmax);
for GM = GMmin:1:GMmax;
 iGM = iGM + 1;
 GM_vector(iGM) = GM;
 iVk = 0;
 for Vk = 1:0.1:60,
  iVk = iVk + 1;
  % Coefficient of the Equation “WHA(θ)=(Coef)*(cosθ)^2”
  % WHA(θ)= [0.0171*Vk^2*A*L/(1000*D)]*(cosθ)^2
  Coef = 0.0171*Vk*Vk*A3*L3/(1000*D3);
  % Equilibrium: GM*sinθ=WHA(θ)
  C = Coef/GM;
  % Determines the Equilibrium Heeling Angle
  sin1 = (-1+sqrt(1+4*C*C))/(2*C);
  theta = 57.3*asin(sin1);
  Vk_vector(iVk) = Vk;
  theta_vector(iGM,iVk) = theta;
 end
end

figure(5)
% Provides Graphical Metacentric Height Values for Various
% Equilibrium States Given by Various Combinations of Heeling
% Angles and Wind Velocities
plot(Vk_vector,theta_vector,’LineWidth’,2),grid
ylabel(‘Static Heel Angle\theta (deg)’)
xlabel(‘Wind Speed (knots)’)
title([‘LCU FULL CARGO GM from ‘,strGMmin,’ m to ‘,strGMmax,’ m - Small Angles
Approximation’])
legend(‘GM=1m’,’GM=2m’,’GM=3m’,’GM=4m’,’GM=5m’,’GM=6m’)

 figure(6)
% Provides Graphical Heeling Angle Values for Various Equilibrium
% States Given by Various Combinations of Metacentric Heights and
% Wind Velocities
contourf(Vk_vector,GM_vector,theta_vector,bar_scale),colorbar
xlabel(‘Wind Speed (knots)’),ylabel(‘GM (m)’)
title(‘LCU FULL CARGO Static Heel Angle\theta (deg) - Small Angles
Approximation’)
shading flat
```

B. ROLL ANGLE RESPONSES IN BRETSCHNEIDER SPECTRUM FOR LCU LIGHTSHIP

Table 12. Roll Angle Responses in Bretschneider (Tm = 7 sec) Short-Crested Sea Waves for LCU Lightship

Sea Heading (Degrees)	LCU Heeling Angle (Degrees)											
	Sea State 2				Sea State 4				Sea state 6			
	Vs=0 m/s	Vs=2 m/s	Vs=4 m/s	Vs=6 m/s	Vs=0 m/s	Vs=2 m/s	Vs=4 m/s	Vs=6 m/s	Vs=0 m/s	Vs=2 m/s	Vs=4 m/s	Vs=6 m/s
0	0.43	0.56	0.75	0.88	2.65	3.49	4.65	5.48	7.02	9.19	12.19	14.36
15	0.51	0.65	0.82	0.95	3.20	4.02	5.13	5.95	8.44	10.55	13.42	15.56
30	0.70	0.83	0.99	1.12	4.36	5.16	6.17	6.96	11.34	13.38	16.04	18.13
45	0.90	1.01	1.16	1.28	5.56	6.28	7.20	7.95	14.26	16.14	18.60	20.62
60	1.06	1.15	1.28	1.38	6.53	7.13	7.92	8.60	16.57	18.19	20.38	22.26
75	1.16	1.23	1.32	1.41	7.15	7.59	8.20	8.77	18.03	19.28	21.08	22.71
90	1.20	1.23	1.29	1.36	7.36	7.60	8.01	8.44	18.53	19.33	20.63	21.91
105	1.16	1.16	1.18	1.23	7.16	7.18	7.36	7.63	18.05	18.33	19.05	19.88
120	1.06	1.02	1.01	1.03	6.54	6.35	6.30	6.41	16.61	16.34	16.44	16.80
135	0.90	0.84	0.80	0.79	5.58	5.19	4.96	4.92	14.13	13.51	13.06	13.00
150	0.71	0.62	0.56	0.54	4.39	3.86	3.51	3.37	11.41	10.16	9.13	8.95
165	0.52	0.42	0.36	0.33	3.24	2.63	2.23	2.04	8.53	6.97	5.95	5.45
180	0.43	0.33	0.26	0.23	2.70	2.04	1.64	1.45	7.13	5.43	4.37	3.87

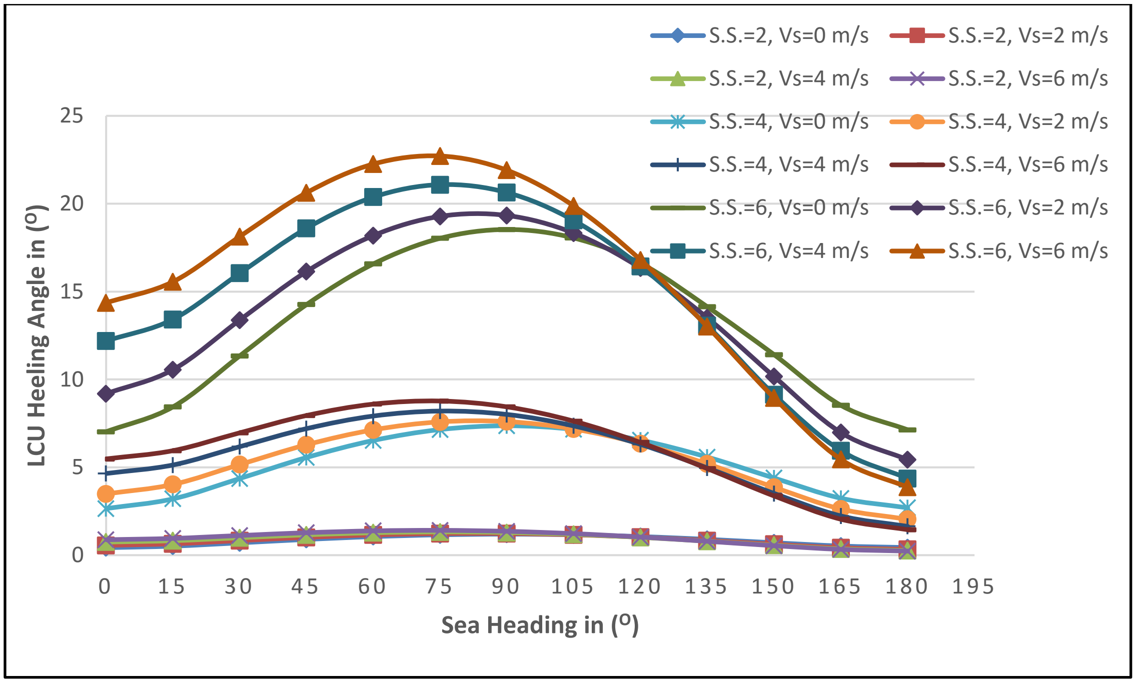

Figure 47. Heeling Angle versus Sea Heading in Bretschneider (Tm = 7 sec) Short-Crested Waves for LCU Lightship

Table 13. Roll Angle Responses in Bretschneider (Tm = 15 sec) Short-Crested Sea Waves for LCU Lightship

Sea Heading (Degrees)	LCU Heeling Angle (Degrees)											
	Sea State 2				Sea State 4				Sea state 6			
	Vs=0 m/s	Vs=2 m/s	Vs=4 m/s	Vs=6 m/s	Vs=0 m/s	Vs=2 m/s	Vs=4 m/s	Vs=6 m/s	Vs=0 m/s	Vs=2 m/s	Vs=4 m/s	Vs=6 m/s
0	0.16	0.19	0.24	0.28	0.99	1.18	1.47	1.74	2.64	3.15	3.92	4.64
15	0.18	0.21	0.26	0.30	1.12	1.31	1.59	1.86	2.98	3.49	4.24	4.94
30	0.23	0.26	0.30	0.34	1.41	1.60	1.86	2.11	3.75	4.25	4.95	5.63
45	0.28	0.30	0.34	0.38	1.73	1.90	2.14	2.38	4.59	5.05	5.69	6.32
60	0.32	0.34	0.38	0.41	1.99	2.14	2.34	2.55	5.30	5.68	6.23	6.79
75	0.35	0.36	0.39	0.42	2.17	2.27	2.43	2.60	5.76	6.04	6.46	6.93
90	0.36	0.37	0.38	0.40	2.23	2.28	2.38	2.51	5.93	6.06	6.34	6.69
105	0.35	0.35	0.35	0.37	2.17	2.17	2.21	2.29	5.77	5.76	5.89	6.10
120	0.32	0.31	0.31	0.31	2.00	1.94	1.93	1.96	5.31	5.17	5.14	5.23
135	0.28	0.26	0.25	0.25	1.73	1.63	1.58	1.57	4.60	4.35	4.21	4.19
150	0.23	0.21	0.19	0.19	1.41	1.29	1.21	1.18	3.76	3.44	3.23	3.14
165	0.18	0.16	0.15	0.14	1.12	0.99	0.91	0.87	3.00	2.64	2.42	2.32
180	0.16	0.14	0.13	0.12	1.00	0.87	0.79	0.75	2.66	2.31	2.10	2.00

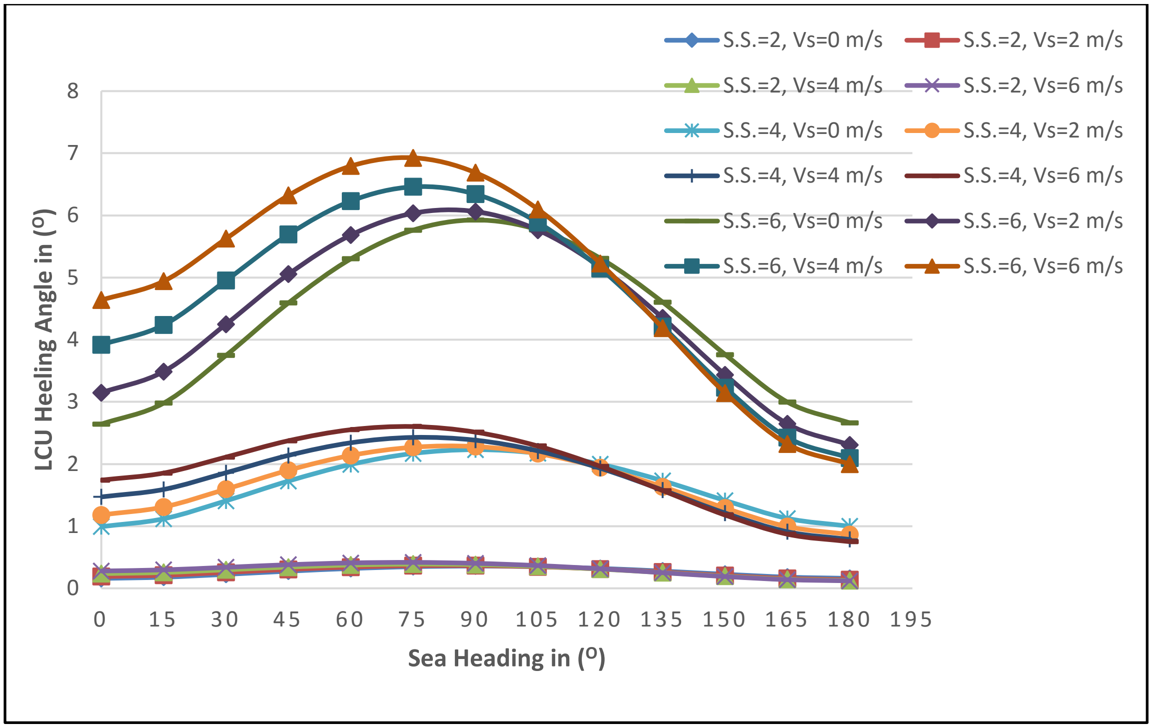

Figure 48. Heeling Angle versus Sea Heading in Bretschneider (Tm = 15 sec) Short-Crested Waves for LCU Lightship

C. ROLL ANGLE RESPONSES IN BRETSCHNEIDER SPECTRUM FOR LCU PLUS HALF CARGO DEADWEIGHT LOADING CASE

Table 14. Angle Responses in Bretschneider (Tm = 7 sec) Short-Crested Sea Waves LCU Carrying Half Cargo Deadweight

Sea Heading (Degrees)	LCU Heeling Angle (Degrees)											
	Sea State 2				Sea State 4				Sea state 6			
	Vs=0 m/s	Vs=2 m/s	Vs=4 m/s	Vs=6 m/s	Vs=0 m/s	Vs=2 m/s	Vs=4 m/s	Vs=6 m/s	Vs=0 m/s	Vs=2 m/s	Vs=4 m/s	Vs=6 m/s
0	0.51	0.72	0.98	1.16	3.14	4.48	6.06	7.14	8.13	11.36	15.32	18.11
15	0.62	0.83	1.08	1.25	3.85	5.13	6.65	7.70	9.80	12.89	16.71	19.48
30	0.87	1.06	1.29	1.45	5.30	6.50	7.91	8.92	13.06	15.98	19.63	22.40
45	1.11	1.29	1.50	1.65	6.73	7.82	9.12	10.09	16.19	18.89	22.38	25.16
60	1.32	1.46	1.64	1.77	7.86	8.79	9.94	10.83	18.57	20.97	24.22	26.89
75	1.45	1.55	1.69	1.80	8.56	9.28	10.22	10.99	20.04	22.03	24.88	27.29
90	1.49	1.55	1.64	1.72	8.81	9.26	9.93	10.51	20.54	22.02	24.29	26.26
105	1.45	1.45	1.49	1.54	8.57	8.72	9.08	9.44	20.06	20.92	22.45	23.83
120	1.32	1.27	1.26	1.27	7.88	7.71	7.75	7.87	18.61	18.76	19.43	20.12
135	1.12	1.03	0.98	0.96	6.76	6.30	6.04	5.97	16.24	15.63	15.42	15.46
150	0.87	0.75	0.67	0.64	5.34	4.63	4.17	3.97	13.14	11.81	10.87	10.44
165	0.64	0.49	0.40	0.36	3.91	3.05	2.49	2.23	9.94	8.00	6.59	5.94
180	0.52	0.37	0.27	0.22	3.22	2.28	1.67	1.39	8.32	6.03	4.44	3.71

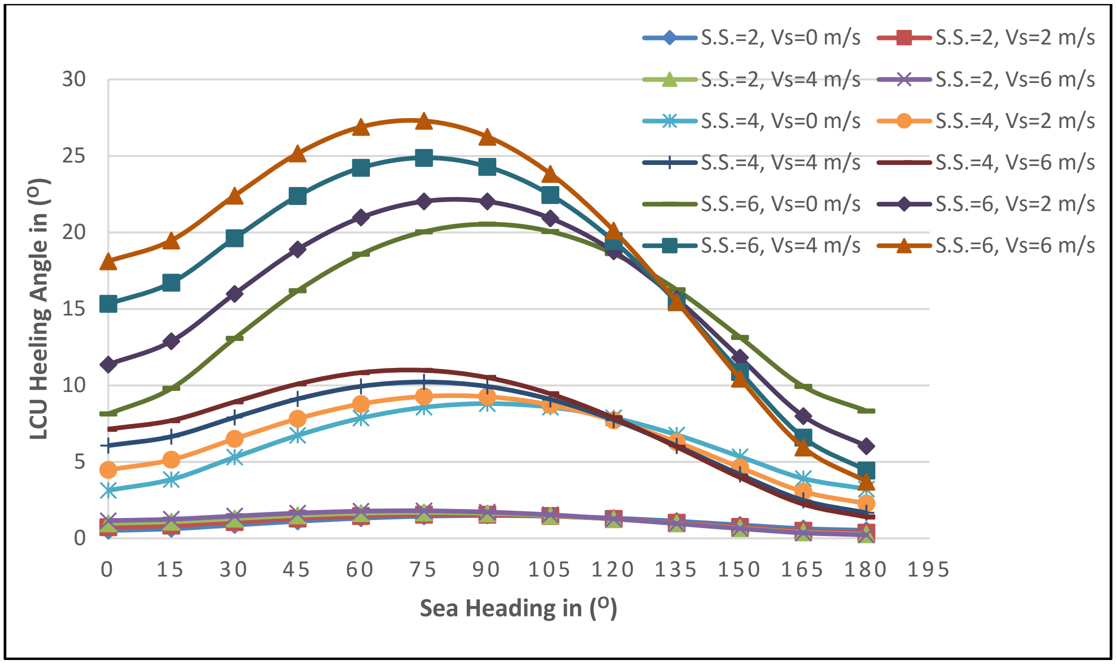

Figure 49. Heeling Angle versus Sea Heading in Bretschneider (Tm = 7 sec) Short-Crested Waves for LCU Carrying Half Cargo Deadweight

Table 15. Roll Angle Responses in Bretschneider (Tm = 15 sec) Short-Crested Sea Waves for LCU Carrying Half Cargo Deadweight

Sea Heading (Degrees)	LCU Heeling Angle (Degrees)											
	Sea State 2				Sea State 4				Sea state 6			
	Vs=0 m/s	Vs=2 m/s	Vs=4 m/s	Vs=6 m/s	Vs=0 m/s	Vs=2 m/s	Vs=4 m/s	Vs=6 m/s	Vs=0 m/s	Vs=2 m/s	Vs=4 m/s	Vs=6 m/s
0	0.17	0.22	0.30	0.36	1.07	1.39	1.84	2.24	2.86	3.70	4.88	5.96
15	0.20	0.25	0.32	0.38	1.24	1.55	1.98	2.38	3.28	4.12	5.26	6.31
30	0.26	0.31	0.37	0.43	1.60	1.90	2.31	2.68	4.23	5.03	6.11	7.10
45	0.32	0.36	0.42	0.48	1.98	2.26	2.63	2.99	5.24	5.97	6.96	7.89
60	0.37	0.41	0.46	0.51	2.31	2.54	2.86	3.18	6.06	6.68	7.54	8.39
75	0.41	0.43	0.47	0.51	2.52	2.69	2.94	3.20	6.59	7.05	7.75	8.46
90	0.42	0.43	0.46	0.49	2.59	2.68	2.85	3.05	6.78	7.04	7.53	8.07
105	0.41	0.41	0.42	0.44	2.52	2.53	2.61	2.73	6.60	6.65	6.91	7.25
120	0.37	0.36	0.36	0.37	2.31	2.24	2.24	2.29	6.07	5.92	5.95	6.09
135	0.32	0.30	0.29	0.29	1.99	1.85	1.79	1.78	5.25	4.92	4.76	4.73
150	0.26	0.23	0.21	0.20	1.61	1.43	1.32	1.28	4.25	3.79	3.51	3.40
165	0.20	0.17	0.15	0.14	1.25	1.05	0.93	0.88	3.31	2.80	2.49	2.36
180	0.17	0.14	0.12	0.12	1.09	0.89	0.78	0.73	2.89	2.37	2.07	1.95

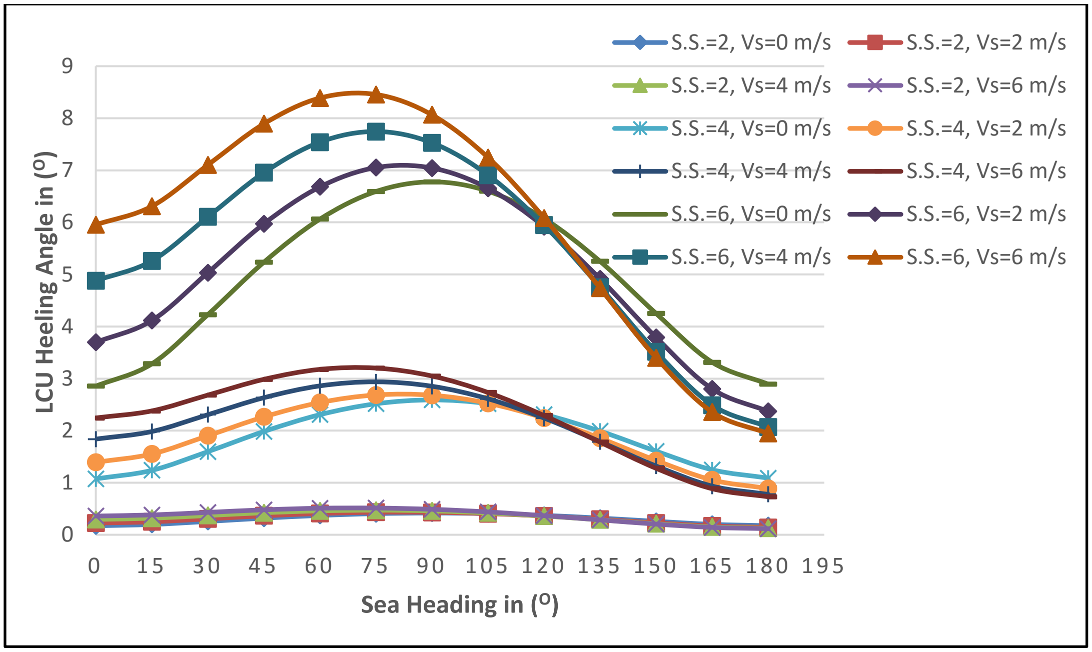

Figure 50. Heeling Angle versus Sea Heading in Bretschneider (Tm = 15 sec) Short-Crested Waves for LCU Carrying Half Cargo Deadweight

D. ROLL ANGLE RESPONSES IN BRETSCHNEIDER SPECTRUM FOR LCU PLUS FULL CARGO DEADWEIGHT LOADING CASE

Table 16. Roll Angle Responses in Bretschneider (Tm = 7 sec) Short-Crested Sea Waves for LCU Carrying Full Cargo Deadweight

Sea Heading (Degrees)	LCU Heeling Angle (Degrees)											
	Sea State 2				Sea State 4				Sea state 6			
	Vs=0 m/s	Vs=2 m/s	Vs=4 m/s	Vs=6 m/s	Vs=0 m/s	Vs=2 m/s	Vs=4 m/s	Vs=6 m/s	Vs=0 m/s	Vs=2 m/s	Vs=4 m/s	Vs=6 m/s
0	0.62	0.94	1.21	1.39	3.76	5.67	7.31	8.44	9.28	13.49	17.68	20.65
15	0.77	1.07	1.32	1.52	4.64	6.40	7.98	9.19	11.07	15.00	19.14	22.29
30	1.08	1.35	1.58	1.80	6.33	7.90	9.39	10.73	14.44	18.06	22.17	25.60
45	1.39	1.63	1.83	2.06	7.92	9.34	10.76	12.18	17.53	20.90	24.99	28.59
60	1.64	1.84	2.00	2.23	9.12	10.37	11.68	13.09	19.81	22.88	26.85	30.45
75	1.81	1.95	2.06	2.27	9.86	10.90	12.00	13.32	21.19	23.88	27.53	30.92
90	1.86	1.94	1.99	2.17	10.12	10.86	11.68	12.81	21.65	23.85	26.95	29.95
105	1.81	1.82	1.82	1.95	9.87	10.28	10.73	11.59	21.21	22.79	25.11	27.51
120	1.65	1.60	1.54	1.62	9.14	9.17	9.21	9.76	19.85	20.68	22.01	23.63
135	1.40	1.29	1.19	1.22	7.96	7.60	7.25	7.45	17.60	17.56	17.76	18.47
150	1.09	0.94	0.82	0.79	6.39	5.69	5.03	4.88	14.55	13.60	12.71	12.50
165	0.79	0.61	0.47	0.41	4.74	3.76	2.93	2.55	11.26	9.43	7.68	6.75
180	0.64	0.45	0.29	0.23	3.90	2.75	1.84	1.41	9.55	7.13	4.88	3.75

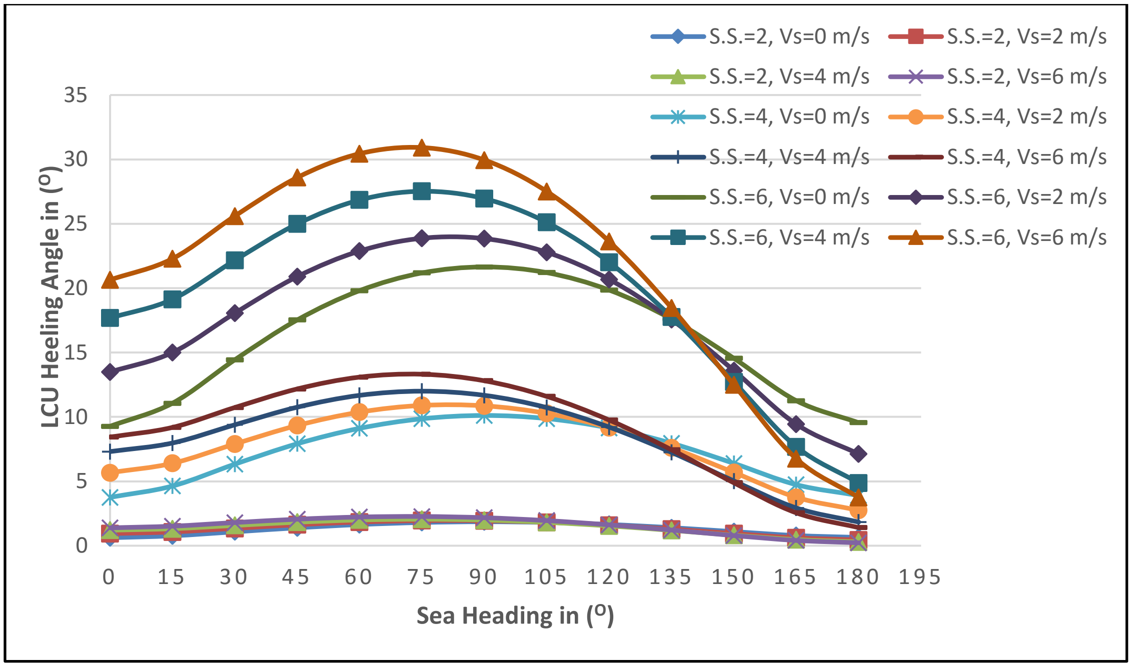

Figure 51. Heeling Angle versus Sea Heading in Bretschneider (Tm = 7 sec) Short-Crested Waves LCU Carrying Full Cargo Deadweight

Table 17. Roll Angle Responses in Bretschneider (Tm = 15 sec) Short-Crested Sea Waves for LCU Carrying Full Cargo Deadweight

Sea Heading (Degrees)	LCU Heeling Angle (Degrees)											
	Sea State 2				Sea State 4				Sea state 6			
	Vs=0 m/s	Vs=2 m/s	Vs=4 m/s	Vs=6 m/s	Vs=0 m/s	Vs=2 m/s	Vs=4 m/s	Vs=6 m/s	Vs=0 m/s	Vs=2 m/s	Vs=4 m/s	Vs=6 m/s
0	0.19	0.28	0.36	0.45	1.20	1.71	2.26	2.77	3.18	4.49	5.94	7.28
15	0.23	0.31	0.39	0.47	1.42	1.90	2.43	2.95	3.72	4.98	6.37	7.74
30	0.30	0.38	0.45	0.54	1.87	2.32	2.80	3.35	4.88	6.04	7.33	8.73
45	0.38	0.45	0.51	0.60	2.35	2.75	3.19	3.73	6.06	7.10	8.28	9.67
60	0.45	0.50	0.56	0.64	2.74	3.08	3.44	3.97	6.99	7.87	8.91	10.25
75	0.49	0.53	0.57	0.64	2.99	3.24	3.52	3.99	7.57	8.26	9.11	10.31
90	0.51	0.53	0.55	0.61	3.08	3.23	3.40	3.79	7.77	8.23	8.83	9.83
105	0.49	0.49	0.50	0.54	3.00	3.03	3.10	3.38	7.58	7.77	8.08	8.82
120	0.45	0.43	0.42	0.45	2.75	2.67	2.64	2.81	7.00	6.91	6.92	7.39
135	0.38	0.36	0.33	0.34	2.36	2.20	2.08	2.14	6.08	5.73	5.49	5.66
150	0.31	0.27	0.24	0.23	1.89	1.66	1.49	1.46	4.92	4.38	3.96	3.89
165	0.23	0.19	0.16	0.15	1.44	1.18	1.00	0.93	3.78	3.13	2.67	2.47
180	0.20	0.15	0.13	0.12	1.23	0.96	0.79	0.72	3.25	2.55	2.11	1.93

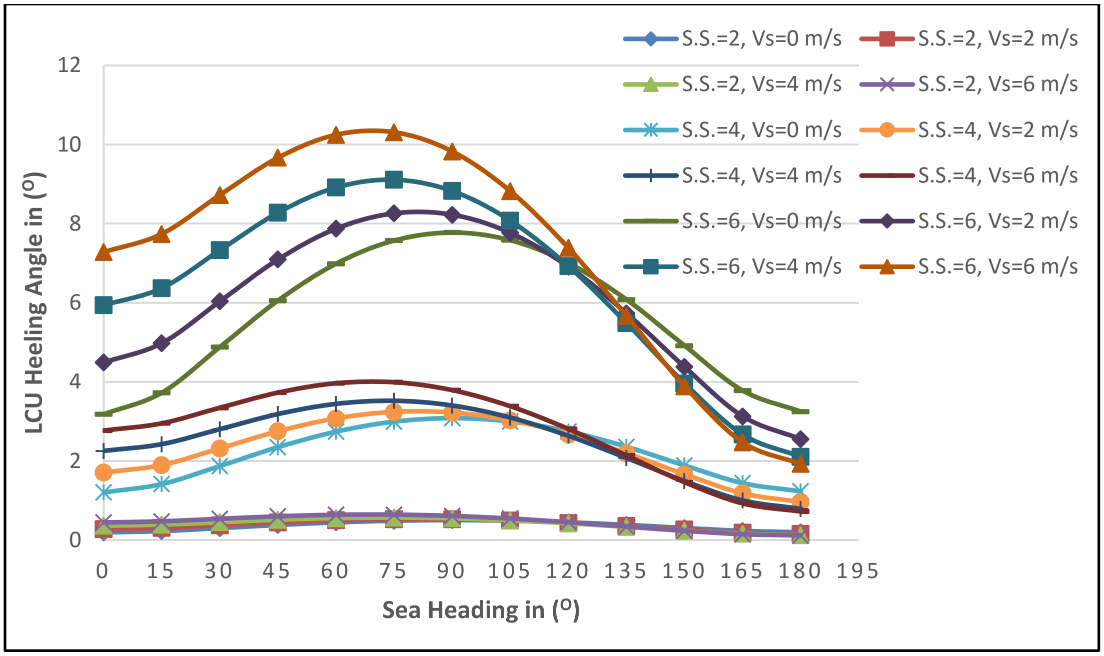

Figure 52. Heeling Angle versus Sea Heading in Bretschneider (Tm = 15 sec) Short-Crested Waves LCU Carrying Full Cargo Deadweight

THIS PAGE INTENTIONALLY LEFT BLANK

LIST OF REFERENCES

[1] "Landing Craft Utility 1600 Class," Jane's by IHS Markit, February 21, 2017 [Online]. Available: https://janes.ihs.com.libproxy.nps.edu/Janes/Display/jfs_a509-jfs.

[2] G. Koelbel. "Procedures manual, dynamic stability analysis for U.S. Navy small craft," Combatant Craft Engineering Naval Ship Engineering Center, Norfolk Division, Norfolk, Virginia, USA, Rep. 23095-1, 1977, pp. 11–40. [Online]. Available: http://www.dtic.mil/dtic/tr/fulltext/u2/a047493.pdf.

[3] T. Sarchin and L. Goldberg, *Stability and Buoyancy Criteria for U.S. Naval Surface Ships,* 1st ed. New York, NY, USA: Society of Naval Architects and Marine Engineers, 1963, ch. 12, sec. 7, pp. 429–433.

[4] "Dynamics of marine vehicles," class notes for Cooperative Control of Multiple Marine Autonomous Vehicles, Dept. of Mechanical and Aerospace Engineering, Naval Postgraduate School, Monterey, CA, USA, summer 1993, pp. 80–83, 86–87, 92–125.

[5] "Seakeeping," class notes for Integration of Naval Engineering Systems, Dept. of Mechanical and Aerospace Engineering, Naval Postgraduate School, Monterey, CA, USA, spring 2017, pp.11, 23.

[6] R. Beck, W. Cummins, and W. Dalzell, *Principles of Naval Architects*. New York, NY, USA: Society of Naval Architects and Marine Engineers, 1989, pp. 18–20, 36–38.

[7] *Ship Motions Program*, 3rd ed., Herbert-ABS, Alameda, CA, USA, 2012, pp. 10–34.

[8] "Ocean Waves," class notes for Ocean Engineering Dept. of Mechanical Engineering, Massachusetts Institute of Technology, Boston, MA, USA, 2005, pp. 7–10. [Online]. Available: https://ocw.mit.edu/courses/mechanical-engineering/2-22-design-principles-for-ocean-vehicles-13-42-spring-2005/readings/lec6_wavespectra.pdf.

[9] K. McCreight, "A Note on Selection of Wave Spectra for Design Evaluation," Naval Surface Warfare Center, Bethesda, MD, USA, Rep. CRDKNSWC-HD-974-02, 1998, pp. 8–9, 12–13. [Online]. Available: https://www.dtic.mil/get-tr-doc.

[10] M. Ochi, N. Hubble, “Coastal Engineering,” in *Proc. of the ASCE of the USA,* 1976, pp. 306–307. [Online]. doi: https://icce-ojs-tamu.tdl.org/icce/index.php/icce/article/view/3066.

[11] R. Conrad, “SMP95: Standard Ship Motions Program user manual,” Naval Surface Warfare Center, Bethesda, MD, USA, Rep. NSWCCD-50-TR-2005/074, 2005, pp. 1–16. [Online]. Available: http://www.dtic.mil/dtic/tr/fulltext/u2/a445093.pdf.

[12] *HECSALV/POSSE User Manual*, 1st ed. Alameda, CA, USA: Herbert-ABS, 2013, pp. 75–79, 115–119, 124–125.

[13] R. Zubaly, *Applied Naval Architecture*, 1st ed. Centerville, MD, USA: Cornell Maritime Press, 1996, ch. 4, sec. 4, pp. 113–127.

LIST OF WORKS CONSULTED

1. *Small Craft-Stability and Buoyancy Assessment and Categorization, Part 1 Non-Sailing Boats of Hull Length Greater than or Equal to 6 m*, ISO Standard 1227–1, 2015. [Online]. Available: https://www.iso.org/standard/68140.html.

2. P. Brown, “A study of small ship stability,” Canberra, Australia, 1986.

3. *Explanatory Notes to the International Code on Intact Stability*, IMO Standard 2008 IS Code, 2008. [Online]. Available: http://imo.udhb.gov.tr/dosyam/EKLER/MSC.1-Circ.1281.pdf.

4. *Adoption of the International Code on Intact Stability,* MSC Standard 2008 IS Code 2008. [Online]. Available: http://www.imo.org/en/Knowledge Centre/IndexofIMO Resolutions/Maritime-Safety-Committee-(MSC)/Documents/MSC.267(85).pdf.

5. S. M. Berg, “Non-linear rolling of ships in large sea waves,” M.S. thesis Dept. of Mech. and Aer. Eng., NPS, Monterey, CA, USA, 2007. [Online]. Available: https://calhoun.nps.edu/bitstream/handle/10945/3003/07VandenBerg.pdf?sequence=1.

6. J. M. Falzarano, “Predicting complicated dynamics leading to vessel capsizing,” Ph.D. dissertation, Dept. of Nav. Arch. and Mar. Eng. University of Michigan, Ann Arbor, MI, USA, 1990.

7. E. Mansard and E. Funke, “On the fitting of Jonswap Spectra to measured sea states,” in *Proc. of the Coastal Engineering Conference of the USA,* 1990. [Online]. doi: https://icce-ojs-tamu.tdl.org/icce/index.php/ice/article/viewFile/4465/4146.

8. C. Mobley, *Modeling Sea Surfaces, a Tutorial on Fourier Transform Techniques*. Washington, DC, USA, 2016.

9. J. Wilson, *Dynamics of Offshore Structures,* 2nd ed. Hoboken, NJ, USA: John Wiley and Sons, 2003.

THIS PAGE INTENTIONALLY LEFT BLANK

INITIAL DISTRIBUTION LIST

1. Defense Technical Information Center
   Ft. Belvoir, Virginia

2. Dudley Knox Library
   Naval Postgraduate School
   Monterey, California